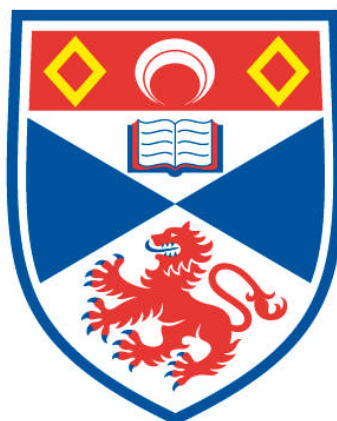


**PD CATALYSED C-C & C-O BOND FORMATION USING
BIS-(DIALKYL/DIARYLPHOSPHINO) FERROCENYL
LIGANDS**

Edward James Milton

**A Thesis Submitted for the Degree of PhD
at the
University of St Andrews**



2010

**Full metadata for this item is available in
Research@StAndrews:FullText
at:**

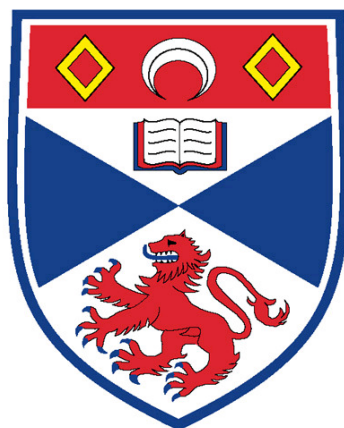
<http://research-repository.st-andrews.ac.uk/>

Please use this identifier to cite or link to this item:

<http://hdl.handle.net/10023/1022>

This item is protected by original copyright

Pd catalysed C-C & C-O bond formation using *bis*-(dialkyl/diarylphosphino) ferrocenyl ligands



University
of
St Andrews

A thesis submitted for the degree of Ph.D. by

Edward James Milton

Under the supervision of Dr Matthew L. Clarke

School of Chemistry

October 2009

Quotes

The most exciting phrase to hear in science, the one that heralds the most discoveries, is not "Eureka!" (I found it!) But "That's funny..."

- Isaac Asimov

Anybody who has been seriously engaged in scientific work of any kind realises that over the entrance to the gates of the temple of science are written the words: "Ye must have faith"

- Max Planck

"If we knew what is was we were doing, it would not be called research, would it?"

- Albert Einstein

Declaration

I, Edward James Milton, hereby certify that this thesis, which is approximately 33,800 words in length, has been written by me, that it is the record of work carried out by me and that it has not been submitted in any previous application for a higher degree.

I was admitted as a research student in September 2005 and as a candidate for the degree of Ph.D. in September 2006; the higher study for which this record was carried out in the University of St Andrews between 2005 and 2009.

Date:

Signature of candidate:

I hereby certify that the candidate has fulfilled the conditions of the Resolution and Regulations appropriate for the degree of Ph.D. in the University of St Andrews and that the candidate is qualified to submit this thesis in application for that degree.

Date:

Signature of supervisor:

In submitting this thesis to the University of St Andrews, we understand that we are giving permission for it to be made available for use in accordance with the regulations of the University Library for the time being in force, subject to any copyright vested in the work not being affected thereby. We also understand that the title and the abstract will be published, and that a copy of the work may be made and supplied to any bone fide library or research worker, that my thesis will be electronically accessible for personal or research use unless exempt by award of an embargo as requested below, and that the library has the right to migrate my thesis into new electronic forms as required to ensure continued access to the thesis. We have obtained any third-party copyright permissions that may be required in order to allow such access and migration, or have requested the appropriate embargo below.

The following is an agreed request by candidate and supervisor regarding the electronic publication of this thesis: Embargo on both all and part of printed copy and electronic copy for the same fixed period of 2 years on the following ground: Publication would be commercially damaging to the researcher, or to the supervisor, or the University.

Date:

Signature of candidate:

Signature of supervisor:

Abbreviations

Å – Ångström (1×10^{-10} m)	Hz – Hertz
Abs. – absorption	IR – Infra-red
Ac – acetyl	<i>i</i> – <i>iso</i>
APC – allyl palladium chloride	IPA – <i>iso</i> -propanol (propan-2-ol)
Aq. – aqueous	ⁱ Pr – <i>iso</i> -propyl
Ar – aryl	IR – Infra Red Spectrometry
Av. – average	K – Kelvin
β_n – “natural” bite angle	L – ligand
BISBI – 2,2'-bis((diphenylphosphino)methyl)-1,1'-biphenyl	Lit – literature
b.p – boiling point	LR-MS – Low Resolution Mass Spectrometry
br – broad	<i>m</i> – <i>meta</i>
CAT – catalyst	M – Molar ($\text{mol} \cdot \text{dm}^{-3}$)
CI – Chemical ionisation	Me – methyl
COD – 1,5-cyclooctadiene	Me-THF – 2-methyltetrahydrofuran
Cp – cyclopentadiene(yl)	MW/ μ W – microwave
Cy – cyclohexyl	min(s) – minute(s)
°C – degrees Celsius	mL – millilitre(s)
δ – parts per million (ppm)	mmol – millimole(s)
d – doublet	mol% – percentage molar equivalent(s)
dd – doublet of doublets	m.p – melting point
D – deuterium	NH ₄ Cl – ammonium chloride
dba – dibenzylideneacetone	NMP – <i>N</i> -methylpyrrolidinone
DCM (or CH ₂ Cl ₂) – dichloromethane	NMR – Nuclear Magnetic Resonance
dcpmp – dicyclohexylphosphino(<i>N,N'</i> -dimethylmorpholine)	<i>o</i> – <i>ortho</i>
dcypb – 1,2- <i>bis</i> -(dicyclohexylphosphino)butane	OAc – acetate
dcype – 1,2- <i>bis</i> -(dicyclohexylphosphino)ethane	OH – hydroxide
depe – 1,2- <i>bis</i> -(diethylphosphino)ethane	OMe – methoxy
dfppe – 1,2- <i>bis</i> -(difluorophenylphosphino)ethane	OR – alkoxide
dippf – 1,2- <i>bis</i> -(diisopropylphosphino)ferrocene	OTf – triflate
dippp – 1,2- <i>bis</i> -(diisopropylphosphino)propane	<i>p</i> – <i>para</i>
dme – 1,2-dimethoxyethane	p.p.m – parts per million
dmf – <i>N,N</i> -dimethylformamide	Ph – phenyl
DPE-Phos – <i>Bis</i> (2-diphenylphosphinophenyl)ether	R.D.S – rate determining step
dppb – 1,4- <i>bis</i> -(diphenylphosphino)butane	RT – room temperature
dppBz – 1,2- <i>bis</i> -(diphenylphosphino)benzene	s – singlet
	S.M. – starting material
	<i>S</i> -Phos – 2-Dicyclohexylphosphino-2',6'-dimethoxybiphenyl

dppe – 1,2- <i>bis</i> -(diphenylphosphino)ethane	t – triplet
dppf – 1,2- <i>bis</i> -(diphenylphosphino)ferrocene	TBAF – tetrabutylammonium fluoride
dppp – 1,2- <i>bis</i> -(diphenylphosphino)propane	TMS – tetramethylsilane
dtbdppf – 1-(diphenylphosphino)-1'- (ditertiarybutylphosphino)ferrocene	^t Bu – tert-butyl
dtbpf – 1,2- <i>bis</i> -(ditertiarybutylphosphino)ferrocene	<i>tert</i> – tertiary
dtbpx – 1,2- <i>bis</i> -(ditertiarybutylphosphino)Xylene	THF – tetrahydrofuran
EI – electron impact	TOF – turnover frequency (h ⁻¹)
eq. – equivalent(s)	Tol – tolyl
Et – ethyl	TON – turnover number
EtOH – Ethanol	Ts – toluenesulfonyl
Et ₃ N - triethylamine	VSEPR – Valence Shell Electron Pair Repulsion Theory
F ⁻ – fluoride	X – halide
FAB – Fast Atom Bombardment	XRD – X-Ray Diffraction
GC-MS – Gas Chromatography Mass Spectrometry	
g – gram(s)	

Contents

Quotes.....	ii
Declaration.....	iii
Abbreviations.....	v
Contents.....	vii
Abstract.....	1
Chapter 1. Introduction.....	3
1.1.0 Pd catalysts in organic synthesis.....	3
1.1.1 Steric effects of ligands: Cone angle (θ) for mono-phosphines.....	3
1.1.2 Bite angle effects of diphosphine ligands.....	4
1.1.3 Electronic effects of phosphine ligands.....	6
1.1.4 Pd catalysed cross-coupling.....	7
1.1.5 Oxidative addition studies of cross-coupling reactions.....	8
1.1.6 Mechanistic studies on transmetalation of nucleophiles.....	16
1.1.7 Ligand steric effects on transmetalation to Pt complexes.....	18
1.1.8 Mechanistic studies on reductive elimination.....	19
1.1.9 Limitations & reactivity of cross-coupling reaction systems.....	22
1.2.0 Negishi cross-coupling reaction.....	23
1.2.1 Suzuki-Miyaura cross-coupling reaction.....	26
1.2.2 Stille cross-coupling reaction.....	33
1.2.3 Hiyama cross-coupling reaction.....	40
1.2.4 Hiyama-Denmark coupling.....	42
1.2.5 Buchwald-Hartwig aryl ether synthesis.....	46
Project Aims.....	49

Chapter 2. Grignard cross-coupling & the reactivity of Pd & Pt complexes of dtbdppf.....	50
2.1 The effect of ferrocenyl phosphine ligands in cross-coupling reactions	50
2.2 “Super-concentrated” 5M Kumada type Grignard cross-coupling reactions....	53
2.3 Transmetalation studies with Pt complexes.....	59
2.4 Synthesis of [Pt(P-P)Br ₂] from [Pt(COD)Br ₂]	59
2.5 Reaction with K ₂ PtBr ₄	62
2.6 Reaction with Pt(COD)(Ph)Br	65
2.7 Transmetalation Studies [Pt(P-P)Br ₂]	72
Chapter 3. Hiyama cross-coupling reaction of alkenyl trialkoxysilanes.....	76
3.1 Varying the concentration of Si nucleophile.....	78
3.2 Competition Experiments – Hiyama Vs Suzuki	80
3.3 Suzuki cross-coupling of heavily fluorinated boronic acids.....	81
Chapter 4. Pd catalysed C-O bond formation using alkoxy silanes as nucleophiles	85
Chapter 5. Conclusions & Further Work	96
Chapter 6. Experimental	98
6.1 Pd /Pt complexes & Transmetalation Studies.....	100
6.2 Hiyama & Suzuki cross-coupling reactions.....	115
6.3 Aryl Ether synthesis	118
Chapter 7. References.....	122
Appendix A - X-Ray Crystallography Data.....	129
[Pt(dtbdppf)Br ₂] – (24).....	130
[Pt(COD)(dippf)Br]Br ⁻ – (26)	132
[Pt(dippf)(Ph)Br] – (28)	136
[Pt(dppe)(<i>p</i> -CF ₃ (C ₆ H ₄))Br] – (54).....	139
Appendix B - Synthesis of [Pt(dppe)(<i>p</i>-CF₃(C₆H₄))Br] (54)	141

Acknowledgements

I would like to thank Dr Matt Clarke for giving me the opportunity to work in his research group and for being a great supervisor. I would also like to thank everyone in the MLC research group for general laboratory banter and for answering all of my daft questions, and giving me hints and tips along the way. Namely, Belén Diaz (for some colourful Spanish and Italian language), Charlotte Jones (pest and official baker of many cakes), Fergus Knight, Mary Gunn, Gary Noonan (for general irish-ness and singalongs), Gareth Lamb (for banter and useful advice on metal complexes), Scott Phillips (for Scottishisms and terrible jokes), Geoff (The HPLC Monkey) Roff (for all of the Slange from Scotshire, practical advice and various quotes), Jamie Frew, José Antonio Fuéntes Garcia (for all of his technical expertise and answering daft questions), Karen Damian (for some colourful Italian language), Nicola Martin (for crazy chat, dancing around the lab and the practical jokes!) I would also like to thank Marcia France (for Americanisms and advice), Ian (Giles) Carpenter (for being pedantic and all things Ian) and Tina Konrad (for allowing me to brush up on my German language skills) and finally Scott for running multi-component TLC systems (in a fish tank?) and wanting Praline, a new amino acid! I have learnt invaluable laboratory skills, had a good laugh and met some great people. Special mentions go to Neil and Katy Keddie for good times, shed demolition, epic BBQ's and mystery spirits, my wonderful Lani and my family (don't worry mum, this can live on the bookshelf quite happily) for supporting me throughout some tough times; you know how you have helped in various ways! Thanks guys (and girls!). Who could forget Kenco[®] and Coca-Cola[®] for all of the caffeine related goodness in the mornings and afternoons when needed and Irn-Bru[®] as a remarkable hang-over cure!

I would also like to thank Mrs. Melanja Smith and Dr Tomas Lebl for their assistance with NMR spectroscopy, Prof. Alexandra M.Z Slawin for X-Ray crystallography, Mrs. Sylvia Williamson for Elemental Analysis, Mrs. Caroline Horsborough and the EPSRC Mass Spectrometry Dept. in Swansea for Mass Spectrometry, Peter Pogorzelec for GC-MS and the EPSRC for funding.

Abstract

A brief introduction explaining phosphine ligand properties, Pd catalysed cross-coupling reactions; the importance of the steps involved in the catalytic cycle (oxidative addition, transmetalation & reductive elimination), mechanistic studies and a comparison of various reactions will give an overview of important cross-coupling reactions and their limitations.

The development of a “super-concentrated” (5M) Pd catalysed Kumada type coupling reaction has been developed for coupling a range of aryl bromide and chloride substrates with the Grignard reagents (*p*-CF₃-C₆H₄)MgBr and PhMgBr in methyl-tetrahydrofuran (Me-THF). Using a range of bidentate ligands such as *bis*-phosphinoferrocenyl ligands, good conversions were achieved using small amounts of solvent; up to 10 times less than typical procedures in THF.

The unsymmetrical Pt complexes of the form [Pt(P-P)Br₂], [Pt(P-P)(Ph)Br] and [Pt(P-P)Ph₂] have been synthesised and characterised. The variations of substituents on the ligand system and the steric bulk have been shown to have a dramatic effect on the rate of transmetalation. The results provide one explanation why 1,1'-bis(*di-tert*-butylphosphino)ferrocene (dtbpf), an excellent ligand for certain Suzuki reactions, is quite poor in reactions where transmetalation is more difficult.

Palladium dichloride complexes of the ferrocenylphosphine based ligands 1,1'-*bis*-(diphenylphosphino)ferrocene (dppf), 1,1'-*bis*-(diisopropylphosphino)ferrocene (dippf) and 1,1'-*bis*-(*di-tert*-butylphosphino)ferrocene (dtbpf) have been shown to be active in the Hiyama cross-coupling of *p*-bromoacetophenone and vinyltrimethoxysilane (CHCH₂Si(OMe₃)) in the presence of TBAF under thermal heating and microwave conditions. Ligands with the optimum balance for promoting the transmetalation, oxidative addition and reductive elimination steps along the reaction pathway have been identified. Competition experiments are consistent with slow transmetalation being an issue with the Hiyama reaction relative to the Suzuki coupling.

A novel protocol has been developed for the synthesis of aryl-alkyl ethers *via* C-O bond activation under Pd catalysed conditions. Utilising the unsymmetrical 1-*bis*-(*di**tert*butyl-1'-*bis*-diphenylphosphino)ferrocene (dtbdppf) under optimised conditions with silicon based nucleophiles and NaOH or TBAF as an activator, the formation of methyl, ethyl, *n*-propyl and *n*-butyl ethers with a range of aryl halides was achieved in good yield.

Chapter 1. Introduction

1.1.0 Pd catalysts in organic synthesis

Transition metal catalysed cross-coupling reactions are a powerful tool for the synthesis of organic compounds and synthesis of natural products.^{1,2} There are many different classes of cross coupling reactions known, dependant on the substrates involved and more industrially viable processes are developed every year. This field of chemistry is fruitful and an active interest exists towards the discovery of cleaner, more efficient methods of catalysis. There are a plethora of catalysts used for C-C, C-O and C-N bond formation. The use of electron rich phosphine ligands in palladium(II) systems has been proved to be successful, especially in the Suzuki³ cross-coupling reaction and more efficient protocols have been introduced.⁴ The flexibility of these reactions proves invaluable within the fine chemical and pharmaceutical industries where both efficiency and versatility are required.

The importance of the ligands around the metal centre is crucial for reactivity, selectivity and regio-selectivity. Perhaps the most important class of ligands are phosphine ligands as they can be easily modified and “tuned” to suit the specific reaction system required. They have the unique ability to stabilise the catalyst in different oxidation states and geometries which leads to reactivity and selectivity.

1.1.1 Steric effects of ligands: Cone angle (θ) for mono-phosphines

The concept of cone angle for mono-phosphine ligands was introduced by Tolman⁵ in 1977. It can be defined as “A quantitative measure of the steric effect of the substituents surrounding the phosphorus atom”. The cone angle (θ) for symmetrical ligands is the apex angle of a cone 2.28 Å from the centre of the phosphorus atom that touches the outer Van Der Waals radii of the substituent atoms (Figure 1).

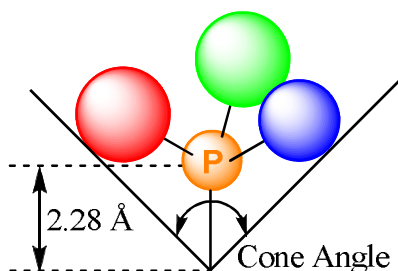


Figure 1. Graphic representation of Tolman's cone angle concept

1.1.2 Bite angle effects of diphosphine ligands

The cone angle can be an important factor in determining the properties of bidentate ligands but bite angle effects are just as crucial. The concept of “natural bite angle” was introduced by Whiteker and Casey⁶ in 1990 to rationalise hydroformylation results obtained with BISBI, a bidentate phosphine ligand (Figure 2) and has been extensively developed by Kamer and Van Leeuwen⁷⁻⁹ with the ground breaking Xantphos family of ligands.

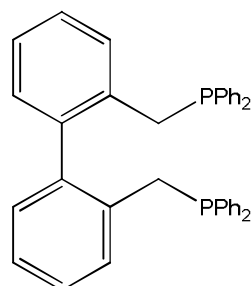


Figure 2. BISBI diphosphine ligand

The “natural bite angle” (β_n) is defined by the preferred chelation angle determined by ligand backbone only.⁶ A wider backbone tends to make the P-M-P bond angle larger and as a result varies the steric and electronic properties of the bidentate ligand (Figure 3).

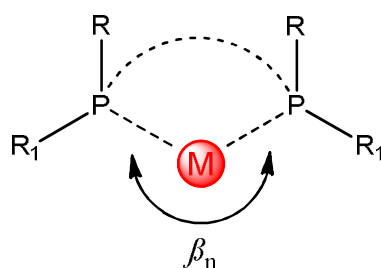


Figure 3. The “natural bite angle”

The natural bite angle β_n is calculated using molecular mechanics (MM2) calculations, using a dummy atom for the metal (M) that has no angular preferences. The metal-to-phosphorus distance, stretching constant (P-M-P bending constant is set to zero) and the dihedral force constant are all taken into account. X-Ray crystallography can also be used to measure a crystallographic bite angle and usually, similar trends are observed compared to the MM2 calculation if the preferred metal geometry is taken into account.

The bite angle of a diphosphine ligand can indicate the degree of distortion from the ideal geometry of a complex based on VSEPR models. Octahedral complexes prefer angles near 90° and tetrahedral complexes prefer 109° .

Since catalysts often interconvert between various geometries, the rigidity of the chelate ring can be decisive.¹⁰ Bidentate phosphines with a natural bite angle of 120° preferentially occupy diequatorial sites in a trigonal bipyramidal complex whereas a bidentate phosphine with a natural bite angle of 90° preferentially occupy apical-equatorial positions¹¹. Diphosphine ligands with bite angles of $\geq 120^\circ$ are obtained using bulky, rigid diphosphine backbones.¹⁰

It is generally considered that a large (wide) bite angle in a metal diphosphine complex can alter both steric and electronic effects;

- 1.) It can increase the effective steric bulk of the ligand which can cause ligand-reactant repulsions and as a result, change the energies of the transition states and catalytic resting states.
- 2.) Electronic changes by changing the bite angle can be described as an orbital effect, due to the bite angle determining metal hybridisation and as a result metal orbital energies. This process can electronically favour (or disfavour) certain geometries of the metal complex and stabilise (or destabilise) various transition states of the reaction.

These properties can be used to “tune” the catalysts needed for effective cross-coupling in each case. For example, square planar geometries of Ni, Pd and Pt complexes can be stabilised by the natural bite angle being close to 90° .

Ligands with larger (wider) bite angles can destabilise the formation of the divalent square planar geometry complexes and favour zero valent geometry and trigonal or tetrahedral geometries about the metal centre. Thus, large bite angles can favour reductive elimination in cross-coupling ($\text{Pd}^{(0)} = 109^\circ / \text{Pd}^{(\text{II})} = 90^\circ$).

1.1.3 Electronic effects of phosphine ligands

The electronic properties of phosphine ligand can be directly observed by differences in CO stretching frequency of metal complexes such as $[\text{Ni}(\text{L})(\text{CO})_3]$ or *trans*- $[\text{Rh}(\text{L})_2(\text{CO})\text{Cl}]$ for monodentate phosphines (As Ni is toxic and nickel carbonyl complexes are extremely volatile). This is a convenient and accurate measurement due to the CO stretching frequency being easily observed and measured by IR spectroscopy (Figure 4). For bidentate phosphines, *cis*- $[\text{Mo}(\text{L})(\text{CO})_4]$ complexes are usually used, due to the fact that bidentate phosphines reacting with $[\text{Rh}(\text{CO})_2]_2(\mu\text{-Cl})_2$ can give either *cis* complexes [*cis*- $\text{Rh}(\text{L})(\text{CO})\text{Cl}$] or dimeric species in which the phosphines adopt a *trans* geometry with a bridging chelate. Only strongly chelating ligands give *cis*-monomeric species.

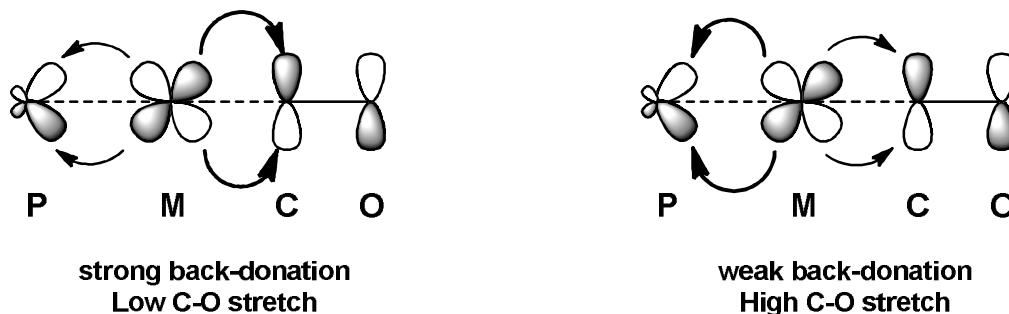


Figure 4. Electronic effects of ligands (Taken from reference¹)

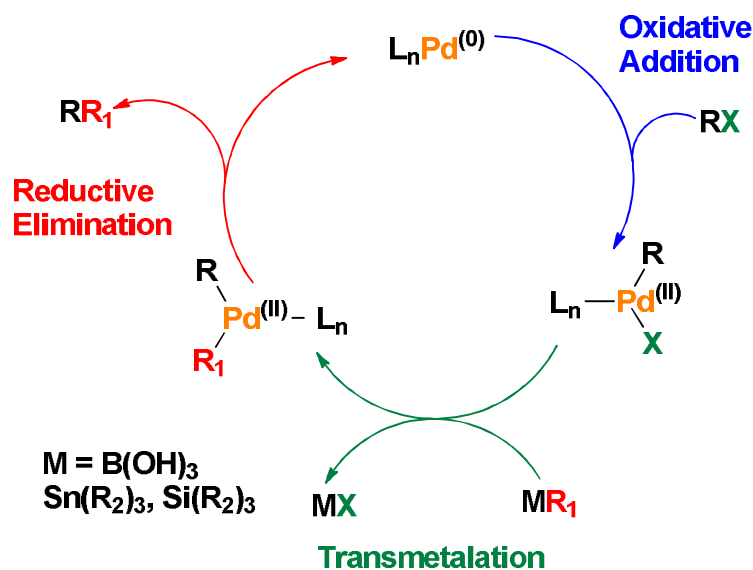
Strong σ -donor ligands give a high electron density on the metal and hence a large back donation to the CO ligands and lower IR frequency. Conversely, strong π -acceptor ligands will compete with CO for the electron back donation and have higher stretching frequency. Some typical values for the Nickel complexes are shown in Table 1.

Ligand (PR₃) R =	IR frequency [NiL(CO)₃] (ν cm⁻¹)
^t Bu	2056
ⁿ Bu	2060
<i>p</i> -(C ₆ H ₄)NMe ₂	2061
Ph	2069
<i>p</i> -(C ₆ H ₄)F	2072
CH ₃ O	2076
PhO	2085
CF ₃ CH ₂ O	2095
Cl	2097
(CF ₃) ₂ CHO	2110
F	2111
CF ₃	2115

Table 1. CO stretching frequency of monodentate phosphines (Taken from reference¹)

1.1.4 Pd catalysed cross-coupling

The three key steps of a basic cross-coupling mechanism are the oxidative addition¹² of the substrate; addition of C-X to Pd⁽⁰⁾ complexes is usually an associative bimolecular process (S_N2 reaction). The leaving anion then adds to the metal centre to give the oxidative addition product. Transmetalation of the R¹ group occurs *via* associative and dissociative pathways¹³ and finally reductive elimination¹⁴ of the product (Scheme 1).



Scheme 1. A general mechanism for a Pd catalysed cross-coupling reaction

1.1.5 Oxidative addition studies of cross-coupling reactions

Various aspects of cross-coupling reactions including the role of anionic Pd species and the reactivity of Pd species towards oxidative addition have been studied by Amatore, Jutand *et al.*,¹⁵⁻¹⁷ resulting in the discovery of several new Pd species suitable for use as catalysts and the publication of a number of important observations.

The relative oxidative addition rates of aryl chlorides and electron rich phosphine ligands to $\text{Pd}^{(0)}$,^{18, 19} and the effect of the ligand bite angle,²⁰ cone angle,²¹ and ligand electronic effects²² have been measured and their roles within the catalytic cycle will be discussed. Pregosin and co-workers²³ have shown the inhibitory effect on oxidative addition of dibenzylideneacetone (dba), as a ligand in $[\text{Pd}(\text{dba})_2]$ a commonly used catalyst pre-cursor in cross-coupling reactions (Figure 5).

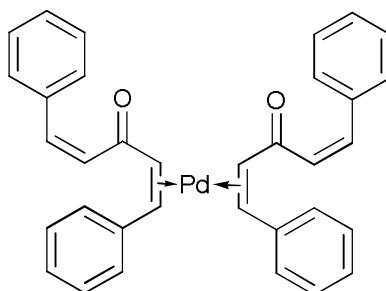


Figure 5. $[\text{Pd}(\text{dba})_2]$

The Heck reaction was used as a model study in this research and both catalytic and stoichiometric reactions with aryl iodides were investigated. The reactivity observed was lower compared to a PdCl_2 based species; this was attributed to the reduced nucleophilicity of the $\text{Pd}^{(0)}$ since dba, an α, β -unsaturated ketone, acts as an electron withdrawing substituent *via* back-bonding. The major $\text{Pd}^{(0)}$ species generated is $[\text{Pd}^{(0)}\text{L}_2(\text{dba})]$ from which dba must dissociate to mediate oxidative addition.

Fairlamb *et al.*^{24, 25} have shown that more electron rich dba analogues (*p*-OMe) have a significant increase in reactivity (rationalised by faster oxidative addition) in the Suzuki-Miyaura reaction of activated aryl chloride, deactivated aryl chlorides (and an activated aryl boronic acid) and deactivated aryl bromides with phenyl boronic acid. By studying a range of *para*-substituted dba ligands, a noticeable increase in oxidative addition of iodobenzene was observed with an OMe group bound to the aryl ring of the dba.

It seems this is an electronic effect (as the aryl rings were *para*-substituted) but not directly. The more electron rich dba ligand has lower backbonding (due to destabilisation) and will thus dissociate readily to form the active species in oxidative addition $[\text{Pd}^{(0)}\text{L}_2]$ (Figure 6).

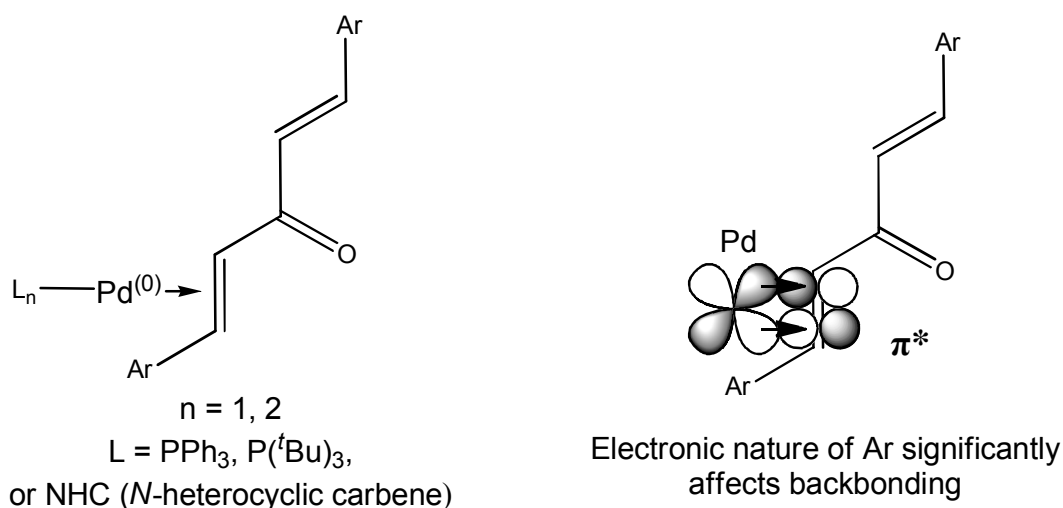
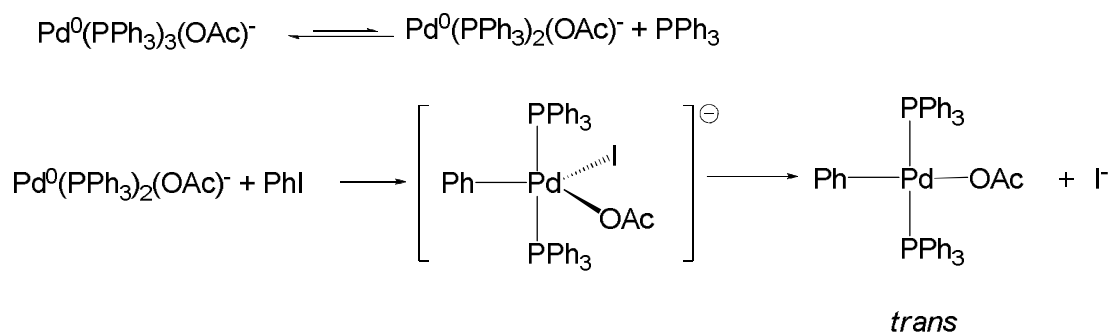


Figure 6. Backbonding in " $\text{L}_n\text{Pd}(\text{dba})$ " complexes

Amatore, Jutand *et al.*¹⁵ however, found that acetate groups bound to the palladium in Pd(OAc)₂ have a positive effect on the Heck reaction and have higher activity in the oxidative addition of Ph-I. This is due to the formation of a pentacoordinate species [Pd(OAc)(Ph)I(PPh₃)₂]. It has been proposed that the acetate anions can coordinate to the Pd⁽⁰⁾ species, which exists in equilibrium with [Pd⁽⁰⁾(PPh₃)₃(OAc)⁻] and [Pd⁽⁰⁾(PPh₃)₂(OAc)⁻].

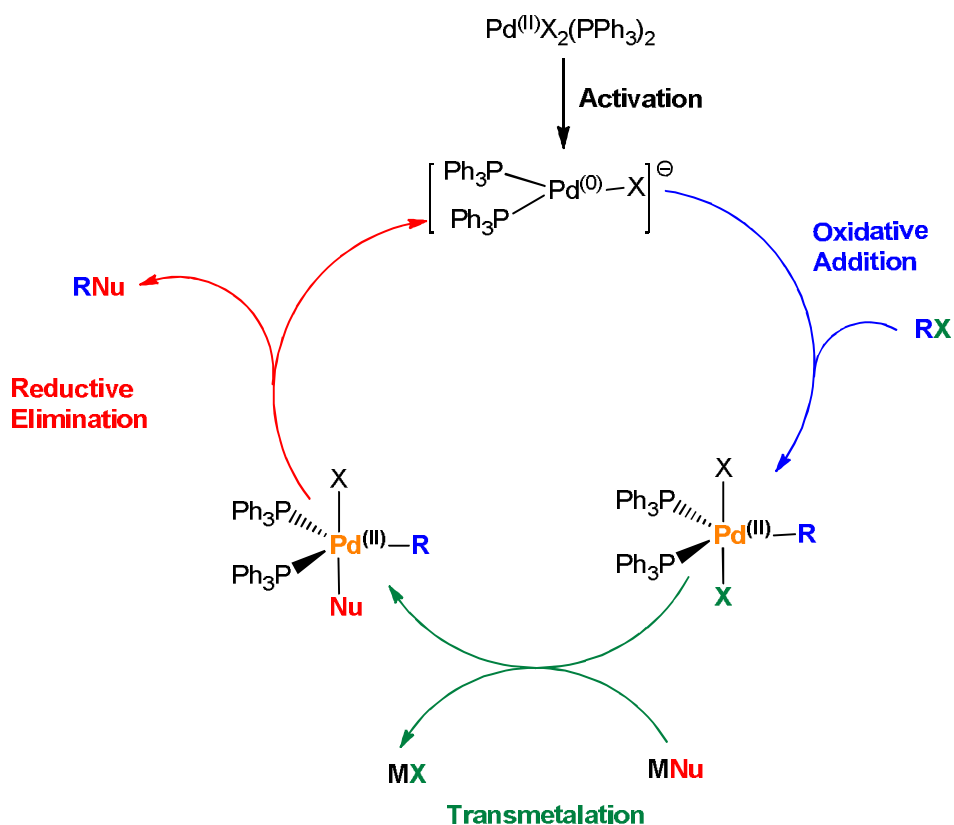
This latter low ligated species has been proved to be active in the oxidative addition step. The formation of new intermediates then occurs with the oxidative addition of PhI. This has led to the conclusion that these species are ideal catalysts for the Heck reaction (Scheme 2).



Scheme 2. Formation of a pentacoordinate [PhPdI(OAc)(PPh₃)₂] species

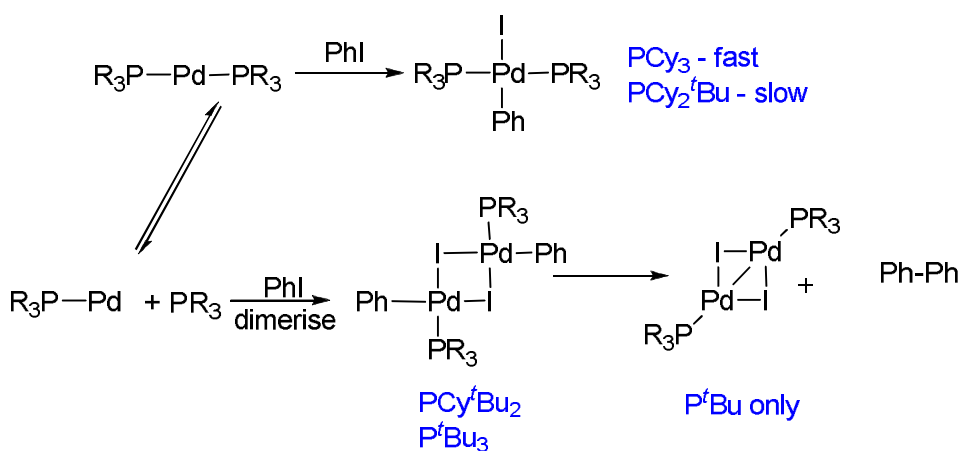
The addition of LiCl to [Pd(AsPPh₃)₂] causes the slow rate of oxidative addition to be accelerated.¹⁶ This increase in rate results from the increased stabilisation of the active species: a chloride ligated Pd⁽⁰⁾ species formed *via* preferential ion-pairing. This intermediate Pd species can then undergo oxidative addition by PhI through a different reaction pathway which leads directly to the *trans*-complex in a more efficient manner than the more common mechanism involving *cis-trans* isomerisation.

Perhaps the most significant discoveries, as shown by Jutand and coworkers²⁶ are concerned with the bulky diphosphine ligand cone angle, which directs the oxidative addition to the Pd *trans*-bisphosphine complexes [Pd(Ar)L₂X] and [Pd₂L₂X₂]. It has been shown that the mechanism of ArX addition to the L₂Pd⁽⁰⁾ complex is highly sensitive to the bulk of the ligand system (Scheme 3).



Scheme 3. Mechanism of Pd-catalysed nucleophilic substitution with free halide ions

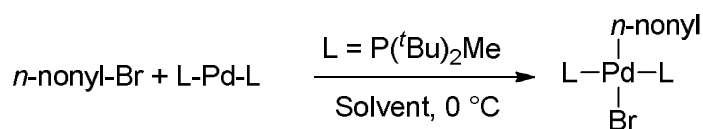
Too much steric bulk proves to be detrimental for the oxidative addition of the substrate; this is demonstrated by the PCy_2^tBu system which can form an iodide bridged dimeric Pd species. With the P^tBu_3 system, reductive elimination of the bi-aryl species occurs by forming an iodide bridged Pd-Pd bonded dimeric species (Scheme 4).



Scheme 4. Reaction pathways for the oxidative addition of Ph-I to $\text{Pd}^{(0)}$ complexes

Fu *et al.*¹⁸ have demonstrated that increasing the polarity of the reaction solvent causes a decrease in activation energy of the oxidative addition of *n*-nonyl-Br (Scheme 5, Table 2). This is consistent with a mechanism involving an S_N2 like attack of PdL₂ on R-X and an increased rate of oxidative addition of Ar-X.¹⁸ The leaving group X (Scheme 6, Table 3) and the increase in steric demand (Scheme 7, Table 4) of the electrophile and ligand both have noticeable effects on the rate of reaction and result in a lowered reactivity.¹⁸

It has also been found that subtle changes to the cone angle (Scheme 8, Table 5) also produce large rate differences by an increase of activation energy of the oxidative addition of *n*-nonyl-Br to the Pd centre.¹⁸



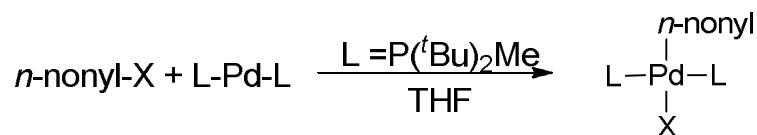
Scheme 5. The effect of the polarity of solvent used

Solvent	Polarity^[d]	ΔG^\ddagger[Kcal.mol⁻¹]
Hexane	0.68	>23 ^[b]
Toluene	1.66	20
THF	2.08	19.5
<i>tert</i> -amyl alcohol	2.46 ^[c]	18.1
NMP	2.62	18
DMF	2.8	17.8

^[a] All data are the average of two runs. ^[b] No reaction at 0-60 °C. ΔG^\ddagger was calculated for 60 °C. ^[c] Value for *tert*-butanol ^[d] Based on the S'' scale. The S'' values are based on a manifold of other solvent dependent processes, and they depend on the proper subjective selection of the appropriate solvent-dependent processes used to calculate them.²⁷

Table 2. Correlation between solvent polarity & activation barrier for oxidative addition^[a]

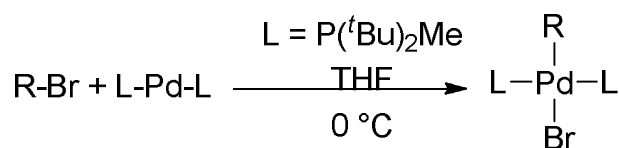
As illustrated in Table 2, an increase in polarity leads to a decrease in the activation energy, consistent with the expectation for an S_N2-type nucleophilic attack of PdL₂ on R-X.



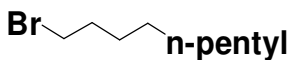
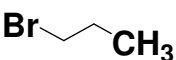
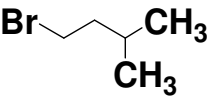
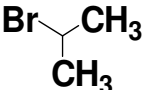
Scheme 6. The effect of the leaving group.

X	t_{1/2}
I	2.2 h at -60 °C
Br	2.3 h at 0 °C
Cl	2.0 days at 60 °C
F	<2% reaction after 43 h at 60 °C
OTs	10.4 h at 40 °C

[a] All data are the average of two runs.

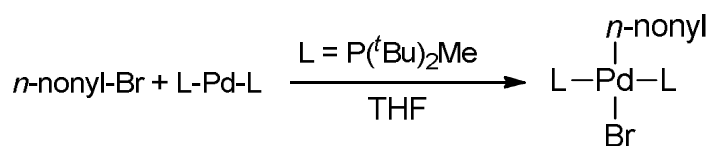
Table 3. Effect of the leaving group on the rate of oxidative addition^[a]

Scheme 7. The effect of the steric demand of the electrophile

R-Br	k_{rel}	ΔG[‡][Kcal.mol⁻¹]
	1	19.5
	0.19	20.3
	0.054	21
	<0.0001	>24 ^[b]

[a] All data are the average of two runs. [b] Extrapolated from a reaction at 60 °C.

Table 4. Correlation between steric demand & activation barrier for oxidative addition^[a]



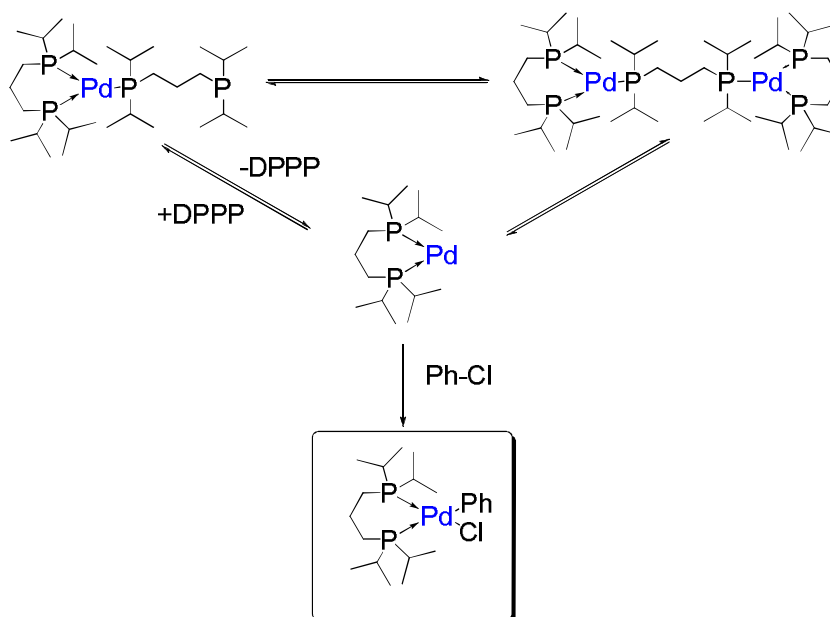
Scheme 8. Effect of the phosphane cone angle of the ligand

L	Cone Angle θ [°]	ΔG^\ddagger [Kcal.mol⁻¹] [b]
P(^t Bu ₂)Me	161	19.5 (0 °C)
PCy ₃	170	20 (0 °C)
P(^t Bu ₂)Et	165	25.4 (60 °C)
P(^t Bu) ₃	182	>28.4 (60 °C)

[a] All data were the average of two runs. [b] The temperature at which ΔG^\ddagger was measured is noted in parentheses.

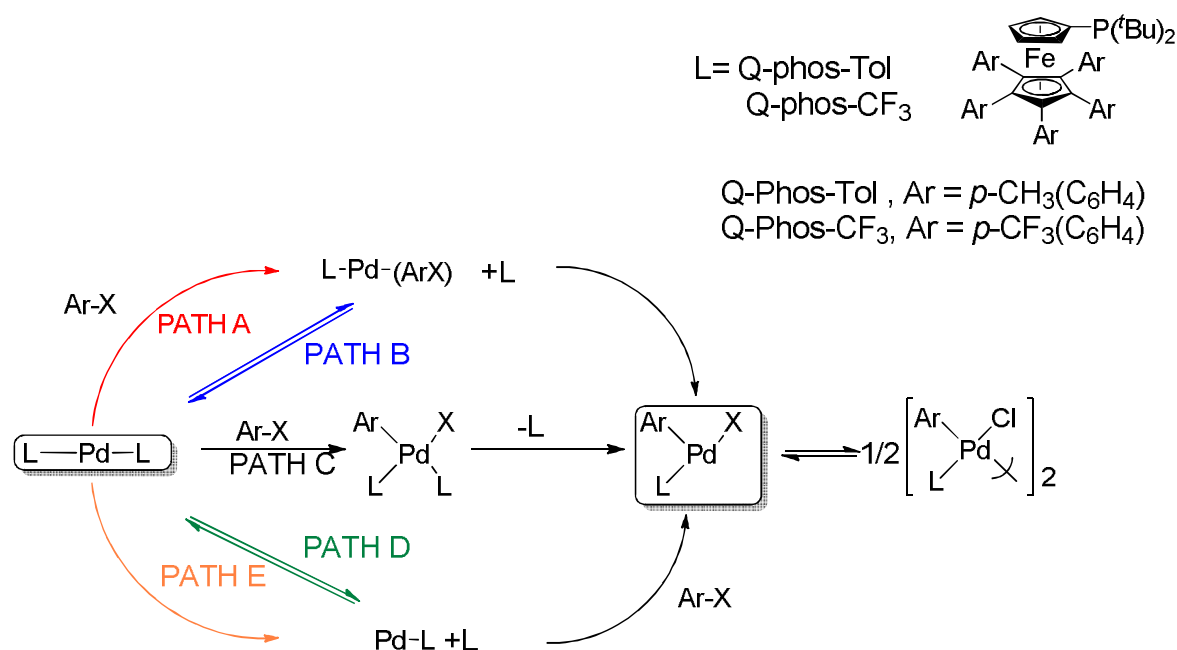
Table 5. Effect of the phosphane on the activation barrier for oxidative addition^[a]

Portnoy, Milstein *et al.*²⁰ have confirmed the ability of the electron rich phosphine ligand 1,3-*bis*-(diisopropylphosphino)propane (dipp) to function as both a chelating and monodentate ligand in a Pd⁽⁰⁾ complex. It has been observed that oxidative addition of an aryl chloride to the trigonal complex [Pd(dipp)₂] involves facile generation of two 14-electron species. These species subsequently undergo the rate determining step of oxidative addition to an aryl chloride (Scheme 9).

Scheme 9. Proposed mechanism for oxidative addition of Ph-Cl to [Pd(dipp)₂]

This reaction is essentially a nucleophilic aromatic substitution process even when using aryl chlorides with electron-donating groups in place. The Pd(dippf) complex behaves as a strong nucleophile, due to its unsaturated nature, high electron density and “bent” P-Pd-P geometry.

An oxidative addition study was performed by Hartwig *et al.*²⁸ using [Pd-(Q-Phos-Tol)₂] and [Pd-(Q-Phos-CF₃)₂] with PhCl, PhBr and PhI as substrates for coupling. They determined that oxidative addition of the PhX species can proceed *via* five possible mechanisms after analysis of the ³¹P NMR spectra (Scheme 10).



Scheme 10. The possible mechanisms of oxidative addition to Pd complexes

(PhI adds *via* **Path A**, PhBr adds *via* **Path D** and PhCl adds *via* **Path E**)

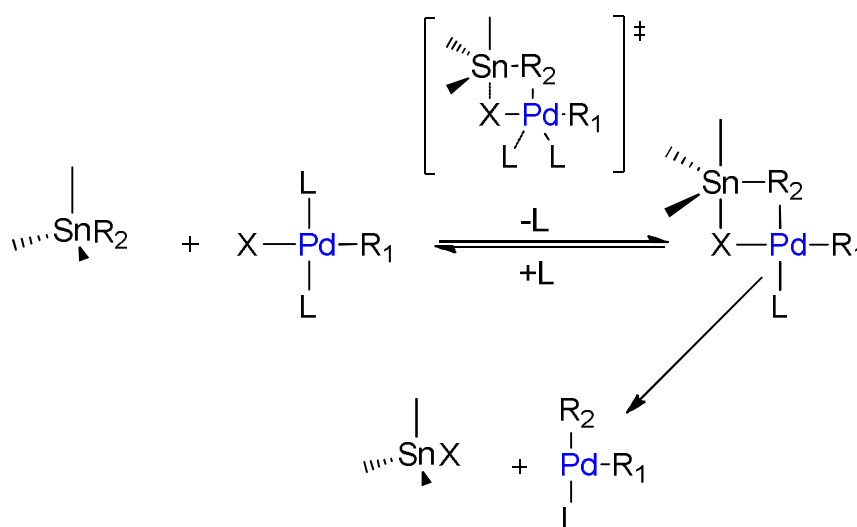
- 1.) **Path A** involves the addition of PhI *via* associative displacement of the phosphine from the Pd centre.
- 2.) **Path B** involves the reversible association/dissociation of substrate and binding of the ligand onto Pd.
- 3.) **Path C** involves the oxidative addition of the Ar-X across the Pd and ligand dissociation to form the L(Ar)Pd(X) species.
- 4.) **Path D** involves the addition of PhBr *via* rate limiting dissociation of phosphine.
- 5.) **Path E** involves the addition of PhCl *via* reversible association/dissociation of phosphine followed by rate limiting oxidative addition.

From these results, can be concluded that electronic effects are perhaps the most important factor; the electronic properties of the diphosphine ligand and the electronegativity of the substrate gave rise to five mechanisms for oxidative addition alone. Electronic effects are crucial in the oxidative addition pathway, and it seems less active R-X bonds need an electron rich phosphine ligand system to mediate the reaction. However, more subtle steric effects can be effective when certain ligand donor strengths have been reached.

1.1.6 Mechanistic studies on transmetalation of nucleophiles

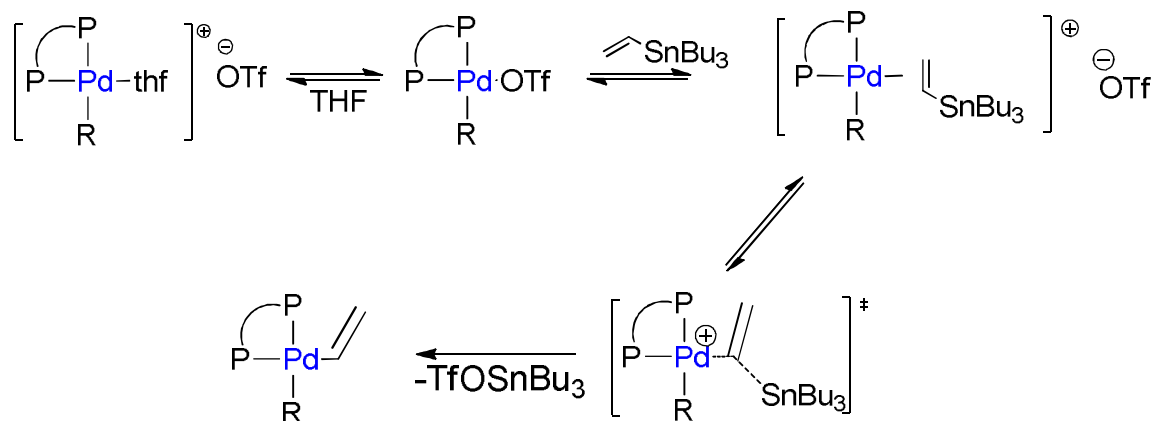
Mechanistic studies on organosilicon coupling reactions are relatively scarce²⁹⁻³⁴ and it has been shown that the rate of transmetalation in a catalytic cycle is one of the key steps in a successful cross-coupling reaction.³⁵ This is particularly important with a Si nucleophile where the RDS could be oxidative addition or transmetalation. Mechanistic studies are observed with Pt catalysts, as they form stable diaryl platinum systems which can be investigated. The work of Nilsson *et al.*³⁶ has reinforced previous work on the Stille reaction and showed that transmetalation occurs with tetraorganostannanes [Sn(vinyl)Me₃] and platinum(II) aryltriflate complexes *trans*-[Pt(L₂)(Ph)X] highlighting the open and closed cyclic transition states shown by Espinet previously (Scheme 11 & 12).¹³

Retention of configuration at carbon *via* an S_E2 cyclic substitution of ligand for R group at the Pd centre (Scheme 11).¹³ This involves a bridged intermediate with the ligand and R group in a *cis*-arrangement to each other, rather than a *trans*-arrangement, which would readily reductively eliminate the coupled product.



Scheme 11. The S_E2 cyclic mechanism of transmetalation

Inversion of configuration at carbon *via* an S_E2 open substitution of ligand for the R group at the Pd centre in the absence of bridging ligands, with competitive formation of *cis* or *trans* intermediates with 1,2-*bis*-(diphenylphosphino)ethane (dppe) as a bidentate ligand (Scheme 12).¹³



Scheme 12. The S_E2 open mechanism of transmetalation

They also showed that co-ordination of a chloro or phosphine ligand in the *cis* and *trans* position inhibits the transmetalation (as phosphine is a relatively strong σ -donor and a π -acceptor ligand). These results suggest that solvolysis and the lability of the leaving group are important for reactivity. A strong steric effect was also identified on the outcome of the transmetalation, indicating associative activation reaction pathways.

This effect was shown by directing the transmetalation to occur over the Sn-C(sp³) bond rather than over the Sn-C(sp²) bond. It was postulated that the initial attack takes place *trans* to the phenyl group, *via* an open transition state. In a subsequent reaction, the intermediate reacts with another molecule of stannane (which catalyses the *cis-trans* isomerisation) and gives the final product *via* a cyclic transition state.³⁶

The most extensive mechanistic study to date was conducted by Denmark and Sweis^{37, 38} and gives a full evaluation of the fluoride promoted cross coupling reaction of alkenyl silanols with aryl iodides. It was shown that a fast and irreversible oxidative addition of the aryl iodide to the metal occurs under these conditions, followed by the rate determining transmetalation *via* a fluoride activated disiloxane species.

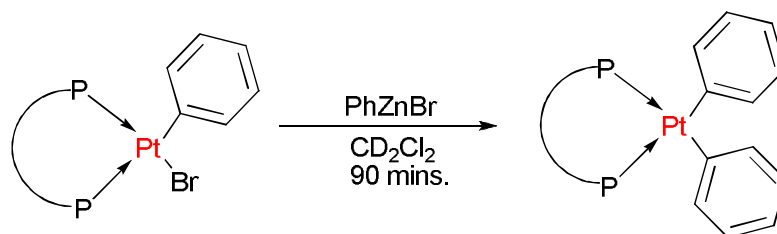
The disiloxane species is derived from the particular silanol employed and undergoes cross-coupling. The observation of an unknown Si species by ^{29}Si NMR proved that a common intermediate is formed. This unknown species was found to be in equilibrium with the fluoride ion and was dependent on the concentration of TBAF used in the study.

An accurate study on these steps in the catalytic cycle will allow better catalyst design, optimisation of the reaction and ultimately, maximise the effectiveness of catalysts required for the coupling of weak nucleophiles.

1.1.7 Ligand steric effects on transmetalation to Pt complexes

Recent work by Clarke and Heydt³⁵ has shown the importance of ligand steric effects on transmetalation. They used *cis*-chelating diphosphine ligands (Figure 7) to distinguish direct stereoelectronic effects from the formation of complexes with different geometry or coordination number, which could occur with mono-phosphines. Platinum was also employed as the stability of palladium diaryl species are known to be highly dependent on the ligands and rapidly reductively eliminate to generate $\text{Pd}^{(0)}$. Platinum avoids this problem and generates a stable diaryl platinum complex, which can be analysed and investigated further.

The diphosphines were chosen for their differences in steric and electronic parameters to give a detailed study with PhZnBr . (dppe), 1,2-*bis*-(diethylphosphino)ethane (depe), (dfppe) and (dppf) gave quantitative yields of the *bis*-aryl compound within minutes. The fact that 1,2-*bis*-(dicyclohexylphosphino)ethane (dcype) and 1,2-*bis*-(ditertiarybutylphosphino)Xylene (dtbpx) systems showed no product even after several days; proves that steric properties can have a more pronounced effect than may have been thought, on the transmetalation reaction (Scheme 13).



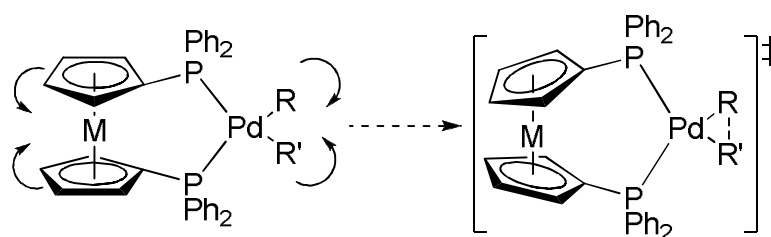
Scheme 13. General transmetalation scheme from bidentate Pt complexes

The effect of the differing halide ligand on the unsymmetrical Pt catalysts was also observed and shown that $[\text{Pt}(\text{dppe})(\text{Ph})\text{Cl}]$ had a very fast rate of transmetalation even at low temperatures compared to the analogous bromide species.³⁵ Further studies to evaluate the effect of changing the ligand, halide and aryl group are required to develop a greater understanding of cross-coupling reactions. These differences need more clarification.

1.1.8 Mechanistic studies on reductive elimination

Brown and Guiry²⁰ have demonstrated the bite angle dependence of diphosphine Pd complexes $[\text{P}_2\text{PdMeR}]$ and the subsequent reactivity of reductive elimination. These studies revealed dppp to be the most stable complex and the observed trends fit with the idea that the reductive elimination step is facilitated by a ligand with a large interchelate angle.

They found that the increase of thermal decomposition of the dialkyl complexes was related to the bite angle of the palladium in the ground state complex; the larger the bite angle, the more facile the elimination. The dppf (bond angle = 97°) and dppp (bond angle = 89°) complexes are consistent with the hypothesis that the transition state for the elimination step has an enhanced P-Pd-P bond angle, and in both cases, the ferrocene (M = Fe) derived ligand systems proved to be more reactive (Scheme 14).



Scheme 14. Distortions along the reductive elimination pathway

Hartwig and Culkin²¹ have proposed that reductive elimination is faster from aryl palladium complexes $[\text{Pd}(\text{dppbz})(\text{Ar})\text{R}]$ (dppbz = 1,2-bis-(diphenylphosphino)benzene; R = methyl, enolate, cyanoalkyl, trifluoroalkyl or malonate) with electron-withdrawing substituents on the Pd bound aryl ligand and with sterically hindered alkyl groups (R) bound to the Pd.

The electronic properties of the alkyl group had the largest influence on the rate of elimination; more electron-withdrawing groups on the α -carbon retarded the rate of elimination. (p -CN > p -CF₃ > p -H > p -Me > p -OMe). It was also observed that steric effects prove to be important when the type of functional group is unchanged, but changes in the type of functional group dominated steric effects.

Studies by Roddick, Merwin *et al.*²² focused on electron-poor complexes of the form [Pt(dfppe)(Ar)₂] (dfppe = 1,2-*bis*-(di-pentafluorophenylphosphino)ethane)). It was found that the elimination of the biaryl species occurs readily at 80 °C. It was also determined that the fate of the Pt(dfppe) fragment released after elimination is solvent-dependent; in aromatic solvents, the tetrahedral bis-chelate species [Pt(dfppe)₂] is the only species observed by ³¹P{¹H} NMR spectroscopy and is confirmed by a large ¹J_{P-Pt} coupling constant of 4269 Hz.

Results from kinetic and mechanistic studies indicated that for the dfppe system, elimination occurred without phosphine loss or significant solvent association *via* a simple concerted 1,1'-coupling process.²² Simple (non-fluorinated) dppe complexes were found not to reductively eliminate bi-aryl species, leading to the determination that there is a strong electronic effect on reductive elimination processes.

The electronic effects of reductive elimination of symmetrical and unsymmetrical *bis*-aryl complexes have already been extensively investigated by Hartwig and co-workers.³⁹ The reductive elimination from the symmetrical bis-aryl platinum complexes [Pt(dppf)(C₆H₄-4-R)₂] [(R) = NMe₂, OMe, CH₃, H, Cl], and the electronically unsymmetrical *bis*-aryl platinum complexes [Pt(dppf)(C₆H₄-4-(R))X] [R = CH₃, X = NMe₂, OMe, H, Cl, F, CF₃; R = OMe, X = NMe₂, H, Cl, F, CF₃; R = CF₃, X = H, Cl, NMe₂; and R = NMe₂, X = H, Cl] (Figure 7) were studied. Two main electronic effects were recorded and also their influence on the selectivity and reaction rate.³⁹

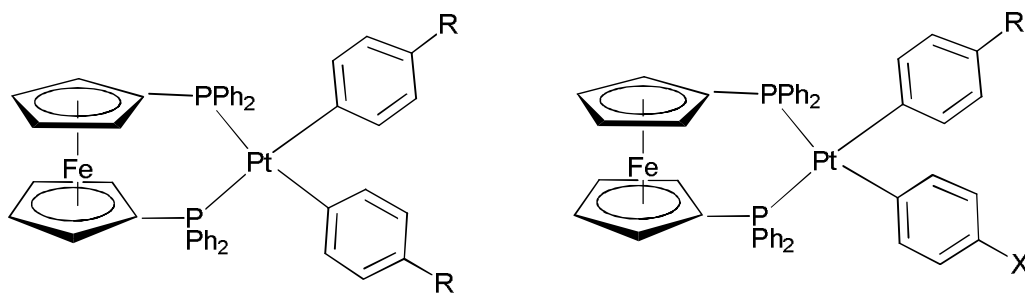


Figure 7. Examples of Pt complexes used by Hartwig

One effect had already been predicted by theoretical methods by Low⁴⁰ and Tatsumi⁴¹ and had determined that reductive elimination was faster with compounds containing more electron-donating groups, which participated in bond formation. The second effect of the same order of magnitude indicated that aryl groups with dissimilar electronic properties increase the rate of reductive elimination. It then seems logical to ascertain that the pairing of an electron-rich and an electron-poor group would lower the energy of the transition state and thereby favour reductive elimination. Therefore, a delicate balance must be struck to favour the reductive elimination process.³⁹

Hayashi *et al.*⁴² have shown that the analogous $[M(\text{dppf})\text{Cl}_2]$ (where $M = \text{Pt}$ and Pd) complexes have similar properties to each other, where the P-Pt-P bond angle is 1.3° larger and the Cl-Pt-Cl bond angle is 3.7° smaller than the corresponding Pd complexes.

The study correlated that compounds with an increased P-Pd-P bite angle and smaller Cl-P-Cl bond angle had superior activity and selectivity in Grignard cross-coupling reactions. It was proposed that this is due to the acceleration of the reductive elimination, resulting from the presence of high steric strain in the chelating system, which can be released on the dissociation of a phosphino group.

The influence of the bite angle has been extensively covered by van Leeuwen *et al.*^{8, 43} of particular interest are the palladium catalysed cross-coupling reactions concentrating on Xantphos type ligands with bite angles $102.9\text{-}110^\circ$.

They observed that an increase in the P-Pd-P bite angle resulted in a decrease in the R-Pd-R' bond angle in the intermediate species of the cross-coupling reaction, which consequently accelerated the reductive elimination process.

An optimum angle was reached with a bite angle equal to 102° (DPE-phos) which suggests a distorted square planar geometry about the Pd centre. When the P-Pd-P bite angle was increased further, the distortion away from square-planar geometry also increased the R-Pd-R' bite angle and as a result, retarded reductive elimination and also the reactivity. This effect was observed when both DPE-Phos and Xantphos were used.⁴²

The Pd catalysed formation of diaryl ethers has also been extensively investigated by Hartwig⁴⁴ and the electronic effects of dppf analogues have shown that electron poor ligands accelerate reductive elimination. By using a *p*-CF₃ form of dppf, an improved yield of aryl ether was observed with *p*-bromobenzonitrile (74% compared to 51% for dppf).

In stoichiometric studies with [Pd(P-P)(Ar)(OR)], the *p*-CF₃ form of dppf was shown to be twice as fast as dppf but the di-*tert*-butyl analogue 100 times faster in the rate of reductive elimination.⁴⁵ This contradicts the electronic argument that an electron rich ligand would be deactivated toward reductive elimination and that steric effects can play a vital role.

The mechanistic pathways involved in cross-coupling reactions have been widely studied and published in the literature, with a great deal of research focused on the oxidative addition^{28, 39, 46} and reductive elimination¹⁵⁻¹⁷ pathways.

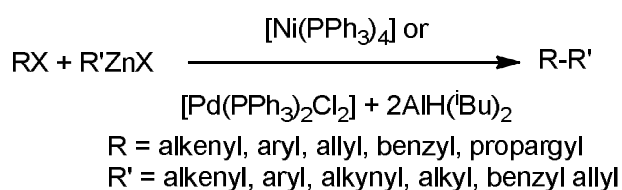
1.1.9 Limitations & reactivity of cross-coupling reaction systems

Each cross-coupling reaction protocol has limitations and these have to be taken into consideration when designing the synthesis of various chemical entities. There is no “generalised” cross-coupling reaction protocol; careful thought has to be used in the choice of nucleophile and cross-coupling partner and in particular the catalyst and ligand system to couple them together.

The use of aryl chlorides is advantageous in cross-coupling reactions due to the relatively low cost and availability compared to aryl/alkyl bromides and iodides. However, if you combine a weak nucleophile (e.g. an organosilane) with an aryl/alkyl chloride coupling partner, the reactivity is significantly lower and requires harsher reaction conditions or higher catalyst loading and higher temperatures, which could be detrimental to product conversion. Therefore performing a Hiyama reaction or aryl ether synthesis with aryl/alkyl chloride substrates is very difficult.

The kinetics of cross-coupling reactions are complex, as one might expect. Yields and selectivities depend on the reaction conditions which are constantly changing. For example, metal-ligand equilibria, the amount of base present (as this is a reagent), the ligand/catalyst may decompose during the reaction and salts are formed during the reaction, all of which are crucial to the reaction pathways and formation of the desired product. Trends in steric/bite angle effects are rare due to the fact that small changes can lead to the population of several intermediates/inactive states which leads to a drastic change in the kinetics of the reaction pathway¹. The following pages aim to illustrate typical reaction conditions and substrate scope for the main type of cross-coupling reactions relevant to this thesis.

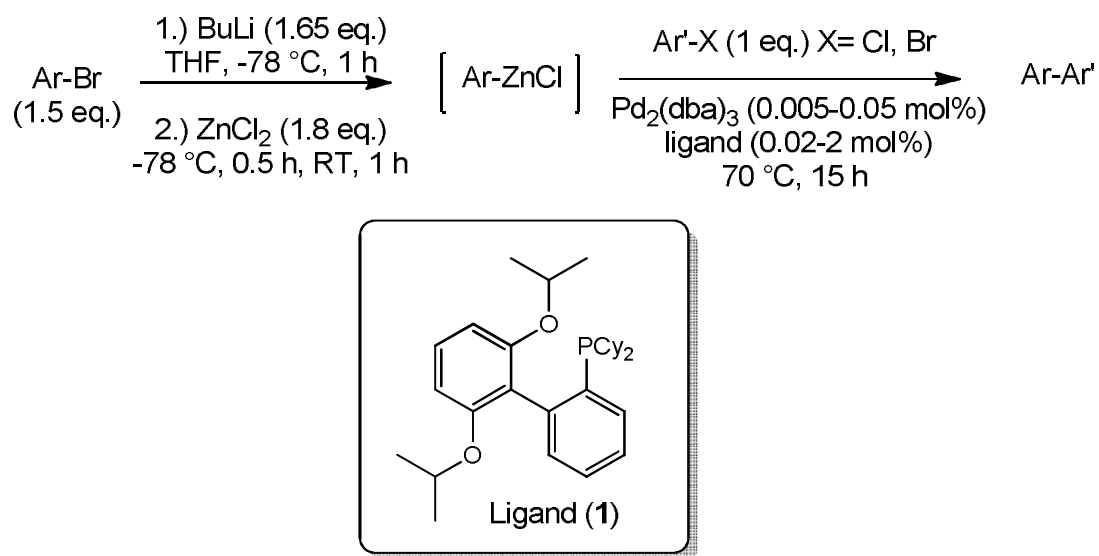
1.2.0 Negishi cross-coupling reaction



Scheme 15. General reaction scheme for Negishi coupling reaction

The use of Zn in the Pd-or Ni-catalyzed cross-coupling (Scheme 15) was first reported in 1977 by Negishi⁴⁷ *et al.* and Fauvarque and Jutand.⁴⁸ A typical Negishi reaction consists of an aryl halide, the generation of the organozinc species *in-situ* followed by Pd catalysed cross coupling of the organozinc species with a second aryl halide to create the bi-aryl moiety. Hayashi⁴² in 1984 proved that bromobenzene can couple effectively with *sec*-butylzinc chloride in >99% with [Pd(dppf)Cl₂] (0.01 mol%) by stirring in THF for 20 h.

Buchwald⁴⁹ *et al.* synthesised a new ligand system (**1**) in 2004 which proved to be active in the Negishi coupling of aryl chlorides and bromides at low Pd catalyst loading giving efficient preparation of hindered biaryls (tri- and tetra-*ortho*-substituted) with a wide range of functional groups and heterocyclic substrates (Scheme 16). A systematic study of ligand structure was performed and was correlated with catalyst activity. Some heteroarylzinc species however, still proved to be problematic giving low conversion.



Scheme 16. Buchwald system for Negishi coupling of aryl chlorides and bromides

Buchwald⁴⁹ demonstrated a tolerance to a variety of common functional groups including cyano, nitro, ester, alkoxy, and amino substituents. Previously reported systems required higher temperatures and quantities of catalyst for similar cross-couplings. For example, 2-cyano-2,3-dimethylbiphenyl was prepared using only 0.01 mol% Pd, which could be the lowest quantity of Pd ever employed for the Negishi cross-coupling of an aryl chloride. The reaction of 1-chloro-4-nitrobenzene with (2,3-dimethylphenyl)zinc chloride in THF at 70 °C resulted in low yields of the desired biaryl.

However, carrying out the process at room temperature provided product in 94% yield using as little as 0.1 mol% Pd. In some cases, a directed ortho-lithiation approach⁵⁰ could be used to access the required arylzinc reagents, obviating the need to start with an aryl bromide.

For example, *ortho*-lithiation of 1,3-dimethoxybenzene, followed by Li/Zn exchange and cross-coupling of the resulting arylzinc reagent with 4-chloroanisole, afforded the biaryl in quantitative yield.

In 2005, Negishi *et al.*⁵¹ have reported high TON's with dppf and DPE-Phos coupling alkenyl and aryl iodides with a range of organozinc species (PhZnBr & (alkenyl)ZnBr)) employing LiBr. RT and 70 °C were needed in some cases in THF with 1-5 mol% catalyst loading (Scheme 17).



Scheme 17. Negishi coupling of alkenyl and aryl iodides with organozinc reagents

Higher conversions were observed with longer reaction times (15 h at RT) or higher temperature and prolonged reaction times (70 °C, 4-10 h). With alkynyl zinc reagents it seems DPE-Phos was superior giving >70% cross coupled product with PhI and (*E*)-1-octenyl iodide at 0.001 mol% loading. *p*-Tol(X) was used in a study of phenyl metals (Zn and Mg) at RT for 23 h. Good results were obtained again with dppf and DPE-Phos for bromides and iodides. However the addition of LiBr inhibited the reaction of bromides whereby PhZnBr(LiBr) with *p*-TolBr only gave 25% conversion, whilst PhZnBr(MgClBr) gave 98% conversion with [Pd(dppf)Cl₂] 0.1 mol% stirring at RT for 23 h. Clearly the choice of nucleophile has an important effect in these reactions.

Recent work by Liu *et al.* has elucidated the mechanism to an extent, whereby a double transmetalation competes with reductive elimination to form cross-coupled or homo-coupled product respectively.⁵² There are limitations to the reaction protocol, whereby the organozinc species has to be synthesised *in-situ* to ensure complete conversion.

More recently Negishi has reported the synthesis of di-tri and tetra substituted alkenes *via* bromoboration to create the boronic ester and subsequent coupling reaction⁵³ and also Pd catalysed alkenylation followed by carbonyl olefination.⁵⁴

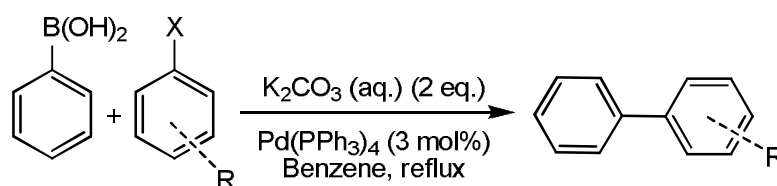
The synthesis of trienoic esters has also been reported which are useful for key reagents for Horner-Wadsworth-Emmons (HWE) chemistry.⁵⁵

Limitations with Negishi coupling still exist whereby aryl-zinc chlorides are still difficult to cross-couple. Heteroaryl and di-alkyl zinc chloride reagents are still problematic. There is still the extra step in the reaction requiring the organozinc reagent to be generated *in-situ* to ensure maximum reactivity.

[Pd(dppf)Cl₂] has been shown to be extremely active in Negishi chemistry and Buchwald has solved some of the problems with aryl chloride substrates by an *ortho*-lithiation approach and gained almost quantitative yield with one of the more deactivated aryl chlorides (*p*-chloroanisole).

In general then, low catalyst loadings can be employed (0.01-0.05 mol% Pd) (Buchwald ligands being favourable for certain aryl chlorides). Most reactions of aryl chlorides need to be heated above 50 °C for prolonged periods to get decent conversion. However there are exceptions which can be stirred at RT overnight. A wide range of functional groups can be achieved but some heteroaryl zinc species still prove to be problematic. There are still limited examples of aryl chlorides and some aryl bromides being used.

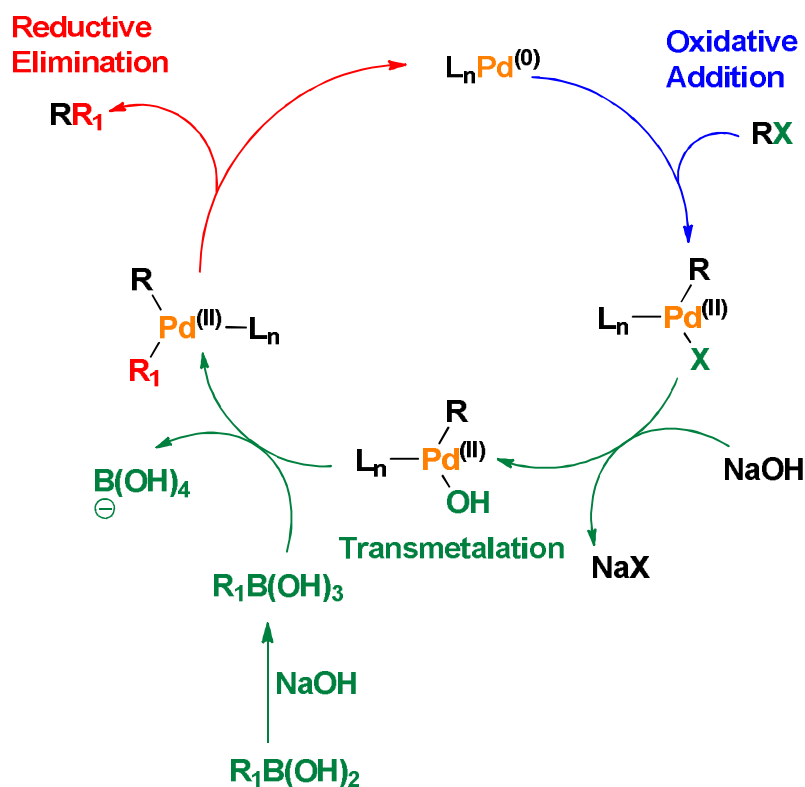
1.2.1 Suzuki-Miyaura cross-coupling reaction



Scheme 18. General reaction scheme for original Suzuki reaction

In the last 10 years, there has been intense research interest in Suzuki reactions of aryl chloride substrates since these substrates are cheaper and more widely available than aryl bromides. A range of catalysts now exist for aryl chloride activation, including diphosphine-Pd catalysts,⁵⁶ mono-phosphine Pd catalysts,^{57, 58} cyclometalated Pd precursors⁵⁹ and potentially hemi-labile bidentate ligands.⁶⁰⁻⁶³

The Suzuki-Miyaura cross-coupling reaction³ (See Bellina *et al.*⁴ for a review) involves the coupling of boronic acids with aryl iodides, bromides, chlorides or triflates (Scheme 19). It has been proved to be an effective route to bi-aryl compounds used by the pharmaceutical and bulk chemical industries.



Scheme 19. Mechanism of the Suzuki-Miyaura reaction

Fu *et al.*,⁶⁴ Buchwald *et al.*⁶⁵ and Bedford *et al.*⁶⁶ have all been successful in optimising the Suzuki reaction with aryl chlorides, by utilising new ligands and different solvent systems. Fu *et al.*,⁶⁴ have optimised the room temperature Suzuki coupling of a wide range of aryl and vinyl bromides and aryl chlorides. Using $Pd_2(dba)_3$ and $P(tBu)_3$ as a catalyst at low loading (0.5–1.5 mol% Pd & 1–4.5 mol% $P(tBu)_3$) and KF as a cheap base, they achieved excellent results with synthesis of bi-aryls in 92–99% yields. Aryl bromides that are electron-poor or electron rich couple cleanly with sterically hindered *o*-tolylboronic acid. Perhaps more importantly *p*-bromo-*N,N'*-dimethylaniline coupled with *o*-tolylboronic acid (98%) and thiophenyl boronic acid (99%), *p*-bromophenol also coupled with phenylboronic acid in 92% in less than 5 h.

Activated aryl chlorides such as *p*-chloroacetophenone, *o/m*-chloropyridine and thiophenes were successfully coupled with sterically hindered, electron rich and electron poor arylboronic acids in 77-99% yields at room temperature.

More vigorous conditions were required to cross-couple unactivated aryl chlorides using higher loading of Pd (1.5 mol%), P(^tBu)₃ (4.5 mol%) and elevated temperatures (70-100 °C) highlighting the difficulties encountered with unactivated aryl chlorides being poor electrophiles to oxidatively add into the Pd catalyst and initiate the reaction.

In general, it can be conceived that aryl boronic acids are easier to couple than alkyl or heterocyclic boronic acids; however the problem still remains with aryl chlorides. *p*-chloroanisole and *o*-tolylboronic acid required heating to 70 °C (88% conversion) whereas *p*-chloroaniline and phenylboronic acid required 90 °C (82% conversion) one of the most difficult aryl chlorides, *p*-chlorotoluene needed heating to 100 °C with cyclopentylboronic acid to achieve 75% conversion. This could be due to the fact that alkyl boronic acids transmetalate at a slower rate than aryl boronic acids.⁶⁷

Through appropriate choice of ligand and catalysts, Fu also selectively cross-coupled an aryl chloride in the presence of an aryl triflate which was unmatched at the time. Low catalyst loadings of 0.5 mol% Pd were also employed and mechanistic studies were undertaken showing that a palladium monophosphine adduct maybe the active species in these Suzuki protocols.⁶⁴

Buchwald *et al.*⁶⁵ also reported an active catalyst at very low loading and successful cross-coupling of aryl bromides and chlorides. Again aryl chlorides requiring prolonged heating times and elevated temperature. They also found Pd(OAc)₂ to be a more effective Pd precursor and K₃PO₄ to be a better base (when combined with the appropriate solvent) with hindered substrates.

Ligands **3** and **5** (Figure 8) have a fine balance of steric and electronic properties which allow accelerated oxidative addition whilst facilitating transmetalation and reductive elimination in the catalytic cycle. These findings reflect the importance of steric bulk and electronic properties of the ligand are vital for reactivity.⁶⁵

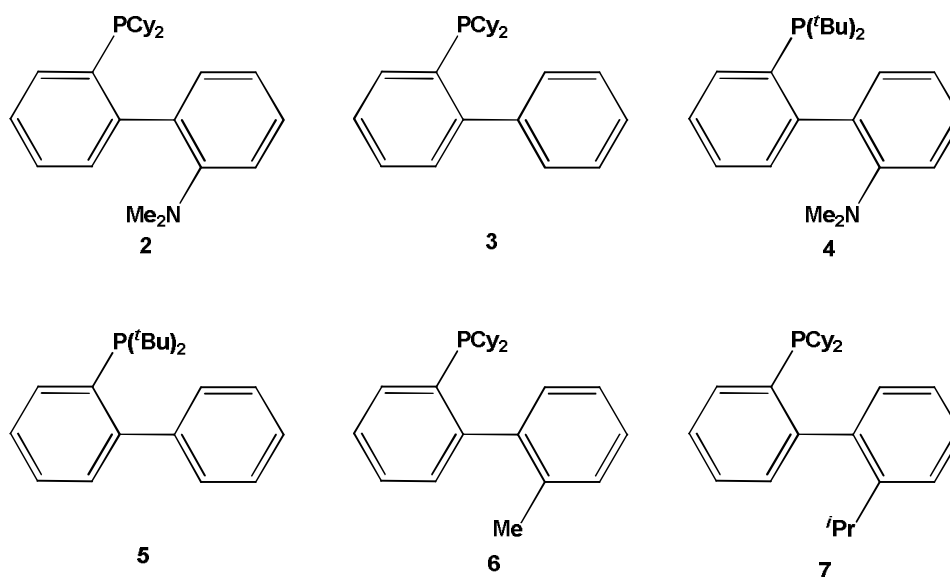


Figure 8. Examples of Buchwald ligands for Suzuki cross-coupling reaction

The basic phosphine group facilitates oxidative addition and binds tightly to the metal (compared to PPh_3) and helps stop the catalyst crashing out of solution. Buchwald also suggests that the *o*-phenyl group may stabilise the complex by an interaction between the aromatic π -system and an empty *d*-orbital on the metal, which can promote reductive elimination and favours the formation of monophosphine Pd species.

This could be due to the aryl group of the substrate being orientated perpendicular to the co-ordination plane and favouring reductive elimination.⁶⁵ Bi-aryls forming from reductive elimination has been shown to occur *via* a transition state in which both arenes are perpendicular to the co-ordination plane from a Pt(II) complex (Figure 9).⁶⁸

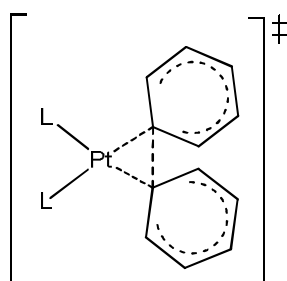
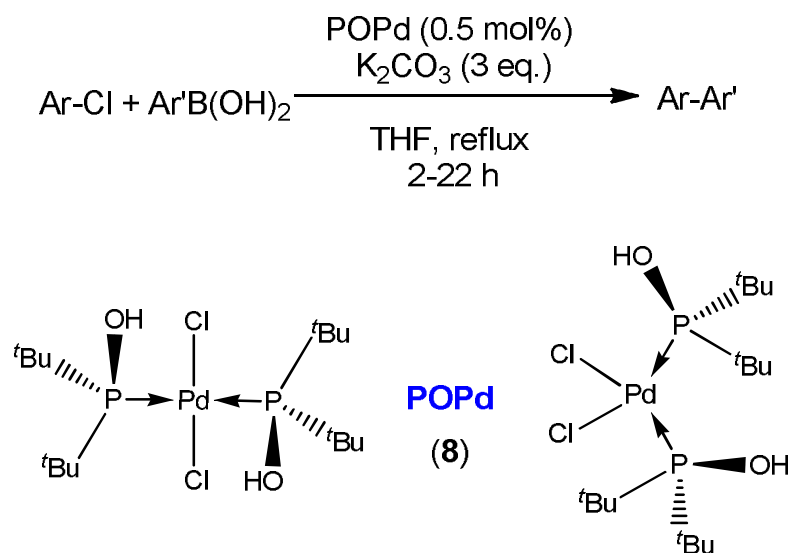


Figure 9. Transition state to show aryl rings perpendicular to the co-ordination plane from a Pt(II) complex to mediate reductive elimination

It was shown by Buchwald⁶⁵ that room temperature Suzuki coupling reactions were catalysed faster by Pd/**5** than Pd/**4**. Ligands **2**, **3**, **6** & **7** were more effective for hindered substrates. It was suggested the smaller size of the ligand allowed relatively facile transmetalation to the $[L_nPd(Ar)X]$ intermediate when sterically encumbered aryl halides or aryl boronic acids are used. The ligand also prevents precipitation of the Pd (which could render the catalyst useless).

The fact that higher turnover numbers (TON's) were obtained with the electron rich dialkyl(biphenyl)phosphine ligands is due to the basic nature of the ligand binding more tightly to the metal thus, increasing catalyst lifetime by keeping the metal in solution for longer periods of time.

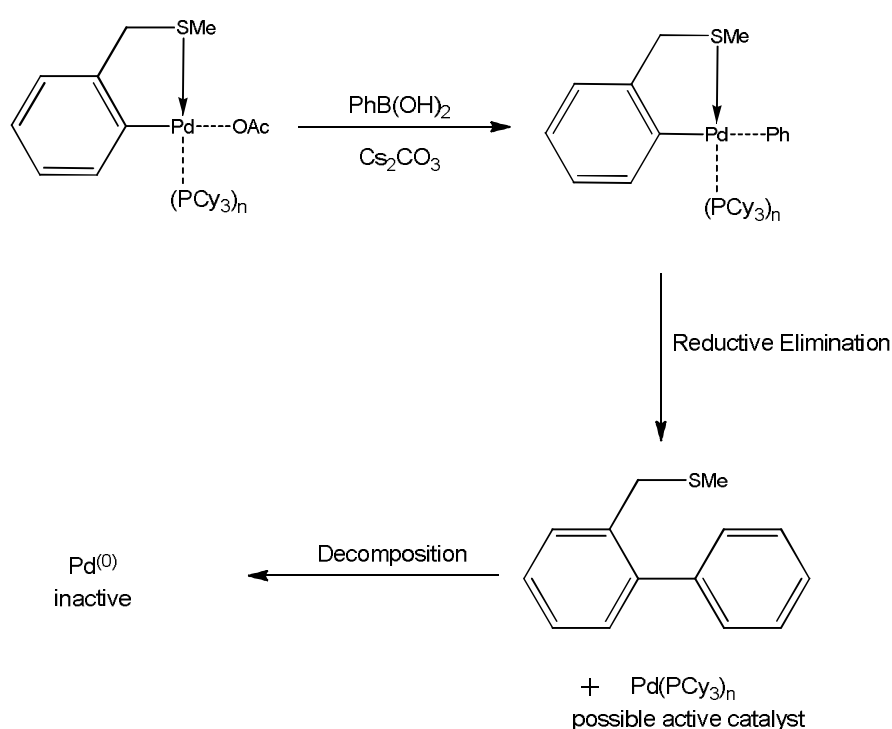
Good results were obtained by Li⁶⁹ in 2002 with POPd (**8**) (0.5 mol%) with chlorobenzene/*p*-tolylboronic acid (1.5 eq.) (refluxing THF, 2 h, 78%) and 2-chloroanisole coupling with $PhB(OH)_2$ (1.5 eq.), ligand (0.5 mol%) and K_2CO_3 (3 eq.) (refluxing THF, 22 h, 82%) again to mediate the more difficult aryl chloride more ligand and a prolonged reaction time was needed highlighting the problematic nature of poor nucleophiles (Scheme 20).



Scheme 20. Suzuki coupling of aryl chlorides with POPd

The work of Bedford *et al.*⁶⁶ has shown an S-based palladacycle to be effective in the Suzuki cross-coupling of a range of deactivated, non-activated and activated aryl chlorides. The addition of di- and tri- alkyl phosphines to the thioether-based palladacycles proved to be more effective. A recurrent trend of chloride coupling catalysis seems to be that active catalysts seem to be mono-dentate. With ligands such as $\text{PCy}_2(o\text{-biphenyl})$ it is possible that the formation of low-coordinate phosphine adducts is favoured, regardless of the amount of excess phosphine used. This could be due to the secondary interaction of the π -system of the aromatic ring co-ordinating to the Pd centre.⁷⁰

Given that N and P-based palladacyclic Suzuki catalysts rapidly generate $\text{Pd}^{(0)}$ due to nucleophilic attack of the aryl boronic acid at the Pd centre, followed by reductive elimination of the biaryl and ortho-metalated ligand, the S-based systems should follow suit. Significant amounts of coupled thioether were observed when combining the catalyst and boronic acid under catalytic conditions. A possible mechanism is shown (Scheme 21). This could be due to the coordination of S and phosphine ligand being labile. This also suggests that the active species are low coordinate $\text{Pd}^{(0)}$ and the reaction conforms to the conventional $\text{Pd}^{(II)}/\text{Pd}^{(0)}$ system. The lower activity could be attributed to a slower induction process or competitive co-ordination of coupled thioether.



Scheme 21. Formation of aryl thioether

Fluorinated boronic acids have proved to be problematic in cross-coupling chemistry under Suzuki conditions. The interest in the Suzuki-Miyaura coupling of these boronic acids exists, in part, because of the difficulty of coupling electron-poor boronic acids. This is thought to be due to the fact that they are less nucleophilic and undergo transmetalation at a slower rate compared to neutral and electron rich nucleophiles. Additionally electron-poor boronic acids are prone to homocoupling⁷¹ and protodeboronation.⁷² Buchwald has observed problems with multi-fluorinated boronic acids.⁶⁰ A particularly challenging example, the coupling of 2,4-difluorophenylboronic acid with 2,6-dimethylbromobenzene, has previously been reported.^{73, 74} This reaction proceeded in 60% isolated yield; however, a reaction temperature of 130 °C and the use of a non-commercially available ligand were required.

Despite the widespread use of boronic acids for Suzuki-Miyaura cross-couplings, and the advantages associated with these reagents, difficulties remain.⁷⁵⁻⁷⁷ Problems include the frequent need for recrystallization of the arylboronic acid prior to use, their tendency to form varying amounts of boroxines, and their propensity to undergo competitive protodeboronation under the reaction conditions used for cross-coupling, as well as problems involving the preparation and application of sterically hindered boronic acids.

The formation of the 2,2'-6,6' substitution pattern (Figure 10) still remains to be challenging with a Suzuki reaction due to the sensitivity toward steric bulk. Buchwald solved this with higher catalyst loading of 4-10 mol% and a special naphthalene based ligand.⁷⁸

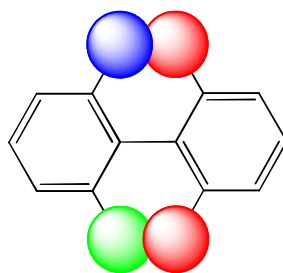
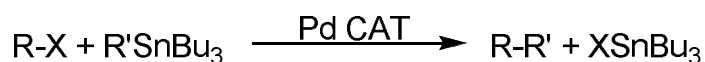


Figure 10. Graphical representation 2,2'-6,6' substitution of a bi-aryl

It seems then, Suzuki-Miyaura cross-coupling chemistry stills proves to be difficult with unactivated aryl chlorides (where higher catalyst loading (1-10 mol%) and elevated temperature (>50 °C) are needed)).

Alkyl and bulky boronic acids require stronger base and/or higher catalyst loading to mediate the reaction (due to a slower rate of transmetalation) and fluorinated boronic acids have been shown to decompose in solution and are unsuitable for cross-coupling chemistry under Suzuki-Miyaura conditions.⁷⁹ These problems need to be addressed due to the demand for fluorinated ring systems for pharmaceuticals and liquid crystal materials. None-the-less Suzuki reactions of aryl chlorides are widespread and couplings of aryl bromides ubiquitous. Overall Suzuki and Negishi can be considered the easiest of coupling reactions. There are numerous examples of Suzuki chemistry and it is widely used within industry.

1.2.2 Stille cross-coupling reaction



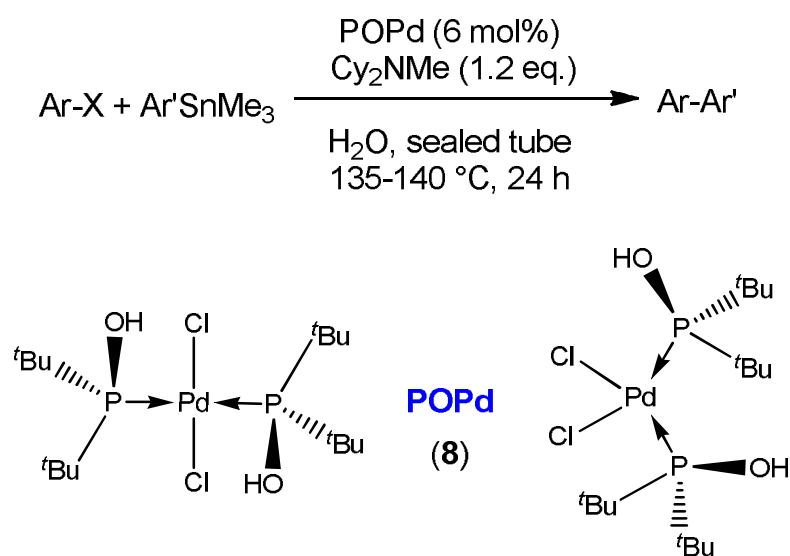
Scheme 22. Stille cross-coupling reaction

An effective protocol determined by Stille *et al.*⁸⁰ for the coupling of aryl halides using organo-tin reagents is the Stille reaction (Scheme 22). This follows the same mechanism as the Suzuki reaction. However, limitations of this reaction also exist. These include the toxic tin by-products generated, which can be harmful to the environment, and the high cost of the nucleophiles required.

An excellent review by Espinet¹³ covers all aspects of the Stille reaction (Sn nucleophiles) from a mechanistic point of view, focusing on the importance of the transmetalation step in the reaction pathway and highlighting the complexity of the Pd⁽⁰⁾ species in solution. It has been found both by Espinet *et al.*^{81, 82} and Amatore and co-workers⁸³ that varying the solvent, reagents or the nature of the Pd catalyst in the Stille reaction complicated the reaction and also the nature of the species involved in the transmetalation step. Its effect on the catalytic cycle has also been evaluated.

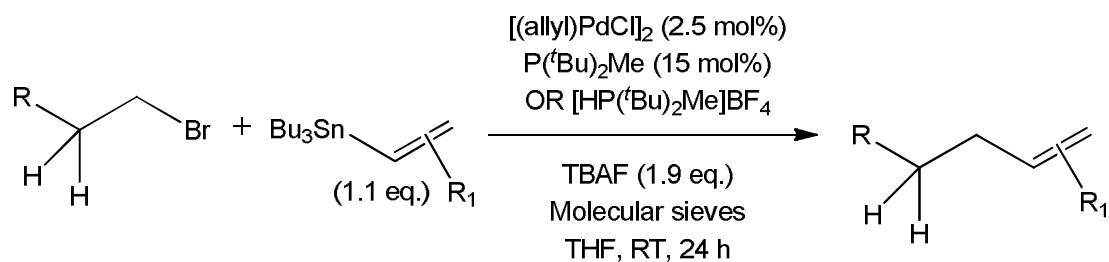
There are examples of various aryl bromides and chlorides utilised in the Stille coupling. Most notably, Wolf and Lerebours⁸⁴ designed a protocol under sealed tube conditions in water (135-140 °C) for 24 h with a loading of 6 mol% [Pd(^tBu₂POH)₂] (POPd) (**8**) with a range of aryl bromides and chlorides (Scheme 23).

Under these conditions, the formation of 3-phenylacetophenone, 2-phenylbenzotrile and 3-phenylpyridine gave higher conversions with the aryl chloride. Functional groups such as ketones and nitriles are tolerated, and organic co-solvents are not required. The air stability and solubility in water of the palladium complexes used in this study allowed simple product isolation and catalyst recyclability. If we compare the POPd system to Suzuki coupling,⁸⁵ much higher catalyst loadings are required and a much higher temperature for a prolonged period of time are required to mediate a Stille reaction.



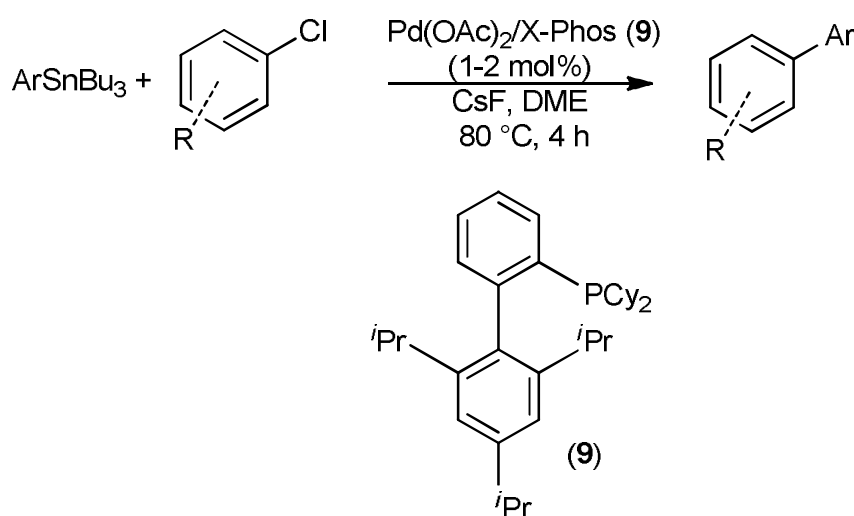
Scheme 23. Stille coupling in water under sealed tube conditions.

Fu *et al.*⁸⁶ has shown that Stille coupling of alkenyl stannanes with alkyl bromides (that possess β -hydrogen atoms) is possible at room temperature, with allyl Pd chloride dimer (APD) (2.5 mol%) in 24h but with high loading of ligand $\text{P}(t\text{-Bu})_2\text{Me}$ (15 mol%) (Scheme 24). Also, it was necessary to add a fluoride salt to promote the reactivity of the stannane. With the diaminophosphane ligand $\text{PCy}(\text{pyrrolidiny})_2$ the reaction can be extended to the coupling of alkyl bromides with aryl stannanes.⁸⁷



Scheme 24. Stille coupling of alkyl bromides with alkenyl stannanes

Buchwald *et al.*⁸⁸ has recently shown that deactivated and unactivated aryl chlorides can be coupled in excellent yields using organostannanes and pre-milled Pd(OAc)₂/X-Phos (**9**) (1 mol%) (Pd/L = 1:1.1) heating to 80 °C for 4 h in DME using CsF as a base (Scheme 25). Examples of fluorinated aryl chlorides have been reported; *o*-chlorobenzotrifluoride/mesitylstannane, (61%), *p*-chlorofluorobenzene/ 2,6-dimethoxyarylstannane (93%) but required slightly higher loading of 2 mol% catalyst. Again, higher catalyst loading of 2 mol% and changing solvent to 1,4-dioxane (to allow a higher reaction temperature of 100 °C) allowed successful coupling of heteroaryl chlorides.



Scheme 25. Stille cross-coupling of deactivated aryl chlorides

Using the Buchwald ligand (**1**) in the Negishi reaction operates at 70 °C for 15 h with aryl chlorides with only 0.05 mol% catalyst. Also Suzuki conditions are typically lower loading (0.5-2 mol%) at RT in some cases with aryl chlorides/bromides. With Buchwald ligand (**5**) 2 mol% catalyst loading at 100 °C for 16h is needed for hindered aryl chloride substrates. This highlights the fact that Stille coupling is inherently more difficult than Negishi and Suzuki coupling reactions.

A remarkable phenomenon in Stille coupling reactions is the effect of the addition of CuI or other Cu^(I) salts, which accelerate couplings catalyzed by [PdL₄]. This so-called “copper effect” was first studied by the research groups of Farina and Liebeskind⁸⁹, they concluded that the role of CuI in systems with “strong” ligands, such as PPh₃, was to scavenge free ligand.

It was also suggested that for “soft ligands” (such as AsPh_3) ligand dissociation from $\text{Pd}^{\text{(II)}}$ is not a problem, and therefore the addition of CuI leads to minimal rate acceleration. Interestingly, Buchwald has observed an inhibitory effect using Cu in the coupling of aryl chlorides and alkynes.⁹⁰

CuI does not promote the dissociation of L from $\text{trans-}[\text{L}_2\text{Pd}(\text{R}^1)\text{I}]$, but it captures part of the neutral ligand L released during the oxidation of $[\text{PdL}_4]$ to $\text{trans-}[\text{L}_2\text{Pd}(\text{R}^1)\text{I}]$, (the species that actually undergoes the transmetalation).

Thus, the effect of CuI is to promote “autoretardation” by free L of the rate-determining associative transmetalation.⁹¹ The effect is strong for PPh_3 and weak for AsPh_3 for two reasons: 1.) The retardation is much more effective for $\text{L}=\text{PPh}_3$ and 2.) CuI is a more effective scavenger of PPh_3 than of AsPh_3 .

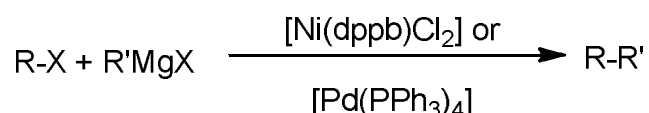
Recent studies on the mechanism of the Stille reaction have shown that each step can be rate determining, depending on the reaction variables. However, it is now better understood how each step can be accelerated. The transmetalation appears particularly complex, as it can operate on several $\text{Pd}^{\text{(II)}}$ species in solution. These species change depending on the solvent, the reagents, and the catalyst involved. The nucleophilicity of the tin reagent can also be influenced by the solvent or by additives.

The use of Pd complexes with sterically demanding ligands as catalysts have overcome problems with electrophiles that were unreactive, such as aryl chlorides, when conventional ligands were used. Some reactions occur with retention of configuration at the carbon atom that is transmetalated and probably proceed by an $\text{S}_{\text{E}}2(\text{cyclic})$ substitution of L for R at the Pd centre.

Other reactions occur with inversion of configuration by an $\text{S}_{\text{E}}2(\text{open})$ mechanism. This behaviour, common to tin and silicon organometallic compounds, strongly suggests that under appropriate conditions similar reaction pathways might be found in reactions involving other organometallic reagents with the less electropositive metals, such as the Suzuki coupling.

If we compare the Stille reaction with the Suzuki reaction; it is more difficult as it requires higher catalyst loading (2-6 mol%), prolonged heating (16-24 h) at higher temperatures (>50 °C) to couple effectively. For example, it even seems that Negishi and Suzuki reactions under comparable conditions with POPd (**8**) are easier than the Stille coupling.

1.1.7 Kumada-Tamao-Corriu cross-coupling reaction



Scheme 26. Kumada-Tamao-Corriu cross coupling reaction

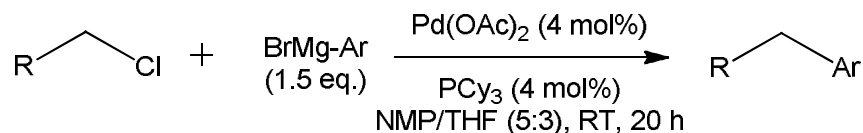
The discovery in 1972⁹² and subsequent systematic investigations⁹³ of the Ni-catalyzed cross-coupling reaction of Grignard reagents by Kumada, Tamao, Corriu and Masse⁹⁴ led to the discovery of magnesium based nucleophiles to cross-couple effectively (Scheme 26). The range of organic compounds that can be readily prepared with Pd catalysts is considerably wider than that with Ni catalysts. For example, alkyne-containing compounds, conjugated dienes, and nitro-substituted arenes are more satisfactorily synthesized by using Pd than Ni. However, Pd should probably be considered first, as it is significantly less toxic than Ni.

The reaction is limited to aryl halides which do not react with organomagnesium species and proves to be sluggish with alkyl magnesium halides. Aryl chlorides require higher catalyst loading and prolonged reaction times to mediate high conversions, highlighting the fact that aryl chlorides still prove to be difficult to cross-couple effectively.

Dppf catalysts have been reported by Hayashi⁴² *et al.* in 1984, coupling primary and secondary alkyl groups with excellent results using [Pd(dppf)Cl₂] (0.01 mol%) with *sec*-butyl magnesium chloride. Successful coupling with bromobenzene (95%, RT, 1 h), β-bromostyrene (97%, 0 °C, 2 h), *p*-bromoanisole (75%, RT, 19h) and *o*-bromotoluene (58%, RT, 19 h) was observed.

Work by Beller *et al.*⁹⁵ showed improved coupling with alkyl chlorides at room temperature (Scheme 27) and in agreement with the results reported by Fu *et al.*⁶⁴ for Suzuki reactions, whereby tricyclohexylphosphine (PCy₃) proved to be the best ligand with Pd(OAc)₂ for the

Grignard coupling of 1-chlorohexane and phenylmagnesium bromide. However, the ligand effect was not pronounced, as Pd/*P*^tBu₃ also gave a significant amount of product.



Scheme 27. Kumada-type coupling of alkyl chlorides with organomagnesium species

Further optimisation of the amount of Grignard reagent by adding 1.5 eq. of NMP (*N*-methylpyrrolidinone) and DMAc (*N,N'*-dimethylacetamide) led to excellent yield (96%) of 1-phenylhexane in the presence of 1.5 equivalents of phenylmagnesium bromide. Apart from the influence of the ligand, the efficiency of the reaction was found to be largely dependent on the solvent as THF, dioxane and DMF gave 1-3% conversion.

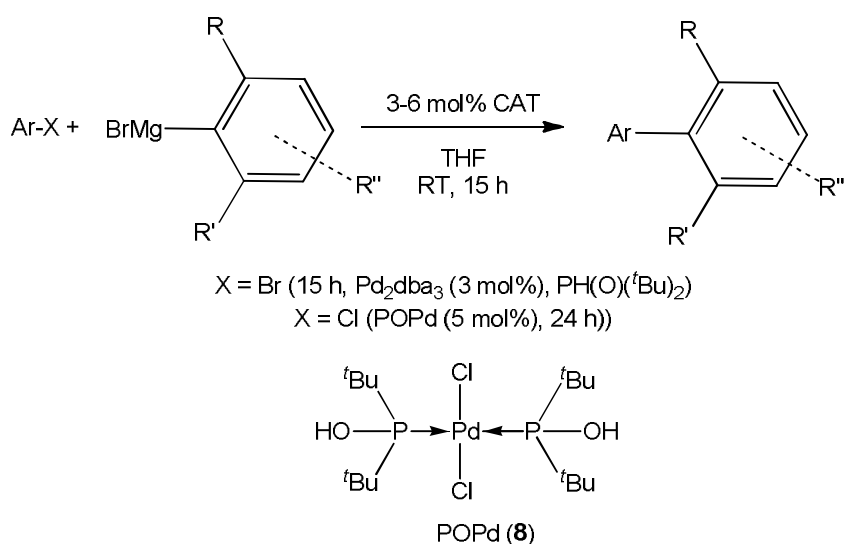
The coupling reactions of 1-chlorohexane and 1-chlorobutane with different tolyl, anisyl, and 4-fluorophenyl Grignard reagents proceeded in good to excellent yields (77-99%). Isobutyl chloride led to a slightly lower yield (72%). Unfortunately, *sec*-butyl chloride and *tert*-butyl chloride did not react under the conditions described, but the method was applicable to functionalized alkyl chlorides.

5-Chloropentanenitrile, methyl 6-chlorohexanoate, and 3-chloropropionaldehyde diethyl acetal gave the corresponding products (99, 58, and 74% respectively). Even coupling reactions with 2-phenylethyl chloride, which is amenable to elimination of HCl to give styrene, proceeded with significant yields (76%, 43% with *p*-fluorophenylmagnesium bromide).

Interestingly, the palladium-catalyzed coupling of organozinc reagents preceded under similar conditions as described for the Kumada coupling. For example, the reaction of 1-chlorohexane with phenylzinc bromide proceeded in the presence of a Pd/PCy₃ catalyst at 60 °C in 41% yield.

Wolf and Xu⁹⁶ have demonstrated that by using phosphinous acids and Pd and POPd, aryl chlorides can be coupled with organomagnesium species at room temperature in 15 h (Scheme 28). More importantly this is the first report of the cross-coupling of *ortho*-substituted aryl chlorides with sterically hindered Grignard reagents.

Heating to 50 °C is necessary when the nickel precatalyst is used, while the palladium-phosphinous acid affords much better results at room temperature. 2-isopropyl-2'-methylbiphenyl (90%), 1-(2-isopropylphenyl)naphthalene (90%), 2-cyclohexyl-2'-isopropylbiphenyl (95%), *N,N*,-2'-trimethylbiphenyl-2-amine (83%).



Scheme 28. Phosphinous acid catalysts for Kumada type coupling reactions

The same yields were obtained by *in situ* formation of the palladium-phosphinous acid from Pd₂(dba)₃ and di-tert-butylphosphine oxide and by direct use of POPd which can be conveniently stored at room temperature and under air. This method provided di- and tri-*ortho*-substituted biaryls in excellent yields even when electron-rich chlorides, which are generally reluctant to oxidative addition under mild conditions, were used.

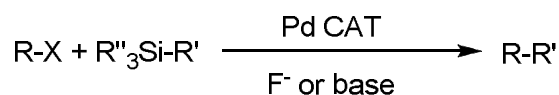
For example, coupling of 1-chloro-2-methoxybenzene, with 2-isopropylphenylmagnesium bromide, or di-*ortho*-substituted aryl Grignards gave biaryls in 89-93% yield. 2-isopropyl-2'-methoxybiphenyl (90%), 2'-methoxy-2,6-dimethylbiphenyl (93%), 1-(2-methoxyphenyl)-2-methylnaphthalene (91%) and 9-(2-methoxyphenyl)anthracene (89%).

However, there are reports where formation of reduced arene and homocoupled side products can complicate these reactions^{92, 97-99} along with a report where improved performance was found in the presence of ZnCl₂.⁹⁹

If we compare the Kumada reaction to Suzuki and Stille we can clearly see that Suzuki requires a lower catalyst loading (0.5-2 mol%) but needs to be heated >50 °C to proceed with aryl chlorides. Stille reactions typically require more than 1 mol% catalyst and require heating. Kumada can work with deactivated and unactivated aryl chlorides 3-6 mol% catalyst (POPd) stirring at RT for 15-20 h. Bulky substrates such as *sec* and *tert* butyl chloride do not react under these conditions. This suggests that under certain conditions, Kumada reactions can be more difficult than Suzuki and easier than Stille reactions.

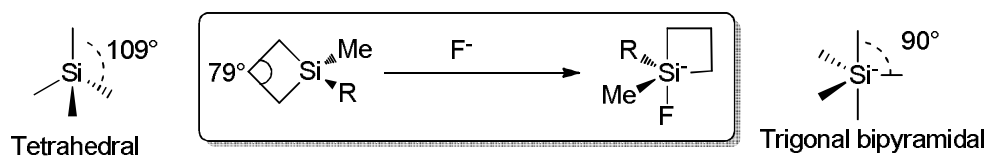
1.2.3 Hiyama cross-coupling reaction

Pioneering work by both Hiyama *et al.*³¹ and Ito *et al.*¹⁰⁰ has shown that organosilanes are also effective in the cross coupling of vinyl or aryl halides/triflates (Scheme 29). Our studies are based around alkenyl trialkoxysilanes.^{33, 101-106} However, the coupling of unactivated aryl bromides and triflates still remains difficult and aryl chlorides still prove to be particularly challenging coupling substrates.



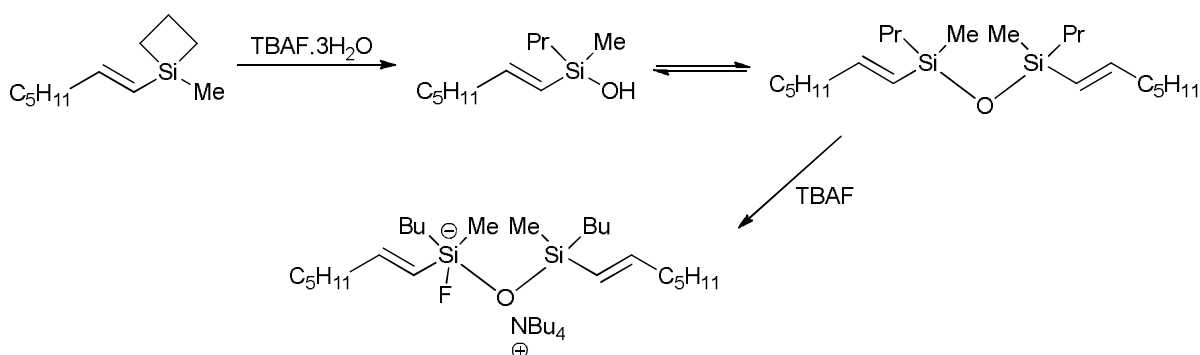
Scheme 29. Hiyama cross-coupling reaction

In addition, high catalyst loading levels are required to increase the activity and some substrates do not react at all. They also observed that the appropriate organosilicon reagent, treated with a source of F⁻ can activate the Hiyama coupling reaction by the formation of a hypervalent anionic silicon intermediate species (Scheme 30). Tetra-*n*-butylammonium fluoride (TBAF) has been found to be one of the most successful fluoride sources for this protocol.^{31,100}



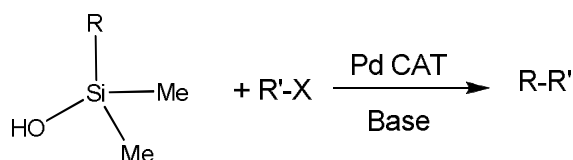
Scheme 32. Activating silacyclobutanes for Hiyama cross-coupling

A careful investigation of the reaction mechanism by Denmark¹⁰⁷ in 2000 revealed that silacyclobutanes undergo rapid ring opening with TBAF·3 H₂O to afford a mixture of silanols and disiloxanes. Transmetalation then occurs from a fluoride-activated disiloxane (Scheme 33).

Scheme 33. Ring opening of silacyclobutanes with TBAF·3H₂O

Both silanols and siloxanes have been synthesized independently and both underwent cross-coupling. These findings paved the way for the use of silanols as cross-coupling partners in the Hiyama-Denmark coupling (Scheme 34).

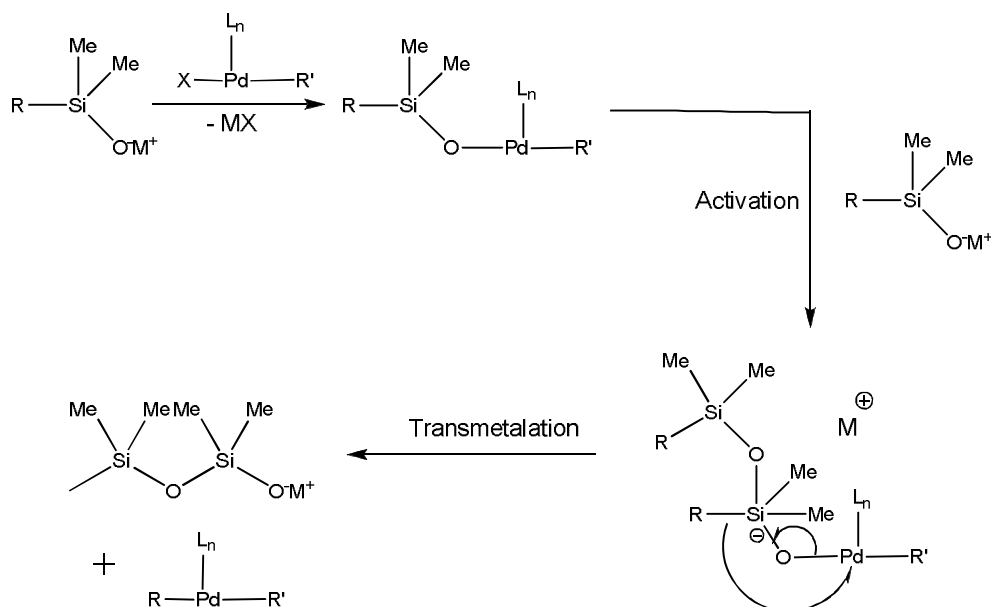
1.2.4 Hiyama-Denmark coupling



Scheme 34. Hiyama-Denmark coupling reaction

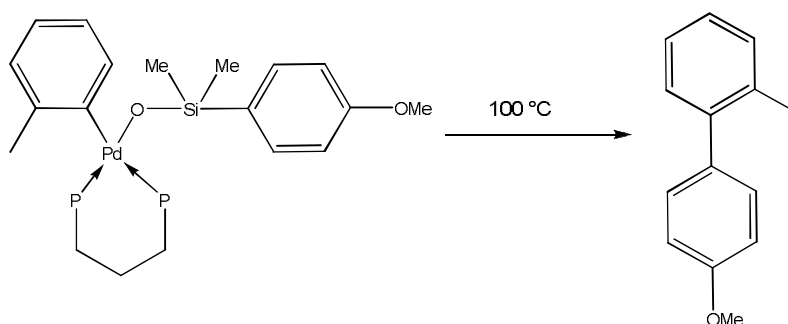
The Hiyama-Denmark Coupling occurs in the presence of a base and strongly depends on the steric and electronic properties of the silicon center, a mechanism for the transmetalation, in which a pentavalent silicon species playing the key role was proposed.

Thus, it was first suggested that the *in situ*-generated silanolate forms an organopalladium complex, which is activated by a second equivalent of the silanolate prior to transmetalation. Later, it has been shown, that the reaction is first-order in silanolate, so the transmetalation proceeds directly from an organopalladium(II) silanolate complex (Scheme 35).^{37, 38, 108}



Scheme 35. Formation of a pentavalent Si species & transmetalation

The new reaction is especially suitable for the conversion of aryl and alkenyl dimethyl silanolates, although aryl dimethyl silanolates react much more slowly than alkenyl derivatives. Further proof was achieved by the isolation and X-ray characterization of a stable palladium silanolate complex of an aryldimethylsilanolate (Scheme 36). Heating to 100 °C provided the biaryl product in quantitative yield in the absence of an activator.



Scheme 36. Formation of biaryl at 100 °C by heating a Pd aryldimethylsilanoate complex

This argued against a requirement for a pentavalent silicon species. In addition, the importance of complexation (Si-O-Pd) for this new transmetalation pathway was shown. Since then, many protocols have been developed that allow the conversion of ester, ketone, and silyl-protected substrates.^{37, 38, 103, 107}

Mild bases such as KOSiMe₃ allow the reversible deprotonation of alkenyl- or alkynyldimethylsilanols. Arylsilanolates need more forcing conditions, for example with Cs₂CO₃ in toluene at 90 °C.¹⁰⁷

Here, the addition of water suppresses homocoupling of the halide. For electron-rich heterocycles, the irreversible deprotonation using NaH for the prior generation of silanolates proved to be a suitable alternative.

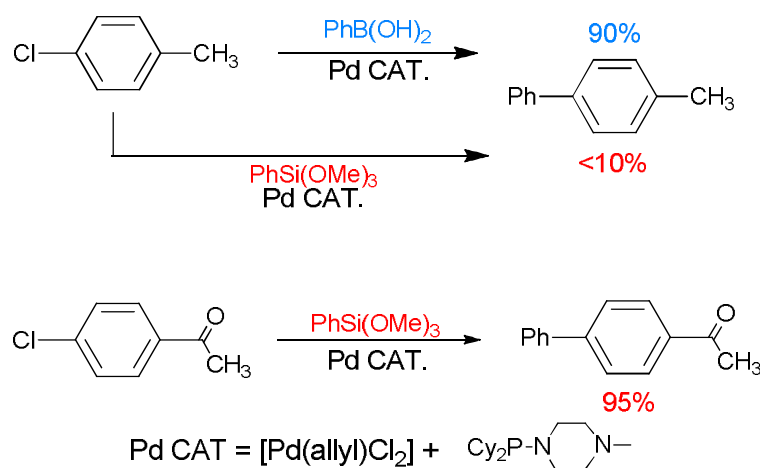
The use of Buchwald ligands, such as (**9**) have been used to mediate the reaction of aryl chlorides with alkenylsilanoates with success.¹⁰³ >90% conversions were observed with a range of aryl chlorides with allyl palladium chloride (APC) at a catalyst loading of (2.5 mol%) and ligand (5 mol%) in THF at 60 °C for 0.5–3 h) with deactivated rings needing longer reaction times. Again the higher catalyst loadings and heating show that Hiyama type reactions are a lot more difficult than Suzuki and Negishi coupling due to the less reactive silicon reagents used.

Organosilicon nucleophiles have the potential to act as highly desirable nucleophilic species in Hiyama cross-coupling reactions as they are stable and easily prepared with low toxicity. However, they remain relatively unexplored due to their lower reactivity in comparison to other nucleophiles, such as organotin reagents used in the Stille⁸⁰ reaction but particularly the organoboron nucleophiles utilised in the Suzuki⁴ reaction.

The main problem with organosilicon nucleophiles is thought to be the slow rate of transmetalation in the cross-coupling catalytic cycle; this is due to the nature of the catalyst commonly used and the interactions between these catalysts and the substrates of the reaction.

It has already been found within the group that under identical conditions, the Hiyama coupling of an unactivated aryl chloride with a methyl group present in the *para*-position with phenyltrimethoxysilane ($\text{PhSi}(\text{OMe})_3$), proves less successful and lower yielding in comparison to the analogous Suzuki coupling reaction (Scheme 37).¹⁰⁹

Mowery, DeShong *et al.*³³ have demonstrated that the incorporation of a more electron-withdrawing COMe group in the *para*-position of the aromatic ring results in the activation of the aryl ring, leading to an increase in the reactivity of the substrate (Scheme 37).



Scheme 37. The nature of the substrate in the cross-coupling reaction

This confirms that electronic properties of the substrate selected in this cross-coupling reaction have a significant effect on the reactivity.

Possible suggestions for this low activity observed using $\text{PhSi}(\text{OMe})_3$ include:

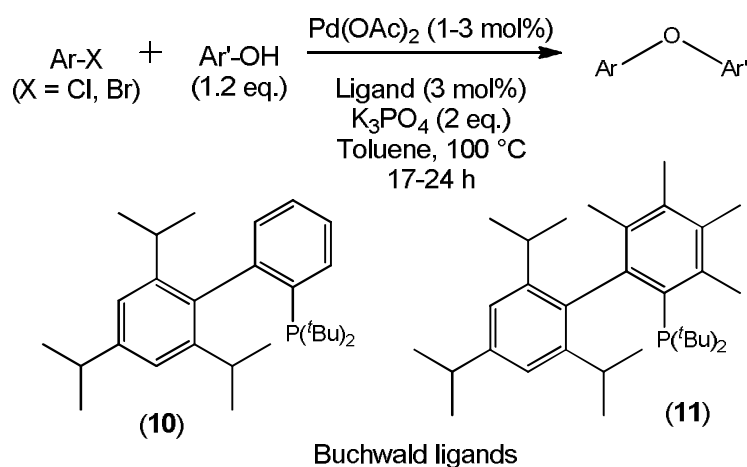
- ✚ Organosilicon compounds could inhibit oxidative addition to the $\text{Pd}^{(0)}$ species.
- ✚ Transmetalation of the organosilicon species could be rate limiting and the aryl substituents of the electrophile and $[\text{Pd}(\text{L-L})(\text{Ar})\text{X}]$ species will have a pronounced effect.

- ✚ Transmetalation and oxidative addition are in equilibrium within the catalytic cycle, and catalyst degradation could occur if either process is slow. This degradation will lead to low productivity of the catalytic cycle.
- ✚ The cross coupling may not proceed *via* commonly accepted routes.

Further investigation is needed to gain a better understanding of the catalytic cycle and the role of the catalyst in the reaction.

1.1 1.2.5 Buchwald-Hartwig aryl ether synthesis

Aryl ethers are a widespread motif in a wide range of natural products, pharmaceuticals, agrochemicals and organic materials, and consequently there has been a considerable amount of research into their synthesis (Scheme 38).¹¹⁰⁻¹¹³ There are limitations in Pd catalysed C-O bond formation however and development of this reaction protocol has been relatively slow compared to C-N bond formation, which has been extensively covered by Hartwig^{45, 114, 115} and co-workers, to whom we owe much of our understanding of Pd catalysed C-X bond formation.

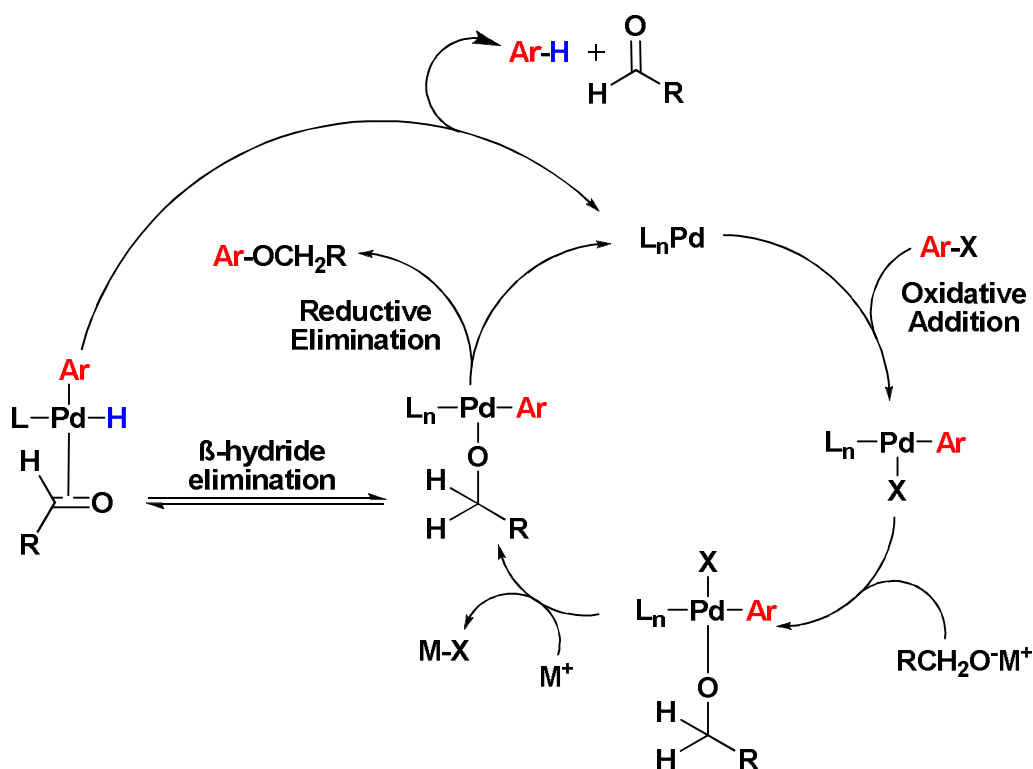


Scheme 38. Buchwald scheme for Pd catalysed C-O bond formation

Nucleophilic aromatic substitution reactions can be a useful procedure for electron deficient aryl chlorides and fluorides under basic conditions. The Cu-promoted Ullman ether synthesis can be a useful method but is limited to certain reactive substrates and only takes place in high boiling polar solvents.¹¹⁶⁻¹¹⁹

Good results have also been readily obtained in the Pd catalysed cross-coupling using tertiary alkoxides as nucleophiles¹²⁰ since Pd-tertiary alkoxides cannot undergo β -hydride elimination during the catalytic cycle. A sustained effort has seen some examples of effective cross-coupling to give aryl-alkyl ethers with specific aryl halide substrates, but no general method has been discovered to date, making this one of the least developed Pd-catalysed cross-coupling reactions. For aryl chlorides and bromides, prolonged heating times of up to 24 h are required at 1-10 mol% catalyst loading, after which time the catalyst is more likely to decompose.

Iron catalysed ether synthesis using aryl iodides is an important recent discovery, but needs significant further research to extend the reaction to aryl bromides and chlorides under mild conditions.^{119, 121, 122} According to Buchwald¹¹⁶, “Using Pd based catalysts the low yields observed in the coupling of certain substrates is due to the slow rate of reductive elimination relative to β -hydride elimination.” Using alkoxides as nucleophiles, bulky substituents promote reductive elimination and give improved yields of product. The reduced arene produced could be due to the basic reaction conditions and accelerated β -hydride elimination (Scheme 39).



Scheme 39. Buchwald-Hartwig mechanism for aryl ether synthesis

Pd catalysed C-O bond formation has been extensively studied and mechanistic work has been carried out by Buchwald¹²³⁻¹²⁸ and rapid C-O reductive elimination of aryl ethers was observed with aryl alkoxo complexes.¹²⁸ Hillhouse and co-workers¹²⁹ reported the selectivity for reductive elimination over β -hydride elimination from Ni alkoxo complexes highlighting the complexity of this reaction protocol.

Again, the higher catalyst loading (1-3 mol%) and prolonged heating time of 16-24 h at 100 °C highlight the difficulty in aryl ether synthesis, compared to the Suzuki (RT, 2 h, 0.5 mol% Pd) and Negishi (RT, 15 h, 0.05 mol% Pd) reactions using Buchwald ligand or POPd cross-coupling procedures. Even Stille and Hiyama reactions can perform better than aryl ether synthesis under optimised conditions. They are however still much more difficult than Suzuki and Negishi reactions.

It seems then in any cross-coupling protocol, aryl/alkyl chlorides require prolonged heating at higher catalyst loading due to their slower oxidative addition compared to aryl/alkyl bromides and iodides.

The rate determining step can change according to the nucleophiles involved and depicts whether oxidative addition (for chlorides), transmetalation (for weak nucleophiles) or reductive elimination (for bulky substrates or ligand system) are accelerated. The reaction also seems to depend on the catalyst, solvent choice and base in each case. Cross-coupling is therefore not straight forward and requires careful thought and optimisation.

The reactivity of the nucleophile plays a crucial role in the catalytic pathway. In the Negishi reaction (organozinc nucleophile), Suzuki reaction (boronic acid nucleophile), Kumada (Grignard) type (organomagnesium nucleophile). Hiyama (organosilicon nucleophile) reactions and C-O bond formation, the order of reactivity (nucleophilicity) in general is as follows: Negishi>Suzuki>Grignard>>Stille>Hiyama>C-O bond formation although the reasons for this may be connected to more factors than just nucleophilic strength.

Project Aims

From the preceding review, it can be seen that Pd catalysed Hiyama, C-O bond formation and Kumada coupling can be more problematic than Suzuki reactions. There is also not enough information that directly compares the performance of various types of nucleophiles in cross-coupling, or in the isolated transmetalation reaction.

This project will also investigate how the rate of transmetalation correlates with a ligands ability to promote Pd catalysed cross-coupling of weak/problematic nucleophiles. We will attempt to find the ligands with the optimum balance for promoting transmetalation, oxidative addition and reductive elimination. Given that steric bulk is desirable for the oxidative addition and transmetalation steps.^{13, 37, 38} A key aspect will be the investigation of non C₂-symmetric ligand system, which constitutes of sterically dissimilar phosphine substituents. It is hoped that this will give us the most efficient catalysts for the cross-coupling of weak/problematic nucleophiles. The project also investigates the use of “green” solvent methyl-THF to carry out cross-coupling of Grignard reagents at high concentration.

One aim of our study on the cross-coupling of organosilicon nucleophiles was to compare the different activators, and this study led us to the unexpected finding of C-O bond formation from alkoxy silanes.

Chapter 2. Grignard cross-coupling & the reactivity of Pd & Pt complexes of dtbdppf

In the last 15 years, there have been a significant number of catalytic processes that have become possible by utilising bulky diphosphines as ligands. This is especially true in cross-coupling chemistry where a plethora of Pd catalysed C-C and C-heteroatom bond forming reactions utilise bulky monodentate,^{57, 58} bidentate⁵⁶ and hemi-labile phosphines⁶⁰⁻⁶³ as ligands. Pronounced steric bulk is a desirable feature for the oxidative addition step in cross-coupling, since it destabilises $[M(P-P)_2]$ species for diphosphine ligands. Steric bulk can also destabilise $[M(P-P)Ar^1Ar^2]$ species with respect to reductive elimination. However, steric bulk is bad for the transmetalation step in cross coupling. In order to identify ligands for cross-coupling of weaker or problematic nucleophiles, a perfect balance of all three steps is required.

We were intrigued by the possibility that 1-*di-tert*butyl-1'-diphenylphosphinoferrocene (dtbdppf) might find this balance. Remarkably despite being commercially available, its organometallic chemistry is relatively unexplored^{56, 130-135}. Since interest was to investigate problematic nucleophiles in cross-coupling catalysis we turned our attention to Grignard cross-coupling (Kumada type reactions).^{92, 97-99} This reaction can suffer from poor functional group tolerance and greater side products relative to Negishi and Suzuki coupling.

2.1 The effect of ferrocenyl phosphine ligands in cross-coupling reactions

Palladium complexes of phosphino ferrocenes (**12**) (Figure 11) have been shown to have a significant activity in the Suzuki coupling reaction by Colacot and Shea.^{56, 136}

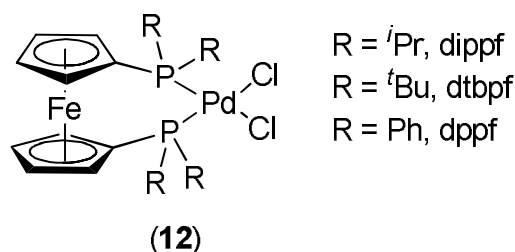


Figure 11. Pd(phosphinoferrocene)Cl₂ complexes

A trend in reactivity of $[\text{Pd}(\text{dppf})\text{Cl}_2] < [\text{Pd}(\text{dippf})\text{Cl}_2] < [\text{Pd}(\text{dtbpf})\text{Cl}_2]$ was noted, which could be attributed to the increase of steric bulk, and electron density, giving optimum rates of oxidative addition and reductive elimination.

It was also found that the $[\text{Pd}(\text{dtbpf})\text{Cl}_2]$ system was the most active catalyst for unactivated and sterically demanding aryl chlorides even at low catalyst loadings. However, this catalyst system has not been tested in the cross-coupling of weaker nucleophiles or in the coupling of nucleophiles that are sometimes problematic. Dppf is renowned for Pd catalysed Kumada and Negishi coupling. For example, $[\text{Pd}(\text{dppf})\text{Cl}_2]$ is highly effective in catalysing the reaction of *n*-butylmagnesium chloride and *n*-butylzinc chloride with organic bromides and *sec*-butylmagnesium chloride with bromobenzene, (*E*)-*p*-bromostyrene, *p*-bromoanisole, and *o*-bromotoluene to give the corresponding cross-coupling products in high yields.⁴²

In order to assess how different nucleophiles behave with this set of ferrocenylphosphino catalysts, we evaluated the cross-coupling of Grignard reagents partly as a comparison to the weaker silicon based nucleophiles discussed later on, but also because despite Grignard reagents being powerful nucleophiles, they can cause a number of side reactions that could be alleviated by the correct choice of catalyst. Special care needs to be taken to prevent metal halide exchange, elimination reactions and homo-coupling.

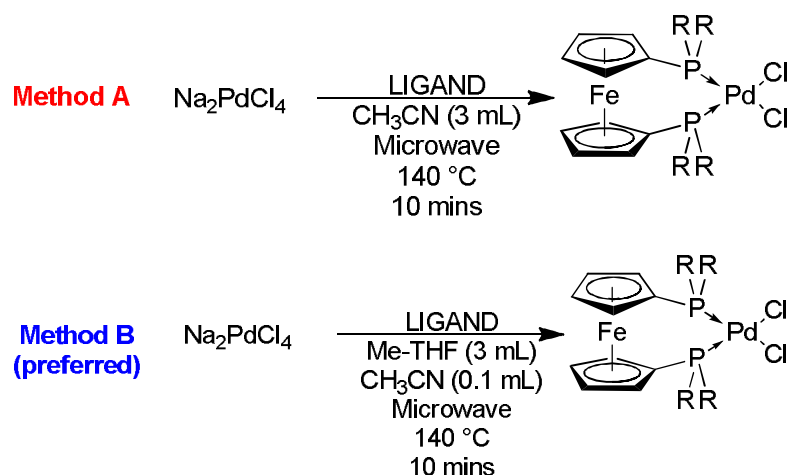
Usually, slow addition of the Grignard reagent facilitates the reaction and prevents side reactions. If oxidative addition is the slowest step in the reaction, the amount of aryl halide should be maximised; whereas if the metalation at Pd (replacing the halide for the aryl group) is fast, the concentration of the Grignard should be kept low.⁹ We were intrigued to investigate Grignard cross-coupling using minimal amounts of solvent in an effort to create a more efficient Pd catalysed transformation of bi-aryls.

Me-THF could be deemed as a "green" solvent as it originates from renewable sources. Me-THF also has less affinity for water than THF; this aids separation as it is completely immiscible. Thus, it is possible to work up reactions without adding any additional volatile organic solvents. Grignard solubility is also an advantage as we achieved 5M concentration in these studies and it seems Me-THF can dissolve magnesium salts such as MgBr_2 (which create emulsions and hinder organic work up) creating a more effective protocol.

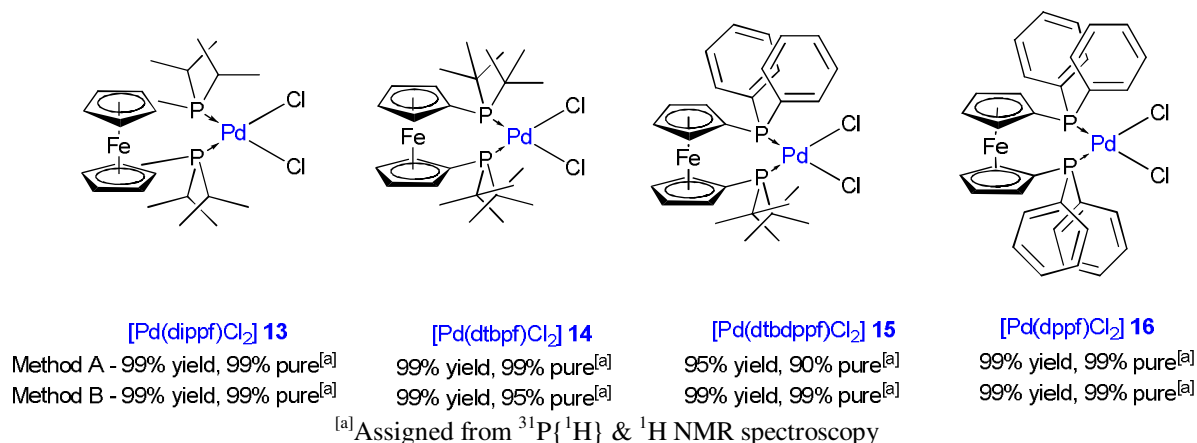
Although complexes of the form **12** can be prepared by reacting the ligands with [Pd(PhCN)₂Cl₂] or [Pd(COD)Cl₂] at room temperature overnight, a more efficient and convenient procedure that saves on reagent solvent was developed. The “phosphinoferrocene” ligands were combined with a stoichiometric amount of Na₂PdCl₄ in acetonitrile at 120 °C under microwave heating for 5 minutes (Method A, Scheme 41).

The pure complexes **13-16** could be isolated after work up from addition of H₂O, extraction and drying over MgSO₄ in quantitative yields (Scheme 41, Figure 12) and were used with success in subsequent cross-coupling reactions.

The synthesis of the Pd complexes of the unsymmetrical ligand was less successful in that a minor impurity (~10%) was formed in the crude product (a mono-oxide species running at $\delta_P = 51$ ppm), however, this could be removed by simply washing away with dry degassed hexanes or by filtration through an alumina plug. This method was further refined by changing MeCN from a solvent into a reagent and using the “green” solvent Me-THF (Method B). In this case, pure solids precipitated from the reaction mixture on cooling and the complexes were obtained after filtration, washing with water and drying. The Pd complexes synthesised remained air stable for 12-18 months stored in a vial under air, after this time oxidation products (mono-oxide $\delta_P = 51$ ppm and di-oxide $\delta_P = 82$ ppm) were observed by ³¹P NMR spectroscopy.

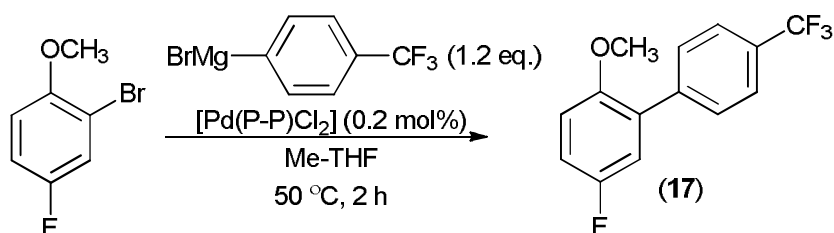


Scheme 41. Preparation of (bis-phosphinoferrocenyl)PdCl₂ complexes

Figure 12. Examples of (bis-phosphinoferrocenyl)PdCl₂ complexes

2.2 “Super-concentrated” 5M Kumada type Grignard cross-coupling reactions

Kumada-type coupling reactions were performed with a super-concentrated (5M) solution of fluorinated Grignard reagent in Me-THF at low catalyst loading of 0.2 mol% [Pd(P-P)Cl₂]¹³⁷. Such high concentration of Grignard reagent was employed in a bid to create an industrially viable process where no additional solvent is required during the course of the reaction. The use of Me-THF also allows for a simplified work up that reduces solvent use. In order for this sustainable solvent to see widespread industrial use, it needs to be both environmentally and economically attractive. A fluorinated aryl-halide was used to allow ¹⁹F NMR as a handle to identify the product (**17**) from the reaction (Scheme 42).

Scheme 42. Super concentrated Kumada type reaction (F₃CArMgBr, 5M)

The formation of the 5M Grignard reagent needed careful optimisation to avoid a large exotherm (as some fluorinated Grignard's can be potentially explosive) being produced and the material being unstable under vacuum and above 50 °C. No activator (iodine crystal, or DME) was needed to initiate the reaction; the aryl bromide was sufficiently activated to promote the Grignard formation.

To prevent homocoupling from excess aryl bromide, heating the Grignard solution (after activation) to 50 °C for 2 h ensured all of the Mg was consumed. (This was checked by working up a small aliquot of the Grignard reagent and hydrolysing with ice cold aqueous NH₄Cl to form benzotrifluoride. This could be confirmed by a single peak in the ¹⁹F NMR spectra (4-bromobenzotrifluoride δ_F = -63.251, benzotrifluoride δ_F = -63.348, Grignard reagent δ_F = -63.079 ppm)). This Grignard reagent starts to hydrolyse even by storage under Argon after a prolonged period of time and gave poor conversions in cross-coupling runs if not used within 24 hours.

Transfer of the super-concentrated Grignard reagent was facilitated by preheating the solution to 50 °C and warming up a glass syringe and stainless steel needle for transfer. A range of bidentate diphosphine ligands were screened for activity (Table 6) with dppp giving 56% (by ¹⁹F NMR) (Entry 2), dtbdppf (**15**) 67% and dppf (**16**) 66% bi-aryl product 5-fluoro-2-methoxy-4'-(trifluoromethyl)biphenyl (**17**) respectively. Two monodentate ligands were also screened (PPh₃ and Me-Cage, entries 9 & 10) giving low conversion suggesting that an electron rich bidentate ligand is needed to facilitate this reaction. The remaining ligands performed poorly with conversions <40%.

Entry	Catalyst	% Product ¹⁹F NMR (¹H NMR)^[a]
1	[Pd(dppe)Cl ₂]	25 (18)
2	[Pd(dppp)Cl ₂]	56 (50)
3	[Pd(dppb)Cl ₂]	21 (12)
4	[Pd(dippf)Cl ₂]	4 (5)
5	[Pd(dtbpf)Cl ₂]	2 (1)
6	[Pd(dtbdppf)Cl ₂]	67 (66)
7	[Pd(dppf)Cl ₂]	66 (67)
8	[Pd(<i>bis</i> -BFP)Cl ₂]	36 (29)
9	[Pd(Me-Cage) ₂ Cl ₂]	11 (7)
10	[Pd(PPh ₃) ₂ Cl ₂]	21 (16)

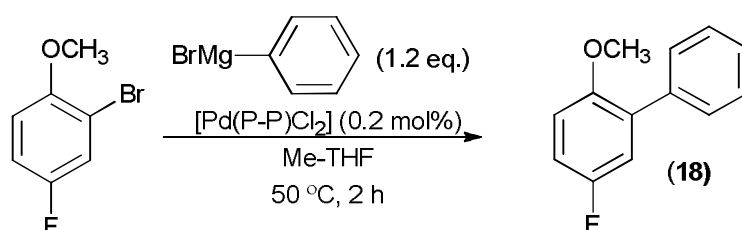
Reagents & Conditions: 2-bromo-4-fluoroanisole: 1 mmol; Grignard solution: 1.2 mmol in Me-THF; Pd catalyst 0.2 mol%; 50 °C, 2 h
^[a]Calculated by ¹H NMR spectra calibrated with internal standard 1-methyl-naphthalene, remaining is SM confirmed by GCMS (uncalibrated).

Table 6. Ligand screen for 5M Kumada coupling

This reaction was scaled up to 4 mmol with an even lower catalyst loading of 0.05 mol% [Pd(dppf)Cl₂] (**16**) with no additional solvent added. The reaction proved to be sluggish,

returning 34% conversion after 24 h and only 37% conversion after 48 h. This is not surprising as most Pd catalysts are deactivated after prolonged heating times and 0.05 mol% must be too low a catalyst loading to enable reasonable catalyst turnover under these conditions.

Kumada-type coupling reactions were also performed with 2-bromo-4-fluoroanisole and a super-concentrated solution of PhMgBr (5M) Grignard reagent in Me-THF at low catalyst loading of 0.2 mol% [Pd(P-P)Cl₂]. The product (**18**) was identified by ¹H, ¹⁹F NMR and GCMS (Scheme 43).



Scheme 43. Kumada type-reaction (PhMgBr, 5M) with 2-bromo-4-fluoroanisole

The formation of the super-concentrated Grignard also needed optimisation. The reaction needed an iodine crystal to initiate and heating to 90 °C for 4 h after activation, to ensure all of the Mg was consumed to prevent homo-coupling of 2-bromo-4-fluoroanisole during catalysis. A range of phosphine ligands were screened giving good results (Table 7) with [Pd(dppf)Cl₂] (**16**) giving 76% conversion (**18**) by ¹⁹F NMR with only 5% homo-coupled product after 2 hours at 50 °C.

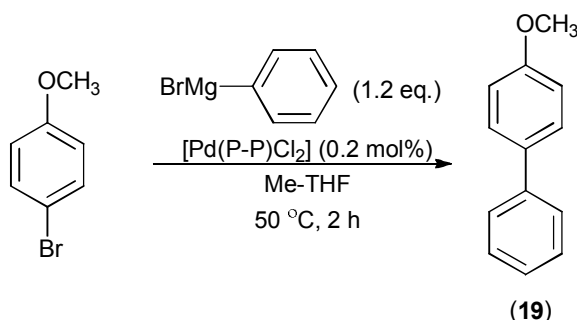
Catalyst	% SM ¹⁹ F { ¹ H} NMR	% Homocoupled ¹⁹ F { ¹ H} NMR	% Product ¹⁹ F { ¹ H} NMR ^[a]
[Pd(dippf)Cl ₂]	60	20	20
[Pd(dtbpf)Cl ₂]	56	14	30
[Pd(dtbdppf)Cl ₂]	28	16	56
[Pd(dppf)Cl ₂]	19	5	76
[Pd(dppf)Cl ₂] ^[b]	92	1	7
[Pd(dppb)Cl ₂]	19	6	75
[Pd(dppe)Cl ₂]	21	8	71
[Pd(dppp)Cl ₂]	1	3	96

Reagents & Conditions: 2-bromo-4-fluoroanisole (1 mmol); Grignard solution (1.2 mmol in Me-THF); Pd catalyst (0.2 mol%); 50 °C, 2 h.^[a] Conversion determined by ¹⁹F {¹H} NMR - Reactions 1-4 were also calculated by ¹H NMR spectra calibrated with internal standard: 1-methyl-naphthalene giving good agreement with ¹⁹F NMR values, identity of products confirmed by GCMS (uncalibrated)^[b] 2 eq. PhMgBr.

Table 7. Kumada type cross-coupling of PhMgBr

In this reaction [Pd(dppp)Cl₂] really stood out giving 96% conversion to product after work up (filtering through MgSO₄ to dry and a further 0.5 mL of Me-THF was added). Although this material could be sufficiently pure for further applications, column chromatography (Petroleum ether 40-60°) delivered the product in 88% isolated yield. Also interestingly [Pd(dppf)Cl₂] with 2 eq. of Grignard gave only 7% product, a considerable amount of dimerized Grignard was observed in the GCMS suggesting more Grignard is problematic under these conditions. This procedure uses less than 1mL Me-THF (per mmol reagent) in total and to the best of our knowledge has not been reported before. Pd cross-coupling reactions, typically Kumada coupling uses over 30 mLs of THF and Et₂O per mmol reaction⁹⁸.

Other substrates that were less activated toward oxidative addition were used to assess the reaction scope, *p*-bromoanisole (Scheme 44) performed reasonably well giving 67% of the desired bi-aryl moiety (**19**) with dppf (**13**) and similar conversion with dtbdppf (**15**) (Table 8) within 2h.



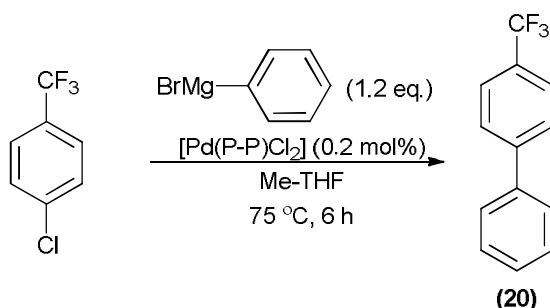
Scheme 44. Super concentrated Kumada reaction (*PhMgBr*, 5M) with 4-bromoanisole

Catalyst	% SM (¹H NMR)	% Product (¹H NMR^[a])
[Pd(dppf)Cl ₂]	33	67
[Pd(dtbpf)Cl ₂]	76	24
[Pd(dtbdppf)Cl ₂]	40	60 ^[b]
[Pd(dppp)Cl ₂]	54	46
[Pd(dppp)Cl ₂]	78	22

Reagents & Conditions: 4-bromoanisole (1 mmol); Grignard solution (1.2 mmol in Me-THF); Pd catalyst (0.2 mol%); 50 °C, 2 h.^[a] Calculated by ¹H NMR spectra calibrated with internal standard: 1-methyl-naphthalene, identity of products confirmed by GCMS (uncalibrated)^[b] Separate reaction run for 6 h at 55 °C, 57% product.

Table 8. Kumada type cross-coupling of *PhMgBr* (5M) with 4-bromoanisole

Excellent results were obtained with an activated aryl chloride *p*-chlorobenzotrifluoride (Scheme 45) which performed well with a prolonged heating time of 6 h at an elevated temperature of 75 °C with [Pd(dppf)Cl₂] (**16**) giving 95% conversion (**20**) (Table 9).



Scheme 45. Super concentrated Kumada reaction (PhMgBr, 5M) with 4-chlorobenzotrifluoride

Catalyst	% SM (¹⁹ F NMR)		% Product (¹⁹ F NMR ^[a])	
	6h	16h	6h	16h
[Pd(dippf)Cl ₂]	15 ^[b]	19	80	82
[Pd(dtbpf)Cl ₂]	74 ^[b]	62	13	37
[Pd(dtbdppf)Cl ₂]	25	10	75	90
[Pd(dppf)Cl ₂]	7	5	93	95

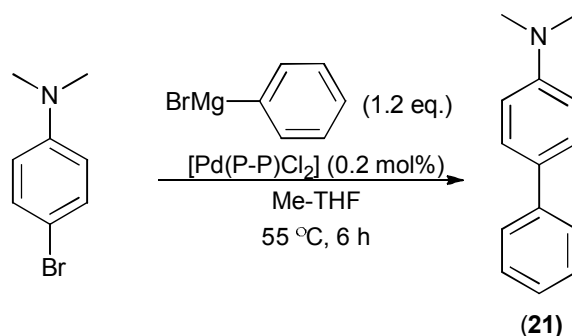
Reagents & Conditions: *p*-chlorobenzotrifluoride (1 mmol); Grignard solution (1.2 mmol in Me-THF, 5M); Pd catalyst (0.2 mol%); 50 °C, 2 h.^[a] Identity of products confirmed by GCMS (uncalibrated)
^[b] Remaining is bis-aryl moiety from homocoupled Grignard reagent.

Table 9. Kumada type cross-coupling of PhMgBr (5M) with 4-chlorobenzotrifluoride

Adding ZnCl₂ (anhydrous) as a promoter to generate a more powerful nucleophile had a detrimental effect on the conversion with dtbpf (**14**) and dtbdppf (**15**) giving 95% SM (5% Product) and 81% SM (19% Product) after 6 h and a slight increase after 16 h. It was hoped that this would accelerate the transmetalation step and facilitate the reaction further, since the work of Farrell and Miller and their use of catalytic ZnCl₂ suggested this.⁹⁹ However our unusual reaction conditions may be the cause of this.

Good results were obtained with a deactivated aryl bromide (*p*-bromo-*N,N'*-dimethylaniline) (Scheme 46) giving 63% conversion to (**21**) with dppf (**16**) and 61% conversion (**21**) with dppp under prolonged heating for 6 h (Table 10). Again the other ferrocenyl based catalysts delivering poorer conversions. It seems an electron-rich bidentate ligand is they key in this cross-coupling process.

Given that, we have demonstrated that these reactions can proceed at very high concentration and with minimal solvent during work-up. It is hoped that academic and industrial researchers will now consider this solvent a more viable proposition; Me-THF has been used within industry but is not widely known.



Scheme 46. Super concentrated Kumada reaction ($PhMgBr$, 5M) with 4-bromo- N,N' -dimethylaniline

Catalyst	% SM (1H NMR)	% Product (1H NMR ^[a])
[Pd(dippf)Cl ₂]	49	51
[Pd(dtbpf)Cl ₂]	59	41
[Pd(dtbdppf)Cl ₂]	77	23
[Pd(dppf)Cl ₂]	37	63
[Pd(dppp)Cl ₂]	39	61

Reagents & Conditions: 4-bromo- N,N' -dimethylaniline (1 mmol); Grignard solution (1.2 mmol in Me-THF); Pd catalyst (0.2 mol%); 50 °C, 6 h.^[a] Calculated by 1H NMR spectra calibrated with internal standard: 1-methyl-naphthalene, identity of products confirmed by GCMS (uncalibrated)

Table 10. Kumada type cross-coupling of $PhMgBr$ (5M) with 4-bromo- N,N' -dimethylaniline

The choice of aryl halide is therefore of importance and has a noticeable effect on a suitable catalyst in each case. With dppp, dippf (**13**), dtbdppf (**15**) and dppf (**16**) all performing well depending on the substrate. Dtbpf (**14**) seems to be too bulky and delivers poor conversion in these reactions even though it has been shown to be an excellent catalyst for Suzuki coupling of aryl bromides and deactivated aryl chlorides where dppf fails.

Given that Suzuki infers activation toward oxidative addition, and that dtbpf has been shown to accelerate reductive elimination (100 times faster than dppf)⁴⁵ it is possible that transmetalation is inefficient. Previous work has shown transmetalation to be sensitive to

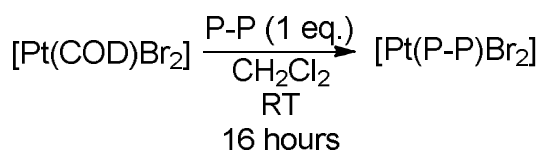
steric effects.³⁵ The non-symmetric dtbdppf however, is worthy of further investigation as it has delivered good conversion with substrate/catalyst ratio of 500/1 at 50-75 °C in 2-6 h.

2.3 Transmetalation studies with Pt complexes

As one might expect, bulky ligands can retard the transmetalation step in cross-coupling catalysis. Indeed, Clarke *et al.* have recently reported that platinum complexes of bulky diphosphines do not undergo reaction with PhZnBr at all, under conditions where simple diphosphines readily react³⁵. In order to shed light on the differences between the four ferrocenyl ligands, transmetalation studies were undertaken with ferrocenylphosphino Pt complexes.

As Pt complexes are more stable than their analogous Pd counterparts (which rapidly reductively eliminate and generate Pd⁰), studies on these complexes can look at the transmetalation step in isolation. In addition, we would learn about the co-ordination chemistry of these ligands. Our target precursors for this study were [Pt(P-P)Br₂] complexes (**22-25**) (Scheme 47, Figure 13).

2.4 Synthesis of [Pt(P-P)Br₂] from [Pt(COD)Br₂]



Scheme 47. Synthesis of [Pt(P-P)Br₂]

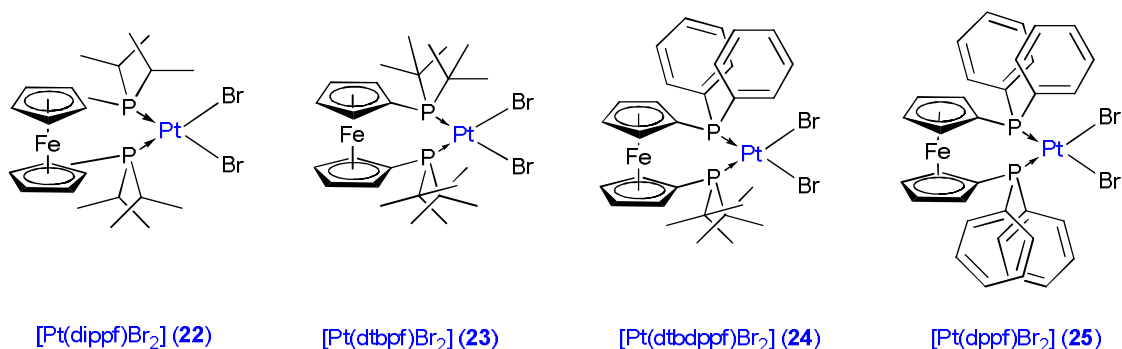
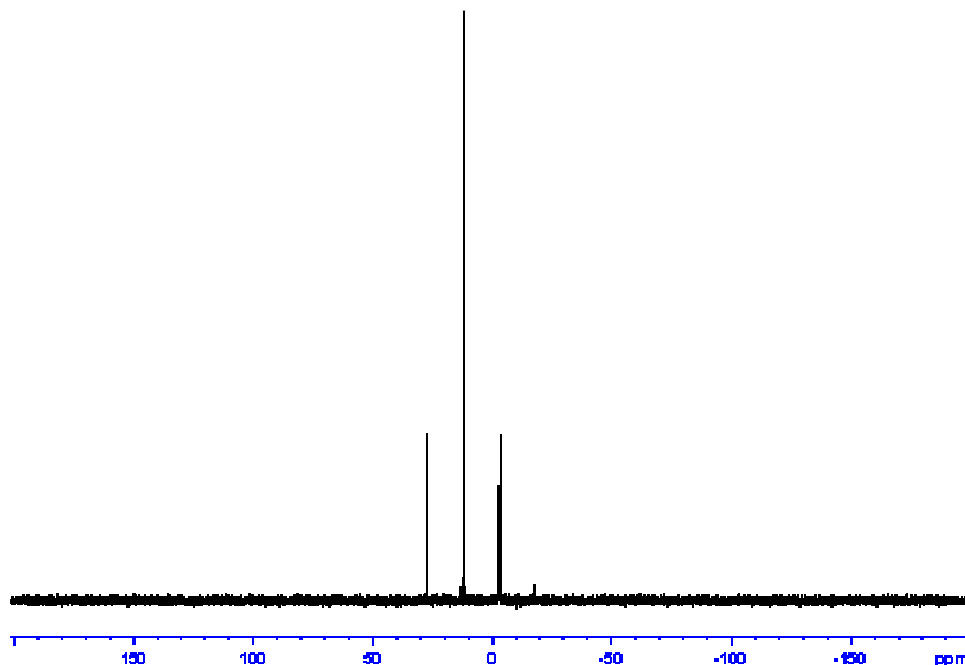


Figure 13. [Pt(P-P)Br₂] target complexes

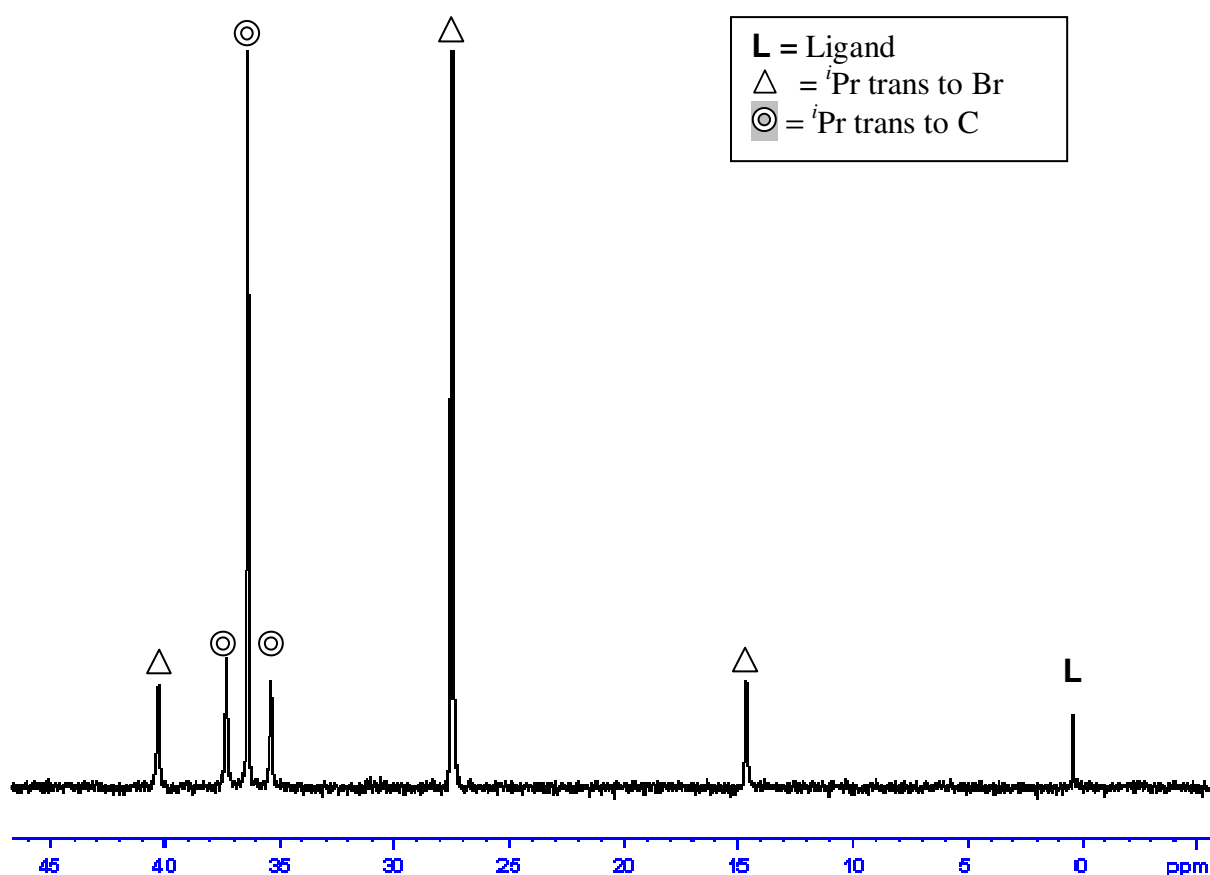
Displacement of COD by the diphosphine ligand after stirring in dry degassed DCM overnight at room temperature provided the desired [Pt(dtbdppf)Br₂] (**24**) and [Pt(dppf)Br₂] (**25**) (Spectra 1).



*Spectra 1. [Pt(dppf)Br₂] (**25**), ³¹P{¹H} NMR showed the desired Pt satellites with trans coupling indicative of a dibromide complex (¹J_{P-Pt} = 3500 – 4500 Hz).*

However, with the bulkier ligands dippf and dtbpf, a novel pincer complex was formed. Instead of P-Pt we observed P-C-Pt bond formation where the COD has inserted, confirmed by ¹H, ³¹P, ¹³C NMR spectroscopy and FAB-MS. The ³¹P{¹H} NMR spectra of [Pt(dippf)(COD)Br]Br⁻ (**26**) is shown below. Instead of the expected ¹J_{P-Pt} coupling of 3500-4500 Hz, the signal at δ_P = 36.35 ppm shows a coupling more typical of a ²J_{P-Pt} coupling of 313 Hz. This indicates a Pt-C-P bond not a Pt-P bond (Spectra 2).

During the reactions, there was little residue of COD left as there was no distinctive smell. In the ¹H NMR alkenyl peaks for the COD were observed ((δ_H = 0.9 (CH₃), 1.2-1.3 (CH₂), 5.40 (Pt-CH)), which integrated correctly and two C resonances in the ¹³C NMR (δ_C = 128.7, 130.9 (CH-PtBr) and the alkenyl signals lead us to believe a COD pincer complex had been formed. This was confirmed by FAB-MS giving an isotope match for the Pt complex (e/z (EI) [M⁺] = 801.14)).



Spectra 2. $^{31}\text{P}\{^1\text{H}\}$ NMR Spectra of $[\text{Pt}(\text{COD})(\text{dippf})\text{Br}]\text{Br}^-$ (**26**)

The dippf analogue was recrystallized to give crystals suitable for XRD which were not perfect (due to disordered CH_2Cl_2 adducts and one of the Cp rings not defined perfectly) but gave data, consistent with the structures assigned by NMR and MS spectroscopy and confirmed the identity of the pincer complex (Figure 14).

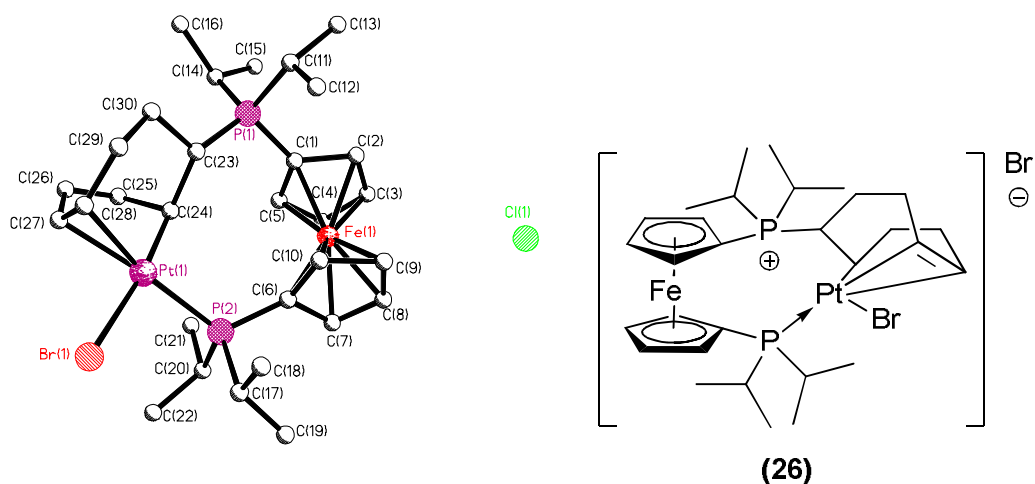
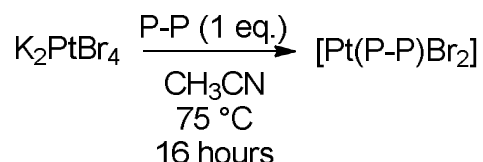


Figure 14. X-Ray Structure and graphical representation of $[\text{Pt}(\text{COD})(\text{dippf})\text{Br}]\text{Br}^-$ (**26**)

Due to the COD inserting into the P-Pt bond, the geometry is distorted from square planar P-Pt-Br = 93.10(18)° and the bond lengths are distorted by being lengthened ((**26**) Pt-Br = 2.547(3) Å) compared to [Pt(dippf)Cl₂] (2.355 Å) and (**26**) Pt-P = 2.284(8) Å) compared to P-Pt in [Pt(dippf)Cl₂] (2.267 Å).¹³² The data was not of sufficient quality to make any more detailed structural observations. The dtbpf analogue (**27**) was recrystallized to give poor quality crystals suitable for XRD and did not return good quality data, so no detailed structural information could be obtained. However the data was completely consistent with the structures assigned by NMR and MS spectroscopy. ³¹P NMR spectroscopy also confirmed the analogous chloride complexes from [Pt(COD)Cl₂]. This suggests that dtbdppf has a different mode of action as it can be synthesised from COD precursors or K₂PtCl₄.

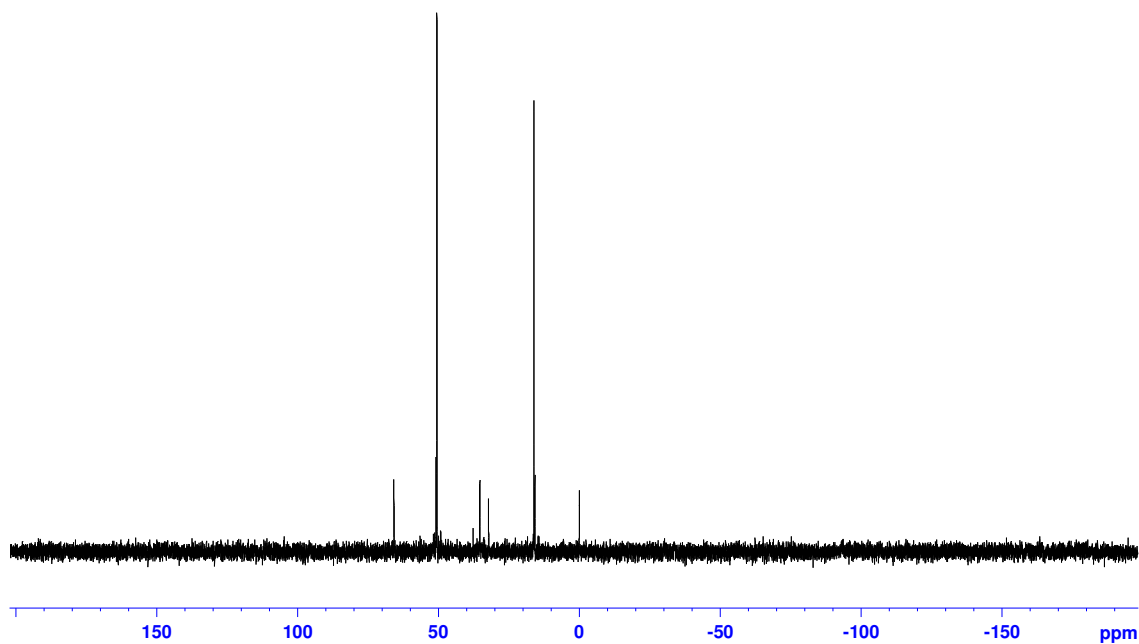
2.5 Reaction with K₂PtBr₄

This problem was solved by changing the COD precursor to K₂PtBr₄ and heating to 75°C overnight in dry degassed acetonitrile to afford the [Pt(P-P)Br₂] complexes we desired (Scheme 48). This could be due to the *bis*-acetonitrile intermediate complex being formed. This can undergo displacement by the diphosphine ligand without consequent C-P bond formation and instead Pt-P bond formation as expected.



Scheme 48. Synthesis of [Pt(P-P)Br₂]

The synthesis of [Pt(dippf)Br₂] (**22**), ³¹P{¹H} NMR (161.976 MHz, CDCl₃) δ_P = 30.494 (s, 2P, ¹J_{P-Pt} = 3762.4 Hz) (Spectra 3) and [Pt(dtbpf)Br₂] (**23**), ³¹P{¹H} NMR (161.976 MHz, CDCl₃) δ_P = 35.951 (s, 2P, ¹J_{P-Pt} = 3858.9 Hz) (Spectra 4) were achieved in this way whereby the NMR showing the expected *trans* coupling across the Pt for Br (¹J_{P-Pt} = 3500-4500 Hz) and MS data correlate. [Pt(dtbdppf)Br₂] (**24**) was also synthesised in this way and corresponded to the MS and NMR data observed. ³¹P{¹H} δ_P = 16.8 ppm (d) (tBu) (¹J_{P-Pt} = 3706.7 Hz, ²J_{P-P} = 5.9 Hz), 50.8 ppm (d) (Ph) (¹J_{P-Pt} = 3912.7 Hz, ²J_{P-P} = 5.9 Hz) showing the expected coupling for a Pt complex with P *trans* to Br (¹J_{P-Pt} = 3500-4500 Hz) (Spectra 3).



Spectra 3. $^{31}\text{P}\{^1\text{H}\}$ NMR spectra of $[\text{Pt}(\text{dtbdppf})\text{Br}_2](\mathbf{24})$

The slow diffusion of DCM in hexanes yielded crystals suitable for X-Ray analysis (Figure 15, Table 11) and the structural information correlated with the NMR and MS evidence.

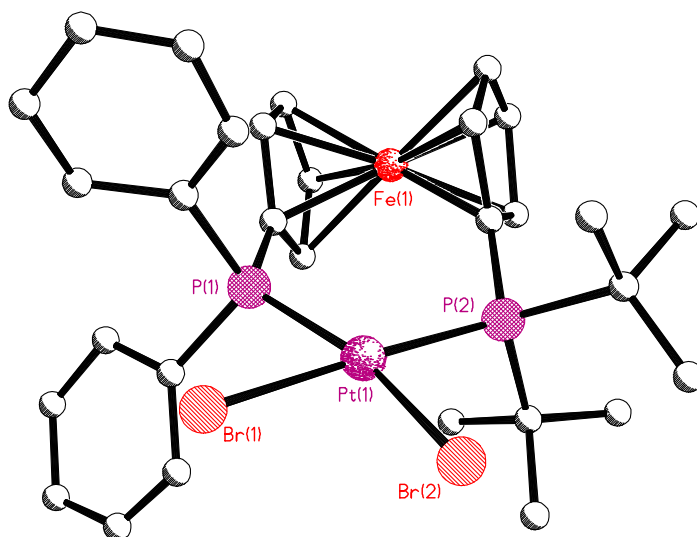


Figure 15. X-Ray Structure of $[\text{Pt}(\text{dtbdppf})\text{Br}_2](\mathbf{24})$

	Bond Angle (°)		Bond Length (Å)
P(2)-Pt(1)-P(1)	101.90(2)	Pt(1)-Br(1) (<i>trans</i> to ^t Bu)	2.494(3)
P(1)-Pt(1)-Br(2)	164.65(17)	Pt(1)-Br(2) (<i>trans</i> to Ph)	2.478(3)
P(2)-Pt(1)-Br(2)	93.46(16)	P(1)-Pt(1)	2.280(5)
P(1)-Pt(1)-Br(1)	81.07(16)	P(2)-Pt(1)	2.328(6)
P(2)-Pt(1)-Br(1)	177.04(15)	Av. Fe-C	2.042(2)
Br(2)-Pt(1)-Br(1)	83.58(10)		
r^a	37.20		
θ^b	4.00		

^[a] The torsion angle $C_A-X_A-X_B-C_B$ where C is the carbon bonded to the P and X is the centroid. ^[b] The dihedral angle between the two Cp rings.

Table 11. Selected X-ray data for $[Pt(dtbdppf)Br_2](\mathbf{24})$

Complex (**24**) has adopted a pseudo-square planar geometry about the Pt with slight distortion for a Pt complex of this type and has a smaller P-Pt-P bond angle (101.90°) compared to $[Pt(dippf)Cl_2]$ (103.78°) both complex **24** and $[Pt(dippf)Cl_2]$ adopt a synclinal staggered arrangement in which the phosphorus atoms are gauche and the Cp rings are staggered.¹³²

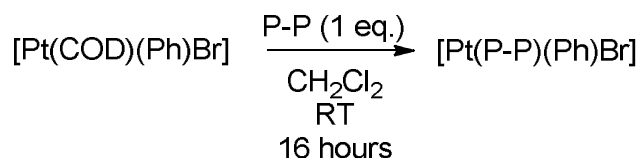
The average P-Pt bond lengths of these ferrocenyl compounds also show similar trends $[Pt(dppf)Cl_2]$ (2.260 Å) < $[Pt(dippf)Cl_2]$ (2.267 Å).¹³² In complex **24**, the P-Pt bond length is longer and there is a small but noticeable difference in *trans* influence of the PPh₂ group apparent as the Br(2)-Pt bond which is *trans* to the PPh₂ is 2.478 Å and the Br(1)-Pt bond which is *trans* to the P(^tBu)₂ group is 2.494 Å. The relatively long bond length and larger bite angle could be due to the steric bulkiness of the phenyl and ^tBu substituents on the metal.

This suggests that the bulkier ^tBu groups compared to the phenyl groups of dtbdppf increased the bite angle of the di-phosphine bonding to the metal.

Although the ³¹P NMR spectra of $[Pt(P-P)(Ph)Br]$ and $[Pt(P-P)Ph_2]$ are very distinctive, we confirmed the identity of complexes we expected to detect in the transmetalation studies by reacting the diphosphine ligands with the precursors $[Pt(COD)(Ph)Br]$ and $[Pt(COD)Ph_2]$ and monitoring the reactions using NMR spectroscopy.

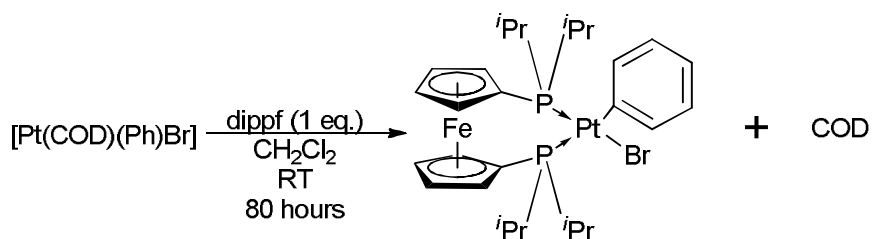
2.6 Reaction with Pt(COD)(Ph)Br

With unsymmetrical substituents *trans* to the ligand, the COD precursor in this case formed the desired [Pt(L)(Ph)Br] complexes (>90% pure by $^{31}\text{P}\{^1\text{H}\}$ NMR) for dippf (**28**), dtbpf (**29**) (which had an interesting mode of interaction with the Pt) and dtbdppf (**30**) by simply stirring the COD precursor with 1 eq. of ligand in dry DCM overnight (Scheme 49). The dtbpf analogue (**29**) formed a complex with the phosphorus atoms *trans* to each other and loss of a bromide. This is due to the steric bulk of the $t\text{Bu}$ groups forcing the complex to adopt this configuration, and become symmetrical. There could also be evidence for a Pt-Fe bond which stabilizes the complex. This suggests a different mode of bonding to the Pt.

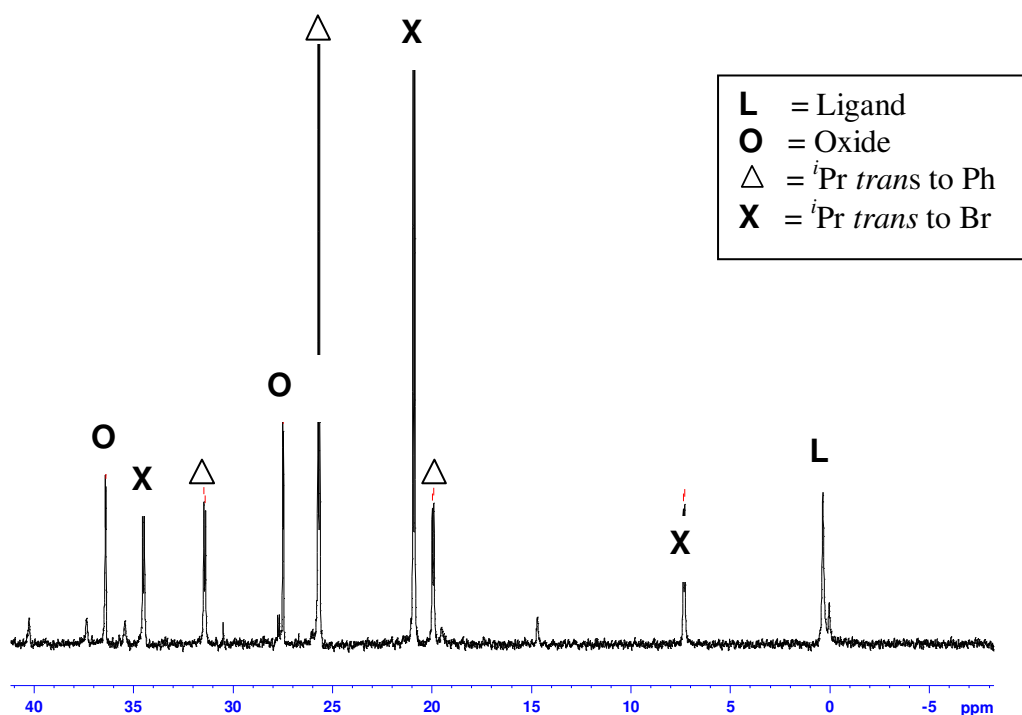


Scheme 49. Synthesis of [Pt(P-P)(Ph)Br]

Dippf proved to be slightly more problematic with some oxide and ligand observed during the reaction. [Pt(dippf)PhBr] (**28**) was formed in 88% yield (90% pure by ^{31}P NMR spectroscopy) (Scheme 50, Spectra 4).



Scheme 50. Synthesis of [Pt(dippf)(Ph)Br](**28**)



Spectra 4. $^{31}\text{P}\{^1\text{H}\}$ NMR spectra of $[\text{Pt}(\text{dippf})(\text{Ph})\text{Br}]$ (**28**), free ligand and oxide

$\delta_{\text{P}} = 20.91$ ppm (d) ($^1J_{\text{P-Pt}} = 4339$ Hz, $^2J_{\text{P-P}} = 12.7$ Hz), 25.70 ppm (d) ($^1J_{\text{P-Pt}} = 1859$ Hz, $^2J_{\text{P-P}} = 12.7$ Hz) showing the expected *trans* coupling across the Pt for Br and Ph respectively. The $^{31}\text{P}\{^1\text{H}\}$ NMR spectra shows that $[\text{Pt}(\text{dippf})(\text{Ph})\text{Br}]$ has been synthesized with some mono- and di-oxide formation and free ligand (running at between 0 and 1 ppm).

X-Ray quality crystals of $[\text{Pt}(\text{dippf})(\text{Ph})\text{Br}]$ (**28**) were obtained from the slow diffusion of CH_2Cl_2 /hexanes (Figure 16). The structure was confirmed by EI-MS, IR, ^1H , ^{31}P and ^{13}C NMR spectroscopy.

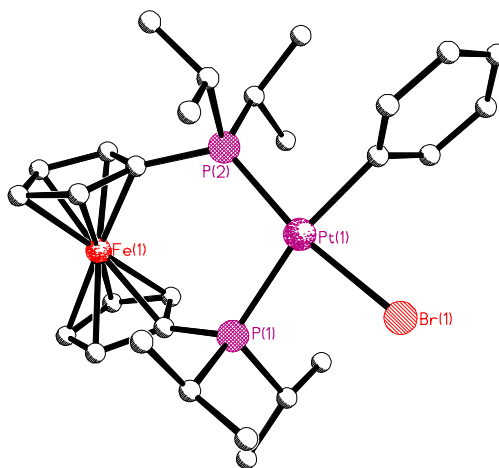


Figure 16. X-Ray structure of $[\text{Pt}(\text{dippf})(\text{Ph})\text{Br}]$ (**28**)

The X-ray structure of complex **28** (Figure 16) confirms the slight distortion from *cis*-square planar geometry expected for a Pt complex of this form (Table 12).

	Bond Angle (°)		Bond Length (Å)
P(2)-Pt(1)-P(1)	102.56(3)	Pt(1)-C(23)	2.070(3)
C(23)-Pt(1)-Br(1)	82.55(10)	Pt(1)-Br(1)	2.504(4)
P(2)-Pt(1)-Br(1)	169.53(2)	P(1)-Pt(1)	2.362(9)
P(1)-Pt(1)-Br(1)	87.56(3)	P(2)-Pt(1)	2.255(9)
C(23)-Pt(1)-P(2)	87.69(10)	Av. Fe-C	2.041
C(23)-Pt(1)-P(1)	168.18(10)		
P(2)-Pt(1)-P(1)	102.56(3)		
τ^a	37.3		
θ^b	3.7		

^[a] The torsion angle $C_A-X_A-X_B-C_B$ where C is the carbon bonded to the P and X is the centroid. ^[b] The dihedral angle between the two Cp rings.

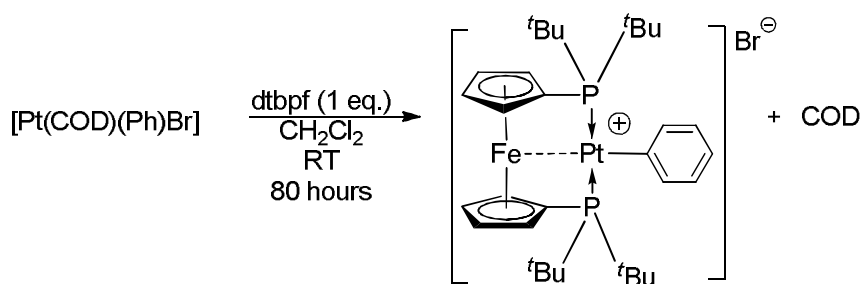
Table 12. Selected Bond Angles and Bond Lengths for [Pt(dippf)(Ph)Br](**28**)

In complex **28**, the Pt has adopted a pseudo-square planar geometry and has a smaller P-Pt-P bond angle (102.56°) compared to [Pt(dippf)Cl₂] (103.78°), [Pt(dppf)Cl₂] (99°)¹³⁰ and [Pt(dppf)Ph₂] (82.90°).¹³⁰ Both complex **28** and [Pt(dippf)Cl₂] adopt a synclinal staggered arrangement in which the phosphorus atoms are gauche and the Cp rings are staggered.¹³² This suggests that the bulkier *iso*-propyl groups of dippf compared to the phenyl groups of dppf increased the bite angle of the di-phosphine bonding to the metal.

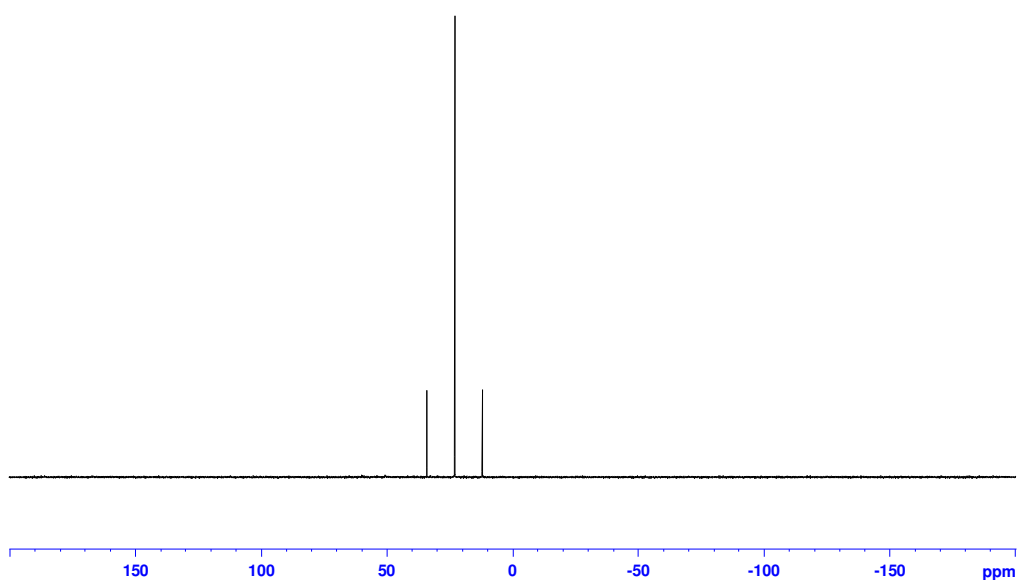
The average P-Pt bond lengths of these compounds also show similar trends [Pt(dppf)Cl₂] (2.260 Å) < [Pt(dippf)Cl₂] (2.267 Å). In complex **28**, the P-Pt bond length is longer still and there is a noticeable *trans* influence of the phenyl group apparent as the P(1)-Pt bond which is *trans* to the carbon of the phenyl ring is 2.362 Å and the P(2)-Pt bond which is *trans* to the bromide is 2.255 Å.

With the sterically hindered dtbpf ligand the expected non-symmetrical pattern in the ³¹P NMR was not observed, instead a complex with a tridentate mode was observed by NMR spectroscopy (Spectra 5).

This indicated the loss of a bromide from the complex and stabilization *via* a Pt-Fe interaction to give the complex shown below **29** (Scheme 51). The phosphorus atoms are *trans* to each other. $\delta_P = 25.6$ ppm, ($^1J_{P-Pt} = 2670$ Hz) (Spectra 5) effectively showing that the *t*Bu groups bound to the phosphorus are in the same chemical environment indicating that the phosphorus atoms are *trans* from the *trans* coupling of 2670 Hz. Further evidence from the 1H NMR is the 2 signals observed for the Cp ring hydrogen atoms (instead of 4 signals expected for *cis*-type chelation) indicating that *trans* geometry is observed in this Pt complex.



Scheme 51. Synthesis of $[Pt(dtbpf)Ph]Br^-$ (**29**)



Spectra 5. $^{31}P\{^1H\}$ NMR spectra of $[Pt(dtbpf)Ph]Br^-$ (**29**)

The work of Van Leeuwen *et al.*¹³⁴ has shown evidence for a dative Pd-Fe bond in very similar complexes. 1H and ^{31}P NMR spectra of complexes **31** and **33** in $CDCl_3$ show two inequivalent phosphorus atoms, a double doublet for the methyl group and four signals of the hydrogen atoms of the cyclopentadienyl (Cp) rings, indicating that the ligands coordinate in a *cis* fashion to palladium (Figure 17).

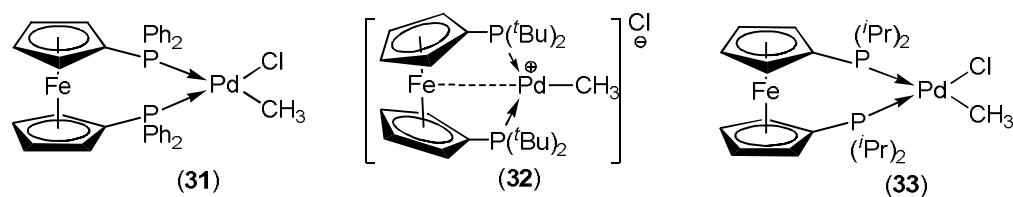


Figure 17. Ring tilting in bulky ferrocenylphosphino palladium complexes

In contrast, complex **32** has two equivalent phosphorus atoms and shows a triplet for the methyl group and only two signals for the hydrogen atoms of the Cp rings. This indicates that the phosphorus atoms in complex **32** are coordinated in a *trans* fashion to palladium.

A *trans*-coordination mode of the dtbpf ligand implies that either the dtbpf ligand is positioned above (and below) the square planar palladium complex or that the iron atom of the ferrocene unit is bonded to palladium. In the latter case, the $14e^-$ configuration that forms after loss of the chloride ligand would be alleviated by a dative palladium-iron bond and the strong basicity of the phosphine ligand. A study by Sato *et al.*¹³³ showed that formation of a palladium-iron bond leads to tilting of the Cp rings.

This causes a large chemical-shift difference ($\Delta\delta$) between the α - and β -H atoms of the Cp rings (~ 1 ppm) compared to the chemical-shift difference in the free ligand (~ 0.2 ppm). A very large chemical shift difference was indeed observed for complex **32**, when the ferrocene unit is positioned above the coordination plane of the palladium centre and the phosphorus atoms are coordinated in a *trans* fashion, the rings can still be tilted as a result of the large intramolecular P–P distance.

Presumably, the larger phosphine substituents cause steric crowding which favours dissociation of the halide and the coordinative unsaturation results in the formation of a Pd-Fe dative bond. Changes in the substituents of the phosphorus atoms of diphosphine ferrocene ligands can have a large effect on their coordination behaviour. A palladium–iron interaction is favoured by bulky alkyl substituents on phosphorus and a lower electron density at palladium.

Reaction of [Pt(COD)(Ph)Br] with a slight excess of dtbdppf gives the expected complex after 24 h at RT in MeCN (**30**) (Figure 18).

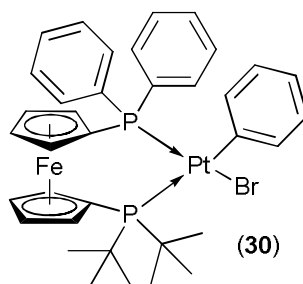
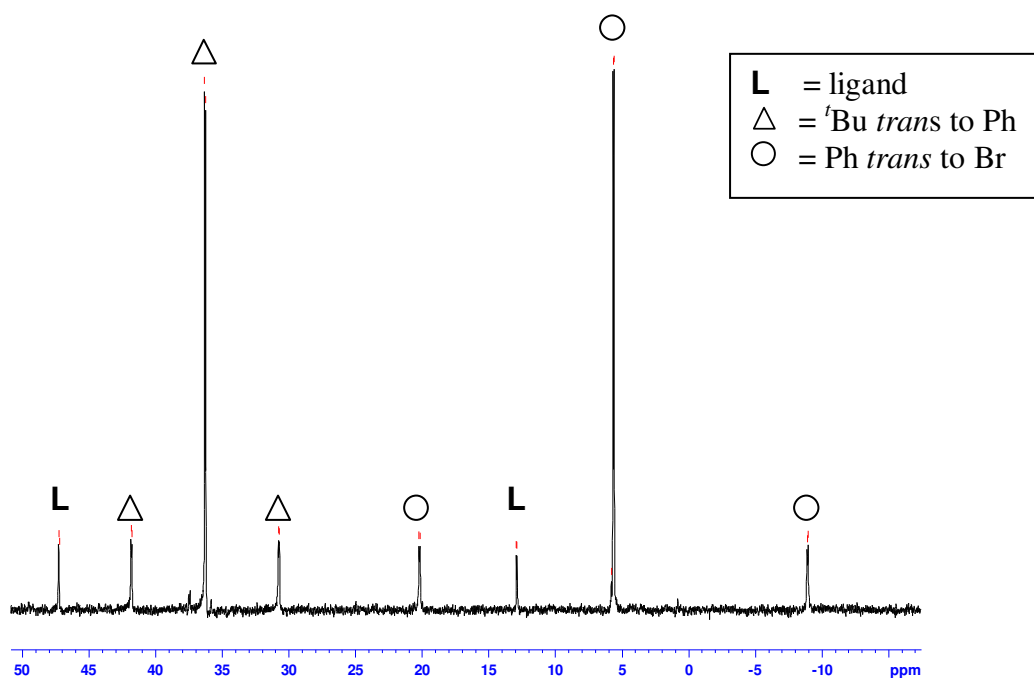


Figure 18. [Pt(dtbdppf)(Ph)Br](**30**)

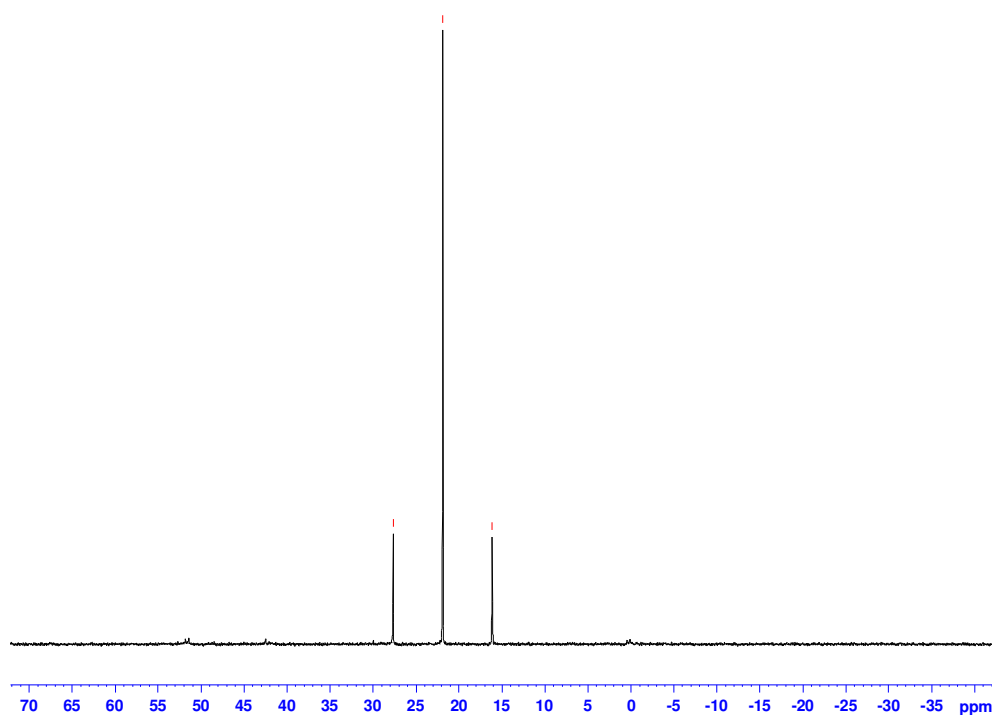
^{31}P { ^1H } NMR showed the correct complex [Pt(dtbdppf)(Ph)Br] (**30**) (Spectra 8) δ_{P} (d) = 36.28 ppm ($^1J_{\text{P-Pt}} = 1776$ Hz, $^2J_{\text{P-P}} = 11.9$ Hz), (d) = 5.70 ppm ($^1J_{\text{P-Pt}} = 4717$ Hz, $^2J_{\text{P-P}} = 11.9$ Hz), which was confirmed by ^1H , ^{13}C NMR, EA and FAB-MS. The ^{31}P NMR spectra also showed that the PPh₂ groups of the ligand are *cis* to the phenyl group due to the smaller *trans* coupling for the ^tBu groups which are characteristic of phosphorus *trans* to a strong *trans* effect ligand such as an aryl ring bound to the Pt (Spectra 6). This could be due to the steric hindrance of the ^tBu groups versus the aryl ring. The π -interactions of the phenyl groups could have a stabilising effect and force the complex to adopt this configuration.



Spectra 6. $^{31}\text{P}\{^1\text{H}\}$ Spectra of [Pt(dtbdppf)(Ph)Br](**30**) & dtbdppf ligand

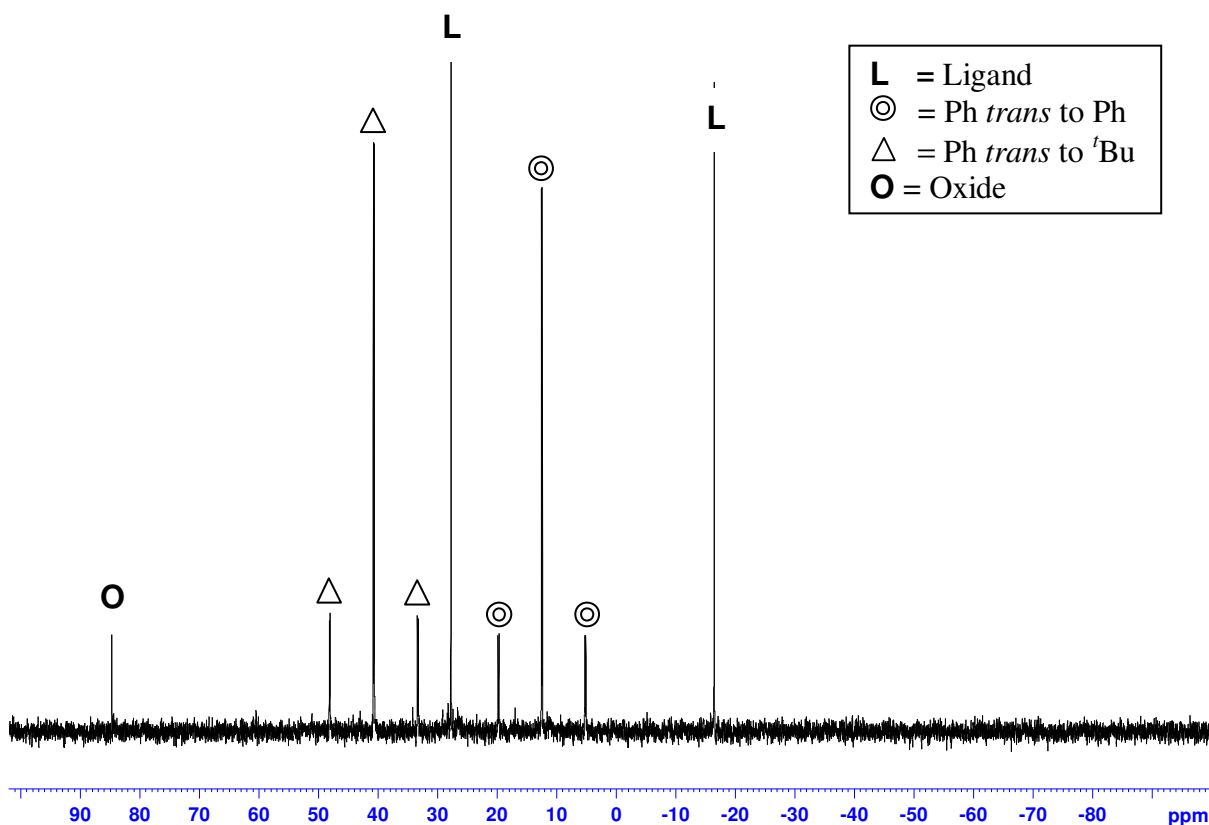
To help with identification of [Pt(P-P)Ph₂] species in the transmetalation reaction, the ligands dippf, dtbdppf and dppe were reacted with [Pt(COD)Ph₂] in dry degassed DCM and monitored by ³¹P{¹H}NMR spectroscopy. With dtbpf no Pt satellites were observed in the ³¹P NMR spectra, indicating no desired [Pt(P-P)Ph₂] complex had been synthesised. It seems introducing two *ditert*-butylphosphino groups' causes too much steric hindrance and prevents P-Pt bond formation.

[Pt(dippf)Ph₂] (**34**) was observed in >90% yield (with 1% ligand and 1% oxide washed away with dry degassed hexanes). Reaction was monitored by ³¹P{¹H}NMR spectroscopy. δ_P = 21.84 ppm (¹J_{P-Pt} = 1880.5 Hz) (Spectra 7).



Spectra 7. ³¹P{¹H}NMR spectra of [Pt(dippf)Ph₂](34)

Dtbdppf reacted with [Pt(COD)Ph₂] to give the desired [Pt(dtbdppf)Ph₂] (**35**) complex δ_P (d) = 12.43 ppm (¹J_{P-Pt} = 1775 Hz, ²J_{P-P} = 15.8 Hz), (d) = 40.67 ppm (¹J_{P-Pt} = 1793 Hz, ²J_{P-P} = 16.4 Hz) The complex was contaminated with free ligand and oxide which resisted attempts at purification (Spectra 9). Nonetheless, this spectrum is characteristic for [Pt(P-P)Ph₂] and is sufficient to confirm product identities from the transmetalation studies we subsequently performed.

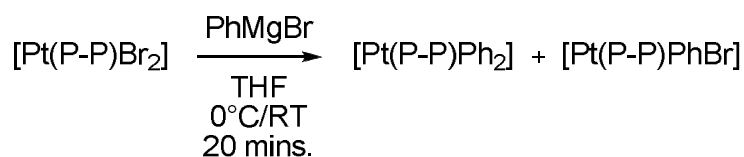


Spectra 9. $^{31}\text{P}\{^1\text{H}\}$ NMR spectra of $[\text{Pt}(\text{dtbdppf})\text{Ph}_2]$ (**35**) oxides & ligand

As a control, DPPE reacts cleanly (>99%) $[\text{Pt}(\text{dppe})\text{Ph}_2]$ (**36**) δ_{P} (s) = 42.00 ppm ($^1J_{\text{P-Pt}}$ = 1702.9 Hz) with little side and oxidation products, by stirring in dry degassed DCM overnight. Indeed, we recommend this reaction for monitoring the purity of $[\text{Pt}(\text{COD})(\text{R})\text{X}]$ and $[\text{Pt}(\text{COD})\text{R}_2]$ during their synthesis³⁵.

2.7 Transmetalation Studies $[\text{Pt}(\text{P-P})\text{Br}_2]$

With authentic samples of $[\text{Pt}(\text{P-P})\text{PhBr}]$ and $[\text{Pt}(\text{P-P})\text{Ph}_2]$ in hand we turned our attention to the transmetalation studies (Scheme 52).



Scheme 52. Transmetalation of $[\text{Pt}(\text{P-P})\text{Br}_2]$ with PhMgBr

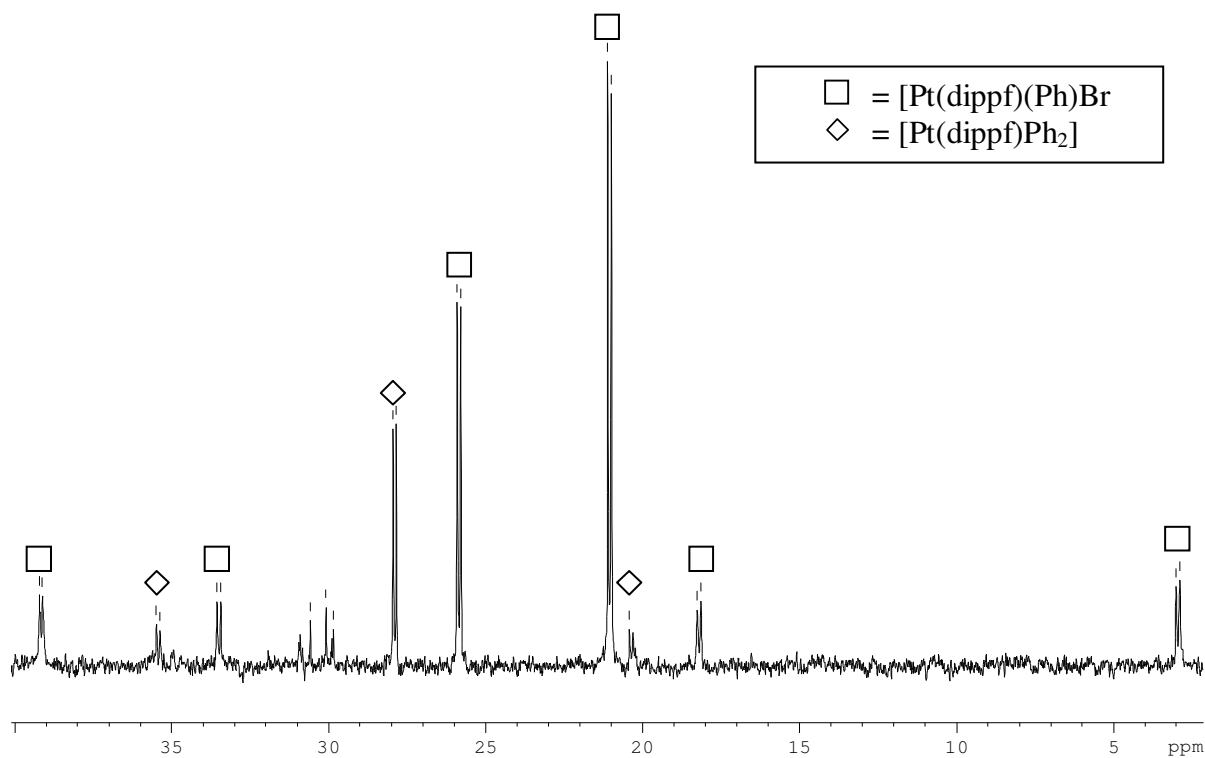
It was found that in all cases 1 eq. of Grignard at 0 °C and RT gave unreacted starting material. With 6 eq. of Grignard at 0 °C, the formation of the [Pt(dppf)PhBr] was apparent for the dppf complex, at RT the dtbdppf and dppf complexes show evidence of the [Pt(P-P)PhBr] species starting to be formed. The spectra were complicated by halide scrambling in deuterated solvents giving rise to extra Pt signals after extended reaction times.

The reaction proved sluggish for the remaining complexes therefore they were subjected to more forcing reaction conditions, 15 eq. of PhMgBr at RT for 2 hours. In all cases, the unsymmetrical products were formed and the dppf, dippf (Spectra 10) and dtbdppf (Spectra 11) complexes showed evidence of the *bis*-aryl species also being formed (Table 13).

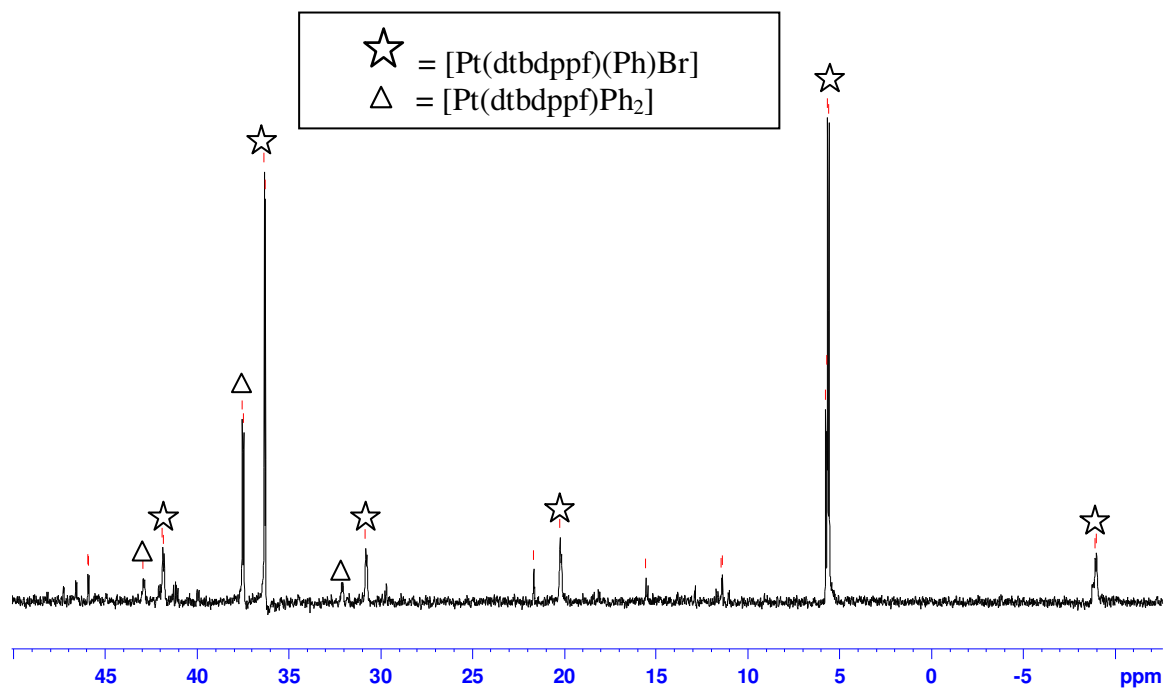
<u>Complex</u>	<u>Yield</u> ^[a] [Pt(P-P)Br ₂]	<u>Yield</u> ^[a] [Pt(P-P)PhBr]	<u>Yield</u> ^[a] [Pt(P-P)Ph ₂]	<u>Yield</u> ^[a] Other P species (No Pt satellites)
[Pt(dippf)Br ₂] (22)	0%	74%	17%	9%
[Pt(dtbpf)Br ₂] (23)	0%	51%	0%	49%
[Pt(dtbdppf)Br ₂] (24)	0%	67%	13%	20%
[Pt(dppf)Br ₂] (25)	0%	48%	36%	16%

Reagents & Conditions: [Pt(P-P)Br₂] (2.2×10^{-5} mol), PhMgBr (0.3 M solution in Et₂O) 15 eq. (0.330 mmol), THF (5 mL), RT, 2h. ^[a]Assigned from ³¹P{¹H} NMR spectra (uncalibrated for potential relaxation times).

Table 13. PhMgBr 15 eq. RT, 2 hours: transmetalation results



Spectra 10. $^{31}\text{P}\{^1\text{H}\}$ NMR of $[\text{Pt}(\text{dippf})\text{PhBr}]$ and $[\text{Pt}(\text{dippf})\text{Ph}_2]$ from reaction of $[\text{Pt}(\text{dippf})\text{Br}_2]$ with PhMgBr



Spectra 11. $^{31}\text{P}\{^1\text{H}\}$ NMR of reaction mixture after addition of PhMgBr to $[\text{Pt}(\text{dtbdppf})\text{Br}_2]$

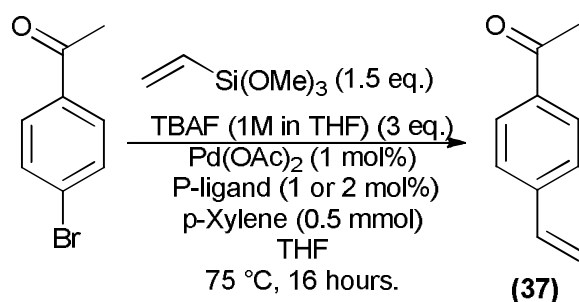
All of the complexes formed the [Pt(P-P)(Ph)Br]. It is interesting to note that the dippf (Spectra 10) formed the highest and the dtbpf formed the lowest amount of [Pt(P-P)(Ph)Br], this can be attributed to increased steric bulk preventing the *bis*-aryl species being formed, in addition, for the dtbpf there are several unidentified phosphorus signals in the NMR spectrum that do not have Pt satellites.

It can also be seen that the dppf species formed the highest amount of the *bis*-aryl complex indicating an increase in the transmetalation of the Grignard reagent. This could be attributed to less steric bulk in the ligand; dtbdppf behaves quite similarly to dippf, undergoing transmetalation more readily than dtbpf. Given that dtbpf performs poorly in several cross-coupling reactions with weak or problematic nucleophiles, we would suggest that this can be directly related to its reluctance to undergo transmetalation.

Chapter 3. Hiyama cross-coupling reaction of alkenyl trialkoxysilanes

Organosilicon nucleophiles can be a useful alternative to organotin (Stille) or organoboron (Suzuki) reagents, as demonstrated in the Hiyama coupling reaction of aryl halides.³¹ This method is advantageous as benign by-products are created and the nucleophiles themselves are also less toxic, less expensive and less oxygen and moisture sensitive than their organoboron and organotin counterparts. Organosilicon compounds are also more tolerant of harsh reaction conditions, such as elevated temperatures and polar solvents and can withstand several synthetic steps before the Pd catalysed coupling reaction. This resilience allows functionalisation around the silicon centre and an increased flexibility in the design of novel organosilicon reagents for catalysis.

An effective protocol was developed for the cross-coupling of *p*-bromoacetophenone (1 mmol.) with vinyltrimethoxysilane (1.5 eq.) under Hiyama conditions to form the aryl-alkene product with 1 mol% of Pd(OAc)₂ and either 1 mol% of bidentate or 2 mol% of monodentate ligand (Table 14). *p*-Xylene (0.5 mmol.) was incorporated as an internal standard as it gave a simple ¹H NMR spectrum (Scheme 53).



Scheme 53. Hiyama cross-coupling of *p*-bromoacetophenone & vinyltrimethoxysilane

A range of mono and bidentate phosphine ligands were screened with some interesting results. Electron rich and electron poor ligands were evaluated along with the series of ferrocenylphosphine ligands discussed in Chapter 2 (Figure 21).

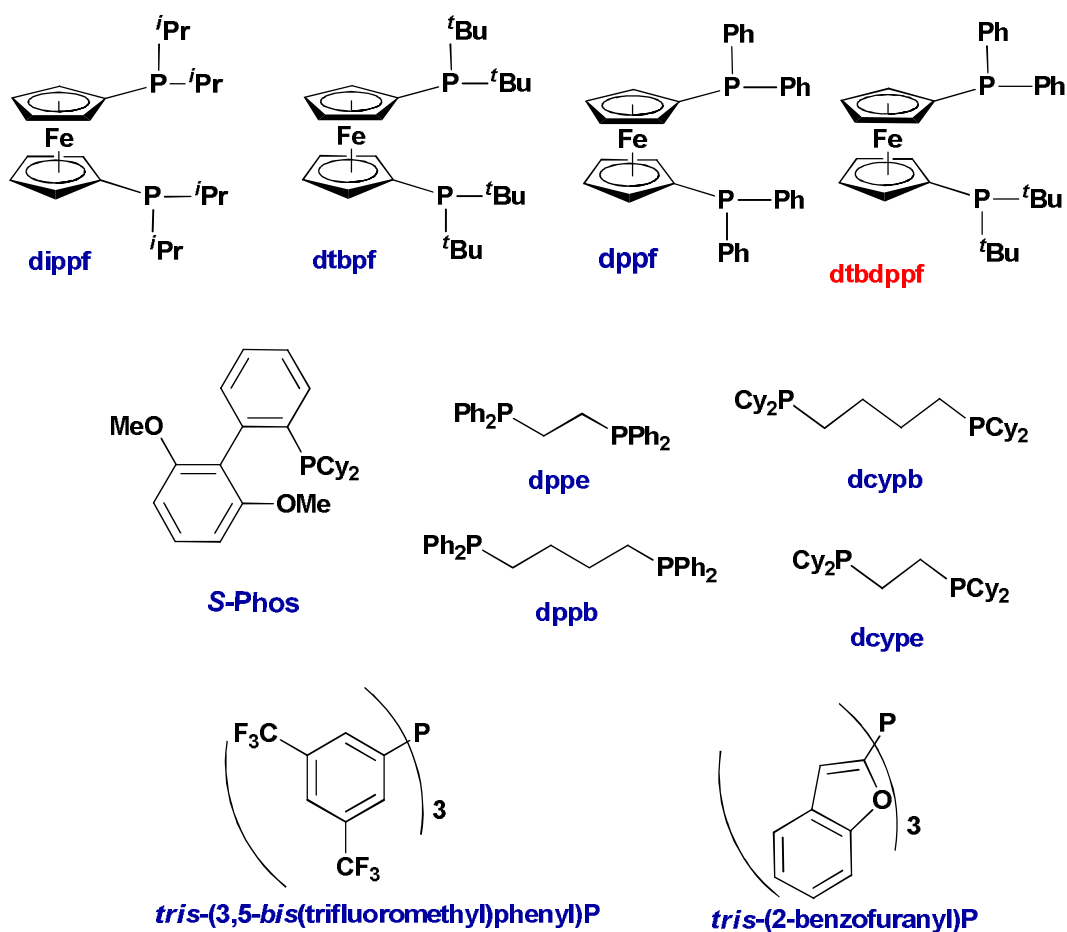


Figure 19. Selected ligand systems for Hiyama cross-coupling

It was observed that monodentate phosphine ligands gave poor conversion (<30%) to the desired coupling product (**37**). Interestingly however, Buchwald's *S*-Phos ligand gave 39% conversion (Table 14), and is thus the best monodentate phosphine screened. However, *S*-Phos/Pd catalysts would give high conversions in a Suzuki reaction of this easy aryl bromide even at room temperature, highlighting the challenges with Hiyama coupling.

Bidentate ligands which were electron rich with relatively large bite angles (Figure 19) proved to give higher conversion with 1,1'-bis(diisopropylphosphino)ferrocene (dippf), 1,1'-bis(diphenylphosphino)ferrocene (dppf) and 1,2-bis-(dicyclohexylphosphino)ethane (dcype) giving good conversions of 56%, 57% and 61% respectively (Table 14).

Catalyst Pd(OAc)₂ (1 mol%) Ligand (2 mol%)	% Conversion by ¹H NMR	Catalyst Pd(OAc)₂/ Ligand (1 mol%)	% Conversion by ¹H NMR
PPh ₃	< 5	dippf	56
PCy ₃	< 5	dtbpf	29
(Me)Cage P	< 5	dtbdppf	47
2-pyridyl-diphenyl P	10.4	dppf	57
<i>tris</i> -(<i>p</i> -methoxyphenyl) P	< 5	dppe	56
<i>tris</i> -(3,5- <i>bis</i> (trifluoromethyl)phenyl) P	4.3	dppb	50
<i>tris</i> -(2-benzofuranyl) P	0	dcypb	60
<i>S</i> -Phos (Buchwald Ligand)	39	dcype	61
		[Pd(dcype)Cl ₂] ^[a]	65
		[Pd(dppe)Cl ₂] ^[a]	39
		[Pd(dppf)Cl ₂] ^[a]	67

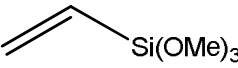
Reagents & Conditions: *p*-bromoacetophenone (1 mmol), vinyltrimethoxysilane (1.5 mmol), TBAF (1M in THF) (3 mmol), THF, 75 °C, 16 h, ^[a] 1 mol% loading.

Table 14. Hiyama cross-coupling with bidentate phosphine ligands

Preformed catalysts were also screened giving pleasing results, and in the case of dppf, perform slightly better if pre-formed (67%). It seems likely that dippf, dppf, dcype, dtbdppf and dcypb could have the correct balance of steric bulk and donor properties desired to accelerate the transmetalation within the Hiyama cross-coupling cycle but still allow oxidative addition. It could be the case that oxidative addition and reductive elimination are accelerated with the other ligands, but the particularly bulky ligand dtbpf could hinder the reaction at the transmetalation step and stop the reaction at that point as has been suggested by the transmetalation study in chapter 2.

3.1 Varying the concentration of Si nucleophile

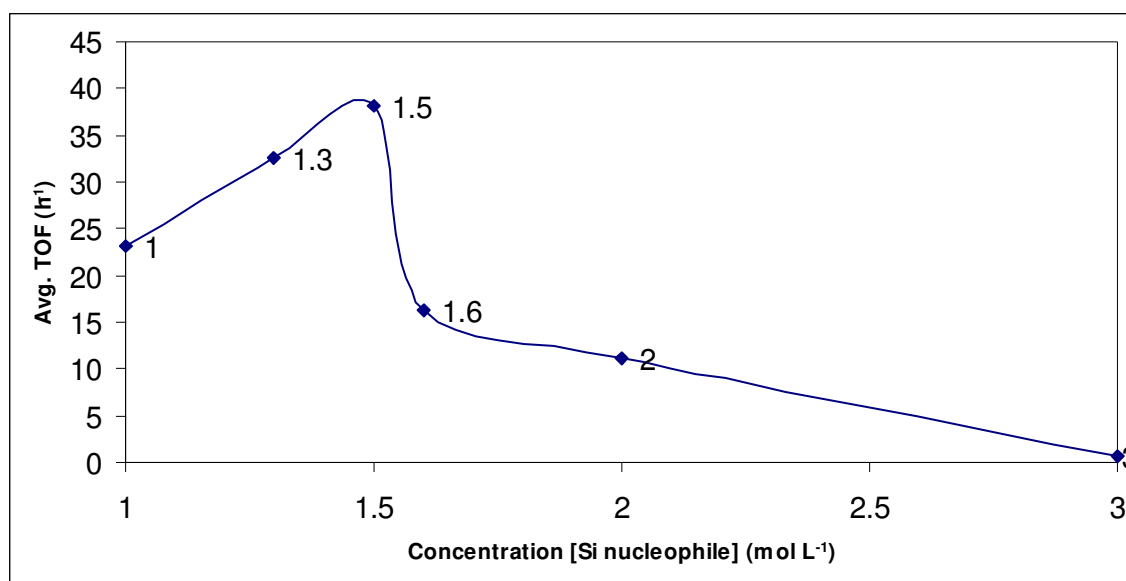
Hiyama reactions could be limited by slow transmetalation or by the vinyl silane binding Pd⁽⁰⁾ and slowing oxidative addition. To probe this, the effect of changing the amount of vinyltrimethoxysilane and TBAF (as the promoter) was examined keeping the total volume constant (Table 15).

 Si(OMe) ₃	TBAF (1M in THF)	Conversion (%)^{[a], [b]}
1.0 eq.	2.0 eq.	37
1.3 eq.	2.6 eq.	52
1.5 eq.	3.0 eq.	61
1.6 eq.	3.2 eq.	26
2.0 eq.	4.0 eq.	18
3.0 eq.	6.0 eq.	1

Reagents & Conditions: *p*-bromoacetophenone (1 mmol), [Pd(*dcype*)Cl₂] (1 mol%), internal standard; 1-methyl-naphthene (0.5 mmol), THF (Total volume 6.6 mL), 75 °C, 16 h, ^[a] Calculated from ¹H NMR spectra, ^[b] Remaining is starting material.

Table 15. Varying the concentration of available Si nucleophile

From these results, it is clear that an inhibitory effect is observed on increasing the concentration of available nucleophile (fluoride activated pentavalent Si species) and decreasing the concentration below 1.5 eq. of silane also has a detrimental effect (Graph 1).



Graph 1. Dependence on Si concentration to mediate Hiyama reaction

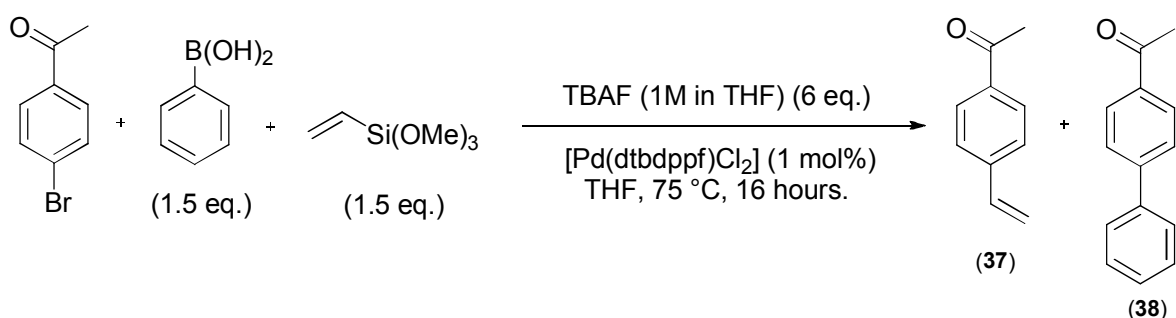
The average Turnover frequency (TOF), defined as “the number of molecules of substrate that a catalyst can convert to product per catalytic site per unit of time” shows that the reaction is dependent on the concentration of activated Si nucleophile available in the reaction. It seems that 1.5 eq. of silane is optimum with a rapid decline in rate on increasing the concentration of

silane. Any conclusions have to be made with caution since a full kinetic profile at various concentrations is not available and therefore the effect of the activation period of the catalyst and catalyst stability are unknown.

Since vinyltrimethoxysilane is a poor nucleophile more than 1 eq. would be needed for this to be effective. It would also make sense that an inhibitory effect is observed as more Si binds to the Pd and saturates the catalyst which could lead to deactivation. The reactive species is effectively competing with itself as more Si binds.

3.2 Competition Experiments – Hiyama Vs Suzuki

Competition experiments were carried out with Suzuki coupling chemistry to assess whether the transmetalation step was rate determining or if vinyltrimethoxysilane inhibits the reaction. This was achieved by reacting the boronic acid and the alkenyl trialkoxysilane in direct competition as the nucleophile in the catalytic cycle, to see if the vinyltrimethoxysilane inhibited the Suzuki reaction to any extent (Scheme 55) Conversion is based on transformation of the starting material being the limiting reagent.

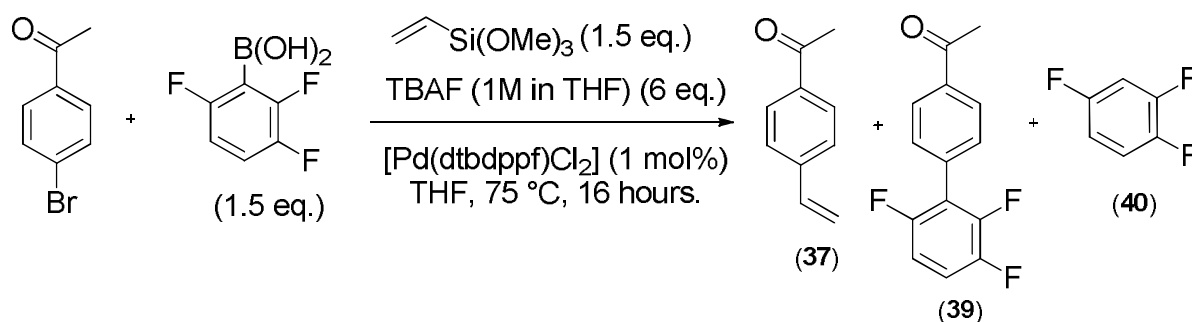


Scheme 55. Competition experiment Suzuki vs. Hiyama

TBAF was used as an activator in these reactions to activate the Si nucleophile for the Hiyama and to act as a base to activate the boronic acid for the Suzuki reaction. Under these conditions the Hiyama reaction (37) gave 40% conversion and the Suzuki (38) 87% respectively. Under competition conditions the Hiyama and Suzuki conversions dropped to 20% and 57% respectively. This shows that transmetalation for the Hiyama with the Silicon nucleophile (vinyltrimethoxysilane) is slower than the phenylboronic acid for the Suzuki.

Due to the Suzuki reaction not being inhibited by vinyltrimethoxysilane anymore than the Hiyama reaction by the boronic acid, this further reinforces the fact that the vinyltrimethoxysilane is a poor nucleophile and cannot compete with the boronic acid.

A highly fluorinated boronic acid (2,3,6-trifluorobenzeneboronic acid) was used under identical conditions as outlined above (Scheme 56) in competition with vinyltrimethoxysilane. The Suzuki reaction performed poorly (34% conversion (**39**), 66% reduced arene (**40**)). Under competition conditions, similar conversion of Suzuki (**39**) (46%) can be attributed to protodeborylation of the boronic acid generating a significant amount of reduced arene (**40**) (44%). There is no evidence of inhibition by the vinyltrimethoxysilane.



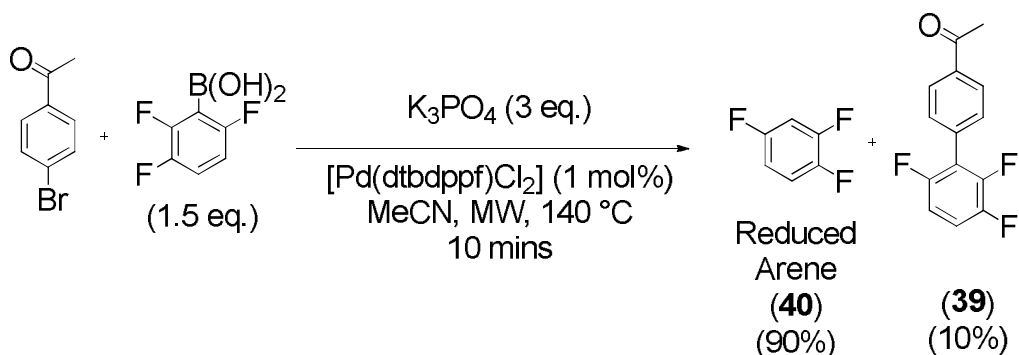
Scheme 56. Competition experiment of a heavily fluorinated Suzuki vs. Hiyama

The Hiyama gave poor conversion (**37**) (10%) highlighting the silicon nucleophile not being able to compete even with this boronic acid sufficiently. The low yield of product with the electron-poor boronic acid is therefore to do with decomposition not slow transmetalation, which seems more likely with Hiyama coupling.

3.3 Suzuki cross-coupling of heavily fluorinated boronic acids

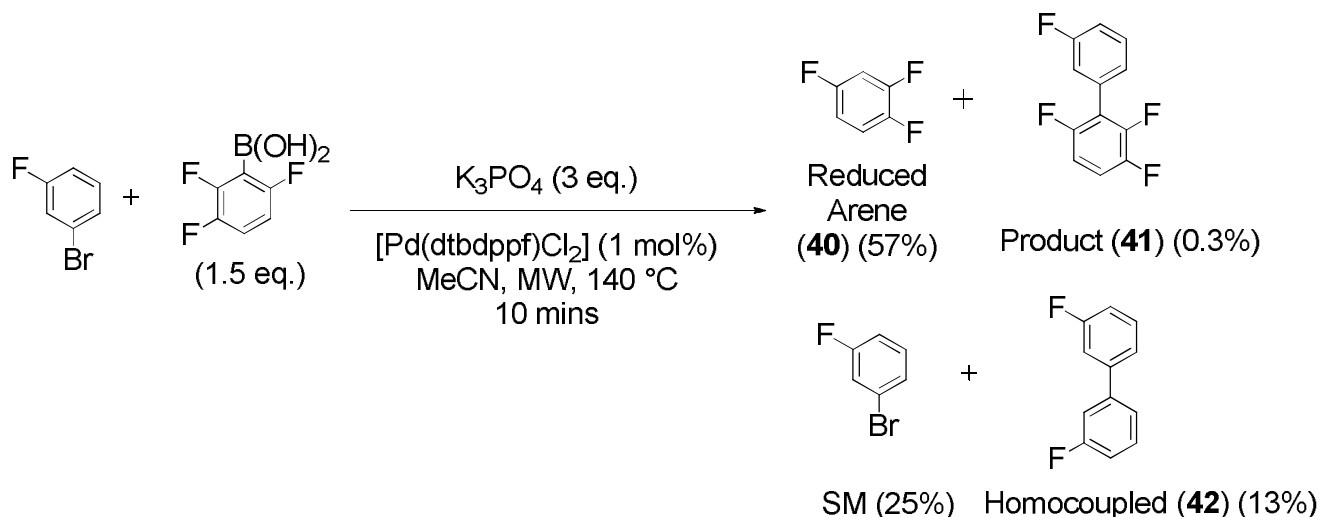
The Suzuki cross-coupling of 2,3,6-trifluorobenzeneboronic acid with *p*-bromoacetophenone was also carried out under typical Suzuki conditions (1.5 eq. boronic acid, 3 eq. base, K₃PO₄ in this case) at 1 mol% loading of [Pd(dtbdppf)Cl₂] (**15**) (Scheme 57). Under microwave heating conditions in MeCN (140 °C, 10 mins) very little cross-coupled bi-aryl was observed by ¹H and ¹⁹F NMR. GC-MS was used to help characterize all of the species present.

In both cases a significant amount of reduced arene (due to protodeborylation) and starting material was observed. With *p*-bromoacetophenone, 90% reduced arene (**40**) and only 10% product (**39**) was observed, indicating that the catalyst is active but the fluorinated boronic acid is decomposing under catalytic conditions (Scheme 57).



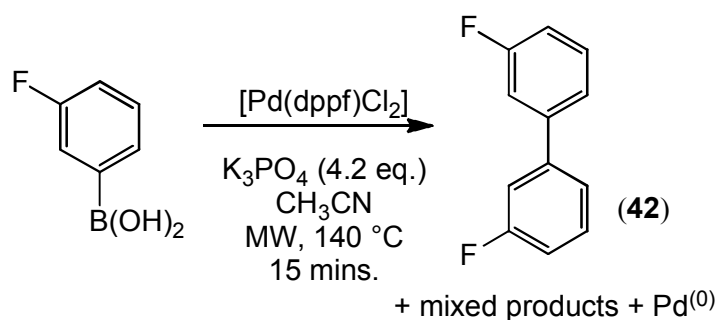
Scheme 57. Evidence of protodeborylation in heavily fluorinated boronic acids

Under identical conditions with 1-bromo-3-fluorobenzene however, only 0.3% product (**42**) was observed with 57% reduced arene (**40**), 13% homo-coupled 3,3'-difluorobiphenyl (**43**) and 25% starting material (Scheme 58). This further reinforces the problem that the boronic acid is breaking down in solution preventing successful cross-coupling. Attempts to improve the cross-coupling of this substrate by using CsF and TBAF as activators or an excess of boronic acid failed, giving only 10% product.



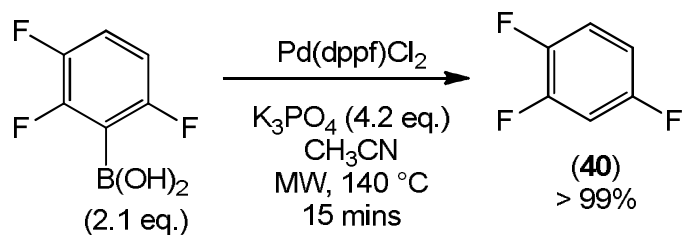
Scheme 58. Attempted Suzuki cross-coupling of 3-fluorobromobenzene with $F_3(C_6H_2)B(OH)_2$

To gain further understanding, stoichiometric experiments between $[\text{Pd}(\text{dppf})\text{Cl}_2]$ (**16**) and boronic acids were carried out (Scheme 59). Given that $[\text{Pd}(\text{dppf})(\text{Ar})_2]$ species rapidly reductively eliminate²⁰ successful transmetalation should result in significant amounts of the symmetrical biaryl (alongside a number of other species such as Pd-aryl intermediates, and base-activated aryl boron species). The reaction between 3-fluorophenylboronic acid (2.1 eq., 4.2. eq. of K_3PO_4 ; CD_3CN , $140\text{ }^\circ\text{C}$, 10 mins) and $[\text{Pd}(\text{dppf})\text{Cl}_2]$ (**16**) gives several species when analysed by ^{19}F NMR spectroscopy. However, the major product is 3,3'-difluorobiphenyl (**42**) as established by spiking NMR samples with a commercial sample (Scheme 59).



Scheme 59. Stoichiometric experiments with $\text{Pd}(\text{dppf})\text{Cl}_2$

The other species have not been identified, but a further spiking experiment shows that fluorobenzene is not present to any great extent. In contrast, reacting 2,3,6-trifluorophenyl boronic acid with $[\text{Pd}(\text{dppf})\text{Cl}_2]$ (**16**) under the same conditions yields only 1,2,5-trifluorobenzene (**40**) as the only fluorine containing product (Scheme 60).



Scheme 60. Protodeboronation of heavily fluorinated boronic acid

Protodeboronation is therefore the cause of the low reactivity observed here, and is a likely problem in other Suzuki couplings of highly fluorinated substrates. Finally, we stirred 2,3,6-trifluorophenyl boronic acid with K_3PO_4 in acetonitrile at room temperature for 15 minutes.

The same quantitative formation of the reduced arene (**40**) was observed even in the absence of Pd catalyst.⁷⁹ We therefore propose that Suzuki coupling between this and similar boronic acids is likely to be difficult under any conditions: alternative strategies or activators are required.

An investigation of ligand effects on the Hiyama coupling of *p*-bromoacetophenone has been carried out; competition experiments were conducted with Suzuki coupling chemistry to assess whether the transmetalation step was rate determining or if vinyltrimethoxysilane inhibits the reaction.

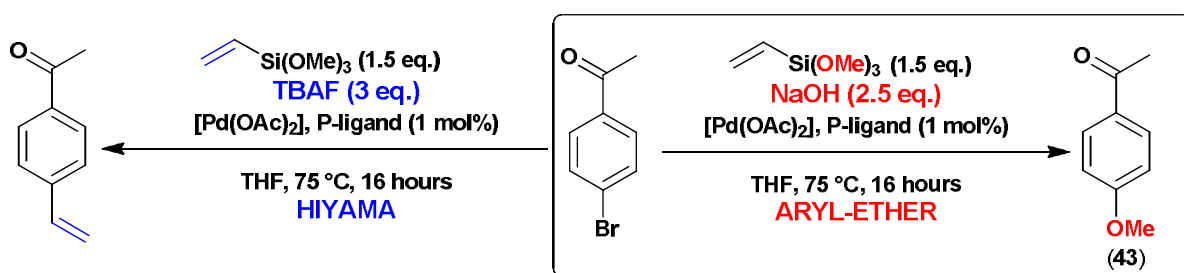
Varying the concentration of the Si nucleophile and competition experiments have shown vinyltrimethoxysilane to be a poor nucleophile in that it cannot compete with phenylboronic acid and fluorinated boronic acids.

Fluorinated boronic acids have been shown to be unstable under cross-coupling and competition conditions and protodeboronate in solution even in the absence of catalyst in solution under typical Suzuki cross-coupling conditions to create significant amounts of reduced arene. These results suggest cross-coupling with fluorinated boronic acids is difficult due to degradation of the boronic acid.

We also wished to investigate if fluoride activation was necessary for cross-coupling reactions with silicon nucleophiles. During optimisation for the Hiyama reactions we found that by replacing TBAF with NaOH as the activator, a novel protocol for the synthesis of aryl-alkyl ethers was discovered and the Pd catalysed C-O bond formation was taken further and comprehensively optimised. This is discussed in the following chapter.

Chapter 4. Pd catalysed C-O bond formation using alkoxy silanes as nucleophiles

During the optimisation of the Hiyama reaction for the arylation of alkenyl trialkoxysilanes, we discovered a novel process for the formation of aryl alkyl-ethers using NaOH as an alternative activator to TBAF. In this chapter, I will discuss this alternative method for Pd-catalysed ether formation that makes use of alkoxy silanes with NaOH and TBAF as an activator (Scheme 61).



Scheme 61. Changing activator: Hiyama vs. aryl ether synthesis

Palladium-catalysed C–O bond forming reactions potentially have several advantages over S_NAr and Ullman reactions, including high functional group tolerance, the use of common, relatively benign solvents, and the use of some less-reactive aryl halide electrophiles under mild conditions. However, in contrast to Pd-catalysed C–N bond forming reactions, developments in Pd-catalysed C–O bond formation have been slow, with many limitations still to overcome. The Pd-catalysed synthesis of diaryl ethers using phenols as nucleophiles has been improved markedly providing that specific bi-aryl phosphines are used.^{45, 124-126, 138-141} However, various reports in the literature have highlighted problems with alkyl aryl ether synthesis or report a very small selection of examples, often in moderate yields.^{120, 125}

A recent example from Buchwald¹¹⁶ who has switched to researching Cu-catalysed C-O bond formation, admits limitations in their previous Pd-catalysed process (However, at present the Cu-system is even less effective).

We decided to use aryl halides and a cheap readily available silicon source in the form of vinyltrimethoxysilane. By simply switching the activator from TBAF (for Hiyama activation) to NaOH we found a significant amount of aryl ether product being formed. Due to reasons above, we felt that optimisation and further study of this, to the best of our knowledge, unprecedented variant of the Pd catalysed C-O bond formation was needed.

One exciting possibility was that the formation of the pentavalent Si species removes the OH^- from solution making the reaction effectively base-free and reducing the possibility of β -hydride elimination (which can compete with reductive elimination) generating a significant amount of reduced arene and aldehyde, one of the key problems in the Buchwald directed C-O coupling reaction (Figure 20, Scheme 62).¹¹⁶

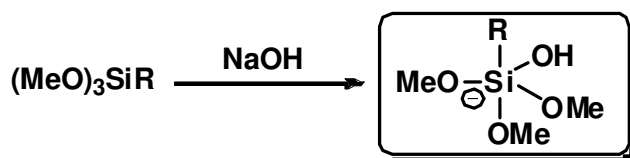
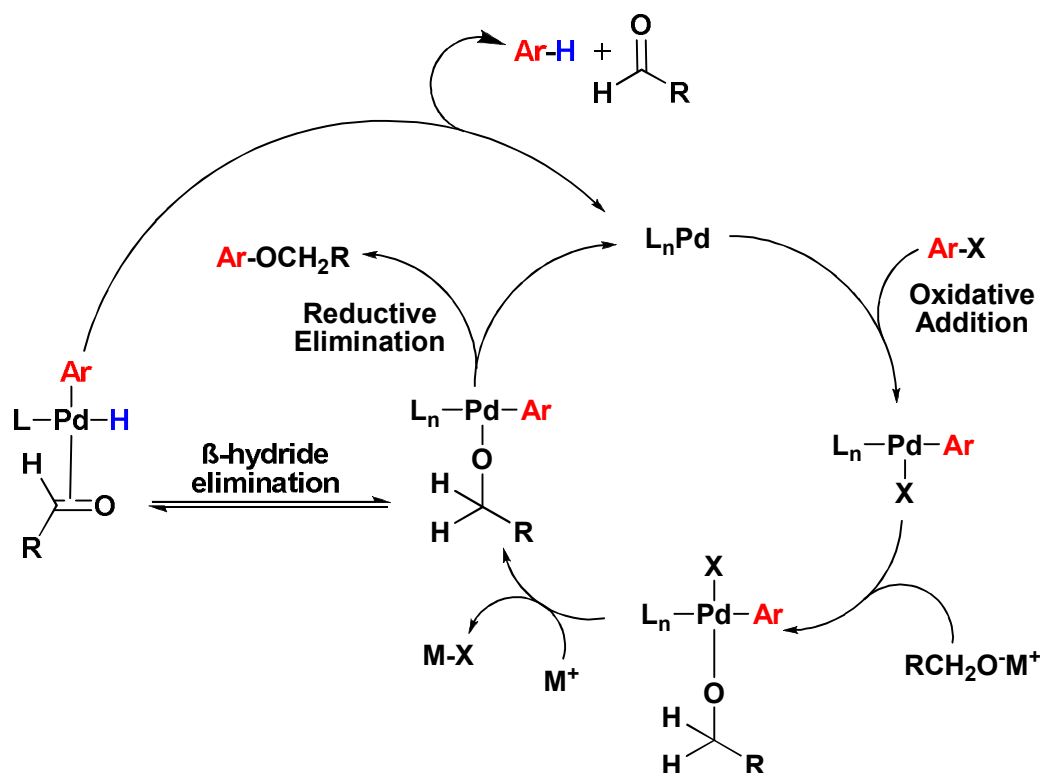
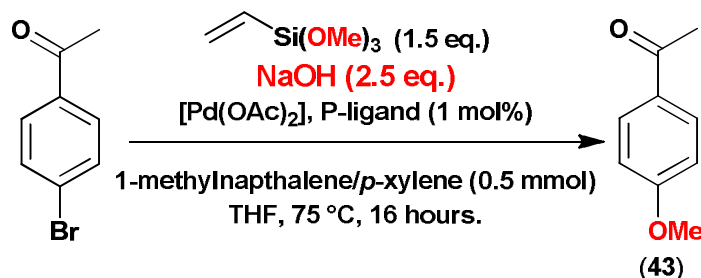


Figure 20. Proposed pentavalent Si species in the aryl ether synthesis



Scheme 62. Buchwald-Hartwig mechanism for aryl ether synthesis

By using the model substrate *p*-bromoacetophenone (1 mmol), and internal standards (*p*-Xylene or 1-methyl naphthalene) to calibrate against, we were able to calculate % conversion to aryl methyl ether (**43**) from ¹H NMR spectroscopy backed up by GCMS (Scheme 63).



Scheme 63. Aryl methyl ether synthesis from *p*-bromoacetophenone

An extensive optimisation process was carried out. A wide range of monodentate and bidentate phosphine ligands were tested and we found that electron rich wide bite angle ferrocenyl phosphine ligands performed best. All of the monodentate ligands performed poorly, returning <20% aryl ether product (**43**) and were not taken further (Table 16).

By altering the Ligand to Pd ratio (Table 16), we were able to tune the catalyst to give better conversion with dtbdppf/Pd(OAc)₂ (2:1) giving 59% conversion to the methyl ether (**43**) (Entry 5). The next step was to assess the source of the Pd in the reaction protocol. Interestingly Pd(dba)₂ performed worse than Pd(OAc)₂ (Entries 7 & 18), this could be due to the lability of the acetate groups making the generation of the active Pd⁽⁰⁾ species in the likely catalytic cycle an easier process.

A range of Pd salts were tested including pre-formed catalyst in the form [Pd(P-P)Cl₂] (Entries 9, 10 & 19) and it was observed that Pd(OAc)₂ and the ligand forming the complex *in-situ* returned the best results (dtbdppf, 2:1, 59%, Entry 5), (dcypb, 3:1, 48%, Entry 17). Reducing the performed precatalyst [Pd(dtbdppf)Cl₂] *in situ* with NaCNBH₃ (Entry 10) shows no net change in reactivity compared to the catalyst alone (Entry 9). This shows that catalyst activation (Pd^(II)-Pd⁽⁰⁾) does not cause a problem since an increase in conversion would have been observed. Control reactions with No Pd and no ligand gave 0% conversion respectively (Entries 29 & 30), indicating the Pd source and ligand are needed to mediate this reaction (Table 16).

Entry	Pd source	Ligand	L/Pd ratio	% Conversion to methyl ether^[a]
1	Pd(OAc) ₂	dippf	(1:1)	38
2	Pd(OAc) ₂	dtbpf	(1:1)	40
3	Pd(OAc) ₂	dtbdppf	(1:1)	42
4	Pd(OAc) ₂	dtbdppf	(1.5:1)	41
5	Pd(OAc) ₂	dtbdppf	(2:1)	59
6	Pd(OAc) ₂	dtbdppf	(3:1)	29
7	Pd(dba) ₂	dtbdppf	(2:1)	26
8	Pd(tfa) ₂	dtbdppf	(2:1)	9
9	[Pd(dtbdppf)Cl ₂]	-	-	20
10	[Pd(dtbdppf)Cl ₂] + NaCNBH ₃ (2 eq.)	-	-	21
11	Pd(OAc) ₂	dppf	(1:1)	20
12	Pd(OAc) ₂	dppe	(1:1)	16
13	Pd(OAc) ₂	dppb	(1:1)	9
14	Pd(OAc) ₂	dcype	(1:1)	21
15	Pd(OAc) ₂	dcypb	(1:1)	41
16	Pd(OAc) ₂	dcypb	(2:1)	46
17	Pd(OAc) ₂	dcypb	(3:1)	48
18	Pd(dba) ₂	dcypb	(2:1)	10
19	[Pd(dcypb)Cl ₂]	-	-	28
20	Pd(OAc) ₂	dcypx	(1:1)	11
21	Pd(OAc) ₂	PPh ₃	(2:1)	16
22	Pd(OAc) ₂	PCy ₃	(2:1)	10
23	Pd(OAc) ₂	(Me)Cage P	(2:1)	16
24	Pd(OAc) ₂	2-pyridyl-diphenyl P	(2:1)	12
25	Pd(OAc) ₂	tris-(<i>p</i> -methoxyphenyl) P	(2:1)	18
26	Pd(OAc) ₂	tris-(3,5-bis-(trifluoromethyl)phenyl) P	(2:1)	7
27	Pd(OAc) ₂	tris-(2-benzofuranyl) P	(2:1)	0
28	Pd(OAc) ₂	S-Phos	(2:1)	8
29	Pd(OAc) ₂	-	-	0
30	-	dtbdppf	-	0

Reagents & conditions: *p*-bromoacetophenone (1 mmol), vinyltrimethoxysilane (1.5 mmol), NaOH (2.5 mmol), Pd source: 1 mol%, THF, reflux, 16 h. ^[a] Calculated by ¹H NMR calibrated against *p*-Xylene/1-methylnaphthalene (0.5 mmol) as an internal standard, remaining is starting material.

Table 16. Ligand & Pd source optimisation for aryl methyl ether synthesis

Solvent effects were investigated (Table 17) and a huge increase was found using toluene at reflux giving 71% conversion to methyl ether (Entry 3). Interestingly H₂O gave 60% conversion (Entry 6) and an aqueous solution of NaOH in THF gave 33% (Entry 9).

This could be due to a large amount of OH^- in solution having an inhibitory effect. 75°C was a sufficient temperature and even compared to favourably refluxing toluene. Pleasingly, *p*-chloroacetophenone could also be coupled in 60% conversion in either THF or toluene (Entries 5 & 8).

<u>Entry</u>	<u>Solvent</u>	<u>Substrate</u>	<u>Oil bath Temperature (°C)</u>	<u>% Conversion by ^1H NMR</u>
1	Butan-2-one	<i>p</i> -bromoacetophenone	80	45
2	EtOH	<i>p</i> -bromoacetophenone	80	44
3	Toluene	<i>p</i>-bromoacetophenone	120	71
4	Toluene	<i>p</i>-bromoacetophenone	75	80
5	Toluene	<i>p</i>-chloroacetophenone	75	60
6	H ₂ O	<i>p</i> -bromoacetophenone	120	60
7	THF	<i>p</i> -bromoacetophenone	80	53
8	THF	<i>p</i>-chloroacetophenone	80	60
9	THF + NaOH (aq)	<i>p</i> -bromoacetophenone	120	33
10	Me-THF	<i>p</i> -bromoacetophenone	80	20

Reagents & conditions: *p*-bromo/chloro acetophenone (1 mmol), vinyltrimethoxysilane (1.5 mmol), NaOH (2.5 mmol), Pd(OAc)₂: 1 mol%, dtbdppf: 2 mol%, 16 h.^[a.] Calculated by ^1H NMR calibrated against *p*-Xylene/1-methylnaphthalene (0.5 mmol) as an internal standard.

Table 17. Solvent effects

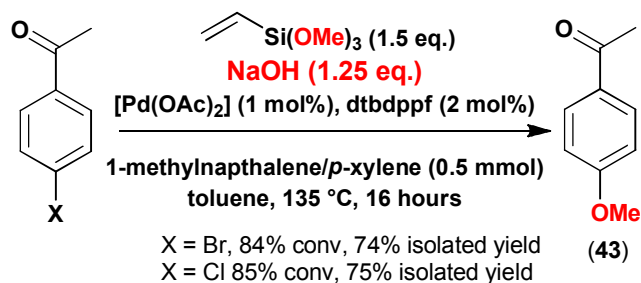
The amount of NaOH was varied from 0.625 eq. to 10 eq. (Table 18). Good results were obtained between 0.625-2.5 eq. with the optimum being 1.25 eq. There was also an inhibitory effect above 3 eq. Initial investigations were performed with NaOH pellets throughout but using powder seemed to improve the conversion slightly, this could be due to the increased surface area of the hydroxide being taken up into solution in small amounts. This could be the key in the formation of the aryl-ether by keeping a small amount of alkoxide in solution forming the pentavalent Si species. To test this theory 1eq. of NaOMe was used as the nucleophile and gave 0% conversion. This could indicate an excess of alkoxide in solution creates an inhibitory effect (Table 18).

<u>Nucleophile/Activator</u>	<u>NaOH/NaOMe</u> <u>(eq.)</u>	<u>% Conversion</u> <u>(by ¹H NMR)</u>
Vinyltrimethoxysilane/NaOH	0.625	60
Vinyltrimethoxysilane/NaOH	1	59
Vinyltrimethoxysilane/NaOH	1.25	85
Vinyltrimethoxysilane/NaOH	2.5	77
Vinyltrimethoxysilane/NaOH	3.5	0
Vinyltrimethoxysilane/NaOH	5	0
Vinyltrimethoxysilane/NaOH	7.5	0
Vinyltrimethoxysilane/NaOH	10	0
NaOMe	1	0

Reagents & conditions: *p*-bromoacetophenone (1 mmol), vinyltrimethoxysilane (1.5 mmol), NaOH (1.25 mmol), Pd(OAc)₂: 1 mol%, dtbdppf: 2 mol%, toluene, 16 h. Calculated by ¹H NMR calibrated against *p*-Xylene/1-methylnaphthalene (0.5 mmol) as an internal standard.

Table 18. Optimisation of the amount of NaOH used

In order to increase the conversion further, we used sealed tubes to conduct the reaction at 135 °C in toluene for 16 h with both *p*-chloroacetophenone and *p*-bromoacetophenone. The product (**43**) could also be isolated in high yield in both cases (Scheme 64).



Scheme 64. Sealed tubes for aryl methyl ether synthesis

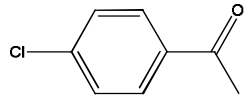
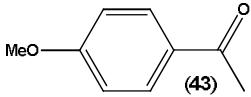
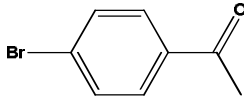
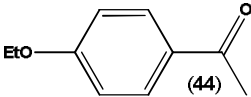
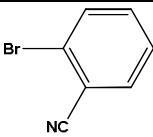
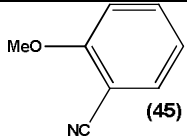
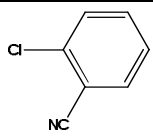
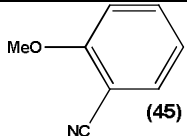
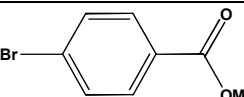
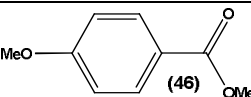
Better results were obtained under microwave heating conditions giving almost quantitative yields of the methyl ether from aryl chloride and bromide at 120 °C for 20 minutes with NaOH in either pellet (Entries 1-4) or powder (Entries 5-8) form (Table 19). The microwave procedure also works well with preformed catalyst [Pd(dtbdppf)Cl₂] (**15**) (Entries 3 & 4, 7 & 8). Presumably the shorter reaction time means less ligand is required, or that formation of the catalytically active species is easier in the microwave.

Entry	Precursor	X	NaOH	% Conversion by ¹ H NMR
1	1 mol% Pd(OAc) ₂ + 2 mol% dtbdppf	Br	Pellets	91, 95
2	1 mol% Pd(OAc) ₂ + 2 mol% dtbdppf	Cl	Pellets	96, 95
3	1 mol% [Pd(dtbdppf)Cl ₂]	Br	Pellets	95
4	1 mol% [Pd(dtbdppf)Cl ₂]	Cl	Pellets	98
5	1 mol% Pd(OAc) ₂ + 2 mol% dtbdppf	Br	Powder	90
6	1 mol% Pd(OAc) ₂ + 2 mol% dtbdppf	Cl	Powder	98
7	1 mol% [Pd(dtbdppf)Cl ₂]	Br	Powder	98
8	1 mol% [Pd(dtbdppf)Cl ₂]	Cl	Powder	94

Reagents & conditions: *p*-bromo/chloro acetophenone (1 mmol), vinyltrimethoxysilane (1.5 mmol), NaOH (1.25 mmol), Pd source: 1 mol%, dtbdppf: 2 mol% (if required), toluene, microwave heating, 120 °C, 20 mins. Calculated by ¹H NMR calibrated against *p*-Xylene/1-methylnaphthalene (0.5 mmol) as an internal standard.

Table 19. Microwave optimisation for the formation of an aryl methyl-ether (**44**)

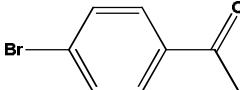
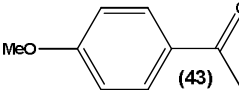
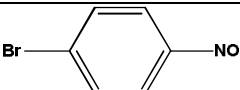
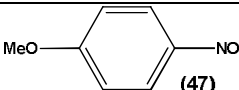
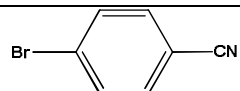
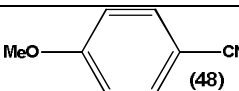
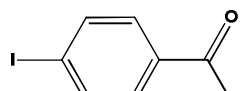
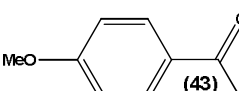
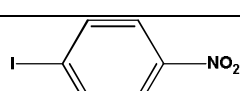
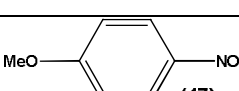
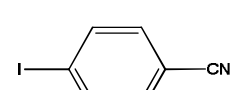
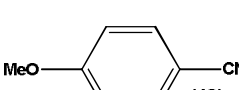
The next stage of the optimisation process was to assess the scope of the reaction protocol for some more aryl-halides (Table 20). The reactions gave excellent results for a range of activated aryl bromides and chlorides under microwave heating protocol. The products formed here could be isolated in high yield by column chromatography. A few other substrates, such as 2-chlorobenzotrifluoride, did seem to couple but decomposed.

Entry	Aryl halide	Product	Conversion (yield) [%]
1			84 (74)
2			85 (77)
3			84 (74)
4			86 (72)
5			75 (66) ^[a]

Reagents & conditions: 1 mol% Pd precursor, 2 mol% dtbdppf as ligand, 1.5 eq. vinyltrimethoxysilane, 1.25 eq. NaOH, 0.5 mmol *p*-Xylene or 1-methyl-naphthalene as internal standard, stirred at 120 °C in toluene under MW heating, 20 mins.; yields refer to pure compounds after chromatography, ^[a] 2.0 eq. vinyltrimethoxysilane.

Table 20. Pd catalysed C-O bond formation with a range of aryl chlorides and bromides

It is interesting to note that aryl iodides compared to their analogous bromide counterparts give lower conversion (Table 21). This could simply be that the aryl iodide oxidatively adds to the Pd catalyst with ease but the size of the iodide prevents transmetalation of the Si nucleophile due to the steric bulk.

Entry	Aryl halide	Product	Conversion (yield) [%]
1		 (43)	84 (77)
2		 (47)	84 (70)
3		 (48)	86 (73)
4		 (43)	26 (30 Reduced arene) (44 SM)
5		 (47)	83 (17 SM)
6		 (48)	61 (19 Reduced arene) (20 SM)

Reagents & conditions: 1 mol% Pd precursor, 2 mol% dtbdppf as ligand, 1.5 eq. vinyltrimethoxysilane, 1.25 eq. NaOH unless otherwise stated, Conversions are calibrated against an internal standard (0.5 mmol *p*-Xylene or 1-methyl-napthalene), stirred at 120 °C in refluxing toluene for 16 h.; yields refer to pure compounds after chromatography, identity of various products and side products were confirmed by GCMS.

Table 21. Pd catalysed C-O bond formation with a range of aryl bromides and iodides

If this were the case and the iodide is sterically encumbering the catalyst and preventing the transmetalation from the Si nucleophile, perhaps the reaction is mediated *via* the cyclic S_E2 mechanism (with retention of configuration) as previously discussed (Figure 21).

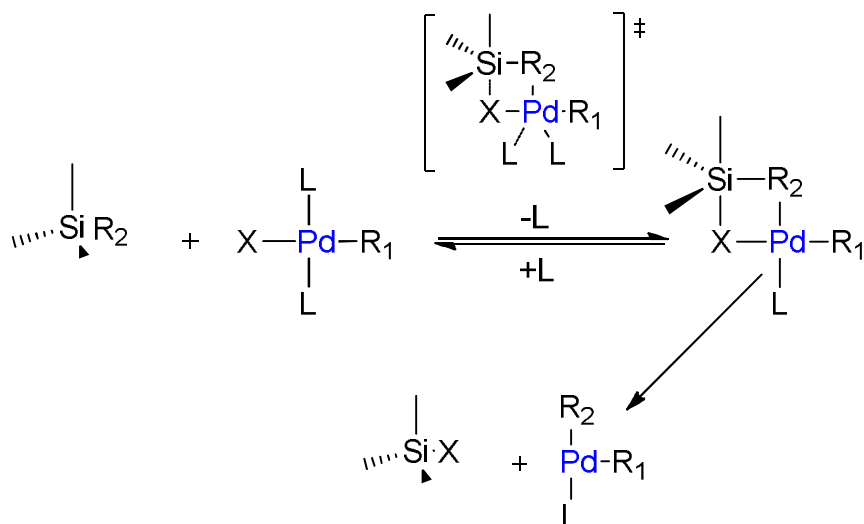


Figure 21. Possible mechanism for Pd mediated aryl ether synthesis

In these studies, using these relatively unoptimised conditions with simple commercially available diphosphine ligands, we have found that several aryl halides gave lower yielding reactions using vinyl trialkoxysilanes or tetraalkoxysilane nucleophiles. For example, *p*-dimethylamino-bromobenzene gave predominantly starting material with some reduced arene, whereas *o*-chloro-anisole, a much deactivated substrate (and perhaps the most challenging from a cross-coupling perspective), returned only starting material.

Vinyl trimethoxy- and vinyl triethoxysilanes are actually cheap fine chemicals and thus could be developed as nucleophiles for the synthesis of methyl and ethyl ethers. However, for this discovery to have a broader impact in the synthesis of aryl-alkyl ethers the reactions needed to be extended to readily available tetraalkoxysilanes; we were therefore delighted to find that simple tetraalkoxysilanes would also undergo this reaction (even more) readily. A range of silyl ether sources were assessed and synthesised where necessary.

By switching from NaOH back to TBAF as the activator, access to OMe (**43**) (80% conversion, Entry 1), OEt (**44**) (79% conversion, Entry 4), O^nPr (**49**) (70% conversion, Entry 6) and O^nBu (**50**) (86 % conversion with TBAF, Entry 9) ethers was obtained from the corresponding tetraalkoxysilanes and *p*-bromoacetophenone with success (Figure 22, Table 22).

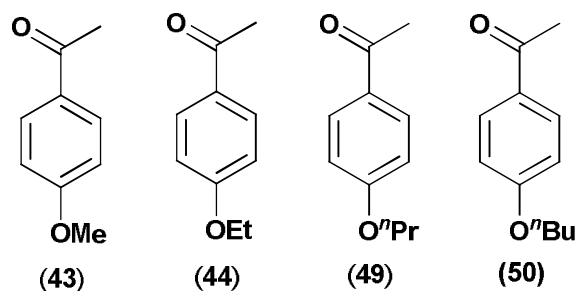


Figure 22. Aryl-alkyl ethers synthesised

Entry	Silane	Activator	Conversion (yield) [%]
1	Si(OMe) ₄	NaOH (1.25 eq.)	80 (72)
2	Si(OMe) ₄	TBAF (3 eq.)	78
3	Si(OEt) ₃ H	NaOH (1.25 eq.)	82 (73)
4	Si(OEt) ₄	NaOH (1.25 eq.)	79 (67)
5	Si(OEt) ₄	TBAF (3 eq.)	68 ^[a]
6	Si(O ⁿ Pr) ₄	NaOH (1.25 eq.)	70 (65)
7	Si(O ⁿ Pr) ₄	TBAF (3 eq.)	80
8	Si(O ⁿ Bu) ₄	NaOH (1.25 eq.)	50 (42)
9	Si(O ⁿ Bu) ₄	TBAF (3 eq.)	86(73)

Reagents & conditions: *p*-bromoacetophenone (1 mmol), Pd(OAc)₂: 1 mol%, dtbdppf: 2 mol%, 1.5 eq. silane, 0.5 mmol *p*-Xylene or 1-methyl-naphthalene as internal standard, stirred at 120 °C in toluene under microwave heating conditions for 20 mins. Conversions are calibrated against internal standards; yields refer to pure compounds after chromatography. ^[a] The coupling of Si(OEt)₄ with *p*-bromonitrobenzene also gave high isolated yield (81%) using TBAF in toluene.

Table 22. Pd catalysed C-O bond formation with various silanes and *p*-bromoacetophenone

Secondary alcohols were utilised in the synthesis of tetraalkoxysilanes, (which proved problematic in the purification stage) and performed poorly. By reacting SiCl₄ with a variety of branched and secondary alcohols, the appropriate tetraalkoxysilane was synthesised. Purification by short-path distillation apparatus proved to be tricky as a statistical mix of products were formed (Si(OR)₄, Si(OR)₃Cl, Si(OR)₂Cl₂ and Si(OR)Cl₃, which were detected by ²⁹Si NMR spectroscopy) with similar boiling points.

The tetraalkoxysilanes also hydrolysed readily and had to be stored under a dry, inert atmosphere. The formation of a mixed Si alkoxy silane (with OEt groups on one side and OCH₂CF₃ on the other) was also attempted in order to probe if the alkoxy group leaves the silane or is transferred from Si to Pd. However, similar problems occurred on purification with mixed products being observed at each attempt.

By introducing branched chains however, it was found that this is not tolerated by the catalyst and no ether product was observed. It seems the reaction process may have to be re-optimised to achieve successful formation of any branched ether.

Tetraisopropoxysilane and alkoxy silanes derived from tertiary alcohols have proven rather unreactive in these first studies; a contrast to the latter being easier nucleophiles¹²⁰ in the direct reaction that possibly reflects that some of the reactions here are limited by slow transmetalation using these relatively bulky catalysts,³⁵ whereas the direct process under harsher conditions just needs to control chemoselectivity (and tertiary alcohols cannot undergo β -hydride elimination).

This reflects that a more in-depth study developing new catalysts for this new variant of C-O coupling is required before it is truly general in scope. The results described here suggest considerable potential for using alkoxy silanes as oxygen nucleophiles, and given that the contrasting reactivity patterns (*e.g.* in the preferred choice of catalyst) were seen to the direct coupling of alcohols, the new procedure may prove to be complementary to the existing methodology.^{123,142}

Chapter 5. Conclusions & Further Work

The development of a “super-concentrated” (5M) Pd catalysed Kumada type coupling reaction has been developed with a few aryl bromide and chloride substrates and a fluorinated Grignard reagent ($(p\text{-CF}_3\text{-C}_6\text{H}_4)\text{MgBr}$). PhMgBr was also synthesised as a 5M solution in Me-THF and employed in these cross-coupling procedures. The use of much smaller volumes of solvent and simpler work-up procedures it is hoped will make an industrially viable process. Me-THF has also been utilised in the synthesis of $[\text{Pd}(\text{P-P})\text{Cl}_2]$ catalysts in a microwave procedure that allows simple filtration of the desired complex, washing with water and drying. Pleasingly, good results were obtained in the Kumada-type coupling of a range of aryl halides at low catalyst loading. For example, 2-bromo-4-fluoroanisole (96% conversion) and *p*-bromoanisole (67% conversion) cross coupled with PhMgBr in 2 h at 50 °C. The deactivated aryl bromide *p*-bromo-*N,N'*-dimethylaniline required heating to 55 °C for 6 h with PhMgBr (61%) and an activated aryl chloride *p*-chlorobenzonitrile required elevated temperature (75 °C) and a prolonged heating time of 6 h with PhMgBr (93%). The fluorinated Grignard pleasingly gave a 67% conversion with 2-bromo-4-fluoroanisole to the desired fluorinated bi-aryl in 2 h at 50 °C.

Further investigation is required for this reaction to be more generalised. It is hoped the use of Me-THF in much smaller quantities will be a viable alternative to current procedures for Grignard cross-coupling reactions.

The reactivity of bulky ferrocenyl phosphino ligands has shown interesting ligand interactions and different modes of bonding when certain geometries are enforced on the metal. A novel $[\text{Pt}(\text{P-P})(\text{COD})\text{X}]\text{X}^-$ (where X = Cl, Br) complex has been synthesised and was discovered in the synthesis of simple $[\text{Pt}(\text{P-P})\text{Br}_2]$ complexes. The unsymmetrical ligand dtbdppf has proved to have different bonding mode to dippf and dtbpf and also proved to be an excellent ligand for promoting C-C and C-O bond formation under Pd catalysed conditions.

An investigation into ligand effects on the Pd catalysed Hiyama coupling of *p*-bromoacetophenone has been performed; competition experiments with Suzuki coupling chemistry have shown vinyltrimethoxysilane to be a poor nucleophile in that it cannot compete with phenylboronic acid and fluorinated boronic acids. Varying the concentration of Si nucleophile has shown an inhibitory effect above and below 1.5 eq.

Fluorinated boronic acids have been shown to be unstable under cross-coupling and competition conditions and protodeboronate in solution; even in the absence of catalyst in solution under typical Suzuki cross-coupling conditions to create significant amounts of reduced arene. These results suggest cross-coupling with fluorinated boronic acids is difficult due to degradation of the boronic acid.

A novel protocol has been developed for the synthesis of aryl-alkyl ethers *via* C-O bond formation under Pd catalysed conditions. Utilising the unsymmetrical 1-*bis*-(ditertiarybutyl-1'-*bis*-diphenylphosphino)ferrocene (dtbdppf) under optimised conditions with silicon based nucleophiles and NaOH or TBAF as an activator, the formation of methyl (85%), ethyl (82%), propyl (80%) and *n*-butyl (76%) ethers was achieved. The scope of the reaction with various aryl halides in >90% conversion demonstrates the versatility of the reaction and allowed the introduction of various functionalities into the molecules synthesised. Branched and secondary alcohols were not tolerated by this system and a complete re-optimisation may be necessary to mediate these reactions and create a general reaction protocol for a wide range of aryl-alkyl ethers similarly, some deactivated.

In the future, the role of the ligand and catalytic species is vital to grasp the concepts involved with successful cross-coupling. A delicate balance between steric and electronic interactions of the ligand-metal relationship must be struck to promote all three steps of the Pd catalysed cycle. A better understanding of these concepts allows rational design for various systems and allows the formation of useful products from “difficult” substrates. Using Pt complexes as models for the analogous Pd catalysts can gain insight and alleviate problems to create a better system.

Chapter 6. Experimental

An inert atmosphere of N₂ or Argon and Schlenk line techniques were used throughout preparative procedures. *In vacuo* refers to the use of a Heidolph[®] Laborota 4000 rotary evaporator with a KNF[®] Laboport pump or a high vacuum line equipped with an Edwards[®] rotary vane pump pulling <0.5 mm Hg. Solvents were degassed by several freeze thaw cycles before use and purified *via* alumina columns in a Grubbs system Braun MSB 8000 still or distilled from sodium-benzophenone (diethyl ether, THF), sodium (toluene), or CaH₂ (CH₂Cl₂). Petroleum ether refers to petroleum ether 40-60°. Acetonitrile and NMR solvents (CDCl₃, CD₂Cl₂, CD₃CN and C₆D₆) were dried over activated 4Å molecular sieves and degassed by several freeze thaw cycles before use.

Na₂PdCl₄ was purchased from Aldrich. K₂PtCl₄ and K₂PtBr₄ were donated from Alfa-Aesar or purchased from Strem and kept under an inert atmosphere. All ferrocene ligands were purchased from Strem or Aldrich, stored under argon and used without further purification. Reagents used for Suzuki, Hiyama and silicon cross-coupling reactions were purchased from Aldrich, dried over activated 4 Å molecular sieves where appropriate and degassed by several freeze thaw cycles before use. Room temperature (RT) refers to 20-25 °C. Temperatures at 0 °C were obtained with a slush-ice bath and at -78 °C were obtained using a dry ice/acetone bath. Reaction reflux conditions were obtained by using an oil bath equipped with a contact thermometer. All microwave syntheses were carried out in a Biotage[®] Initiator Microwave reactor in 10 mL heavy-walled glass reactor vials equipped with an air tight seal. The temperature is measured by an infra red temperature probe that measures the temperature on the surface of the vial. The pressure is measured by direct reading of the deflection of the septa on the vial using a load cell behind the inner part of the cavity lid.

¹H, ¹³C, ¹⁹F and ³¹P Nuclear Magnetic Resonance (NMR) spectra were acquired with a Bruker[®] Avance DPX 300/Avance II 400 Ultrashield spectrometer at 298K in the deuterated solvent stated and referenced to Si(CH₃)₄, residual solvent resonances (¹H) or external references (¹³C, ¹⁹F and ³¹P).

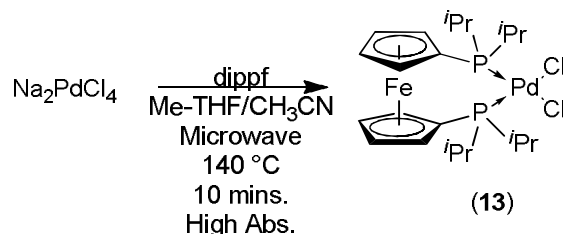
Signal positions were recorded in δ p.p.m with the abbreviations s, bs, d, dd, t, q, br and m denoting singlet, broad singlet, doublet, doublet of doublets, triplet, quartet, broad and multiplet respectively. The abbreviation Ar is used to denote aromatic. All NMR chemical shifts are quoted in ppm. All coupling constants, J are quoted in Hertz (Hz).

GC-MS spectra were acquired with an Agilent® 6890+ Series GC system equipped with an Agilent® 5973 Network Mass Selective Detector (MSD). Using a Supelco® MDN-35 column, (30 m x 250 μ m, 0.25 μ m) and He as the carrier gas at a constant flow rate of 1 mL/min. The temperature was ramped up from 50-280 °C over a period of 26 mins, using an injection of 1 μ L of sample.

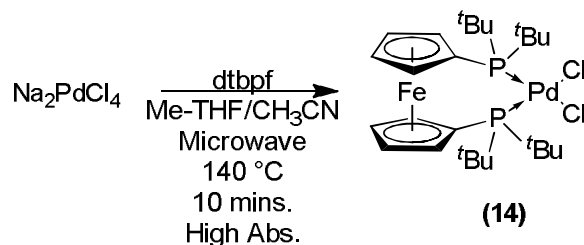
X-ray crystallography data for complexes **24**, **26**, **28** & **54** were collected at 93 K by using a Rigaku MM007 High brilliance RA generator and Mercury CCD system. Intensities were corrected for Lorentz-polarisation and for absorption. The structures were solved by direct methods. Hydrogen atoms bound to carbon were idealised. Structural refinements were obtained with full-matrix least-squares based on F^2 by using the program SHELXTL.

Mass Spectrometry data were obtained from the EPSRC National Mass Spectrometry Service Centre, Swansea by LSIMS fast atom bombardment methods. Complexes **13-28**, **54** and [Pt(dppe)R₂] (where R = Cl, I, *o*-Tol and *p*-Tol) were prepared by well known literature methods.^{143,144,145}

6.1 Pd /Pt complexes & Transmetalation Studies

1,1'-bis(diisopropylphosphino)ferrocene palladium(II) dichloride [Pd(dippf)Cl₂] (13)

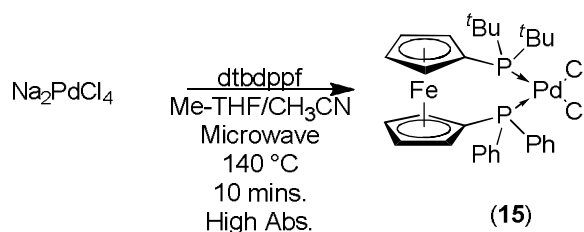
Using Method B, 1,1'-bis(diisopropylphosphino) ferrocene (dippf) (1 eq., 0.142 g, 0.339 mmol) was added to a solution of Na₂PdCl₄ (0.1 g, 0.339 mmol) in Me-THF/acetonitrile (3 mL / 0.1 mL) to give a dark orange solution, which was subjected to microwave conditions at 140 °C for 10 minutes at high absorption to give a red precipitate. The precipitate was filtered, washed with water (2 mL to remove NaCl) and dried under vacuum. (Distilled water (5 mL) was then added to the remaining reaction mixture, the aqueous phases were extracted, dried over MgSO₄ and concentrated *in vacuo* to give no further material) (0.201 g, 0.339 mmol, >99%, (>95% pure by ³¹P{¹H} NMR). ¹H NMR (300.06 MHz, CDCl₃) δ_H = 1.15 (dd, 12H, *J* = 7.1, 15.3 Hz, CH₃), 1.56 (dd, 12H, *J* = 7.1, 15.3 Hz, CH₃), 2.95 (dq, 4H, *J* = 7.1 Hz, CHP), 4.45 (s, 4H, CpH), 4.54 (s, 4H, CpH); ³¹P{¹H} NMR (121.466 MHz, CDCl₃) δ_P = 64.47 (s) [Lit (C₆D₆) δ_P = 65.8 (s)]; ¹³¹LR-MS: [FAB] [M-Cl]⁺ = 559.0.

1,1'-bis(ditertiarybutylphosphino)ferrocene palladium(II) dichloride [Pd(dtbpf)Cl₂] (14)

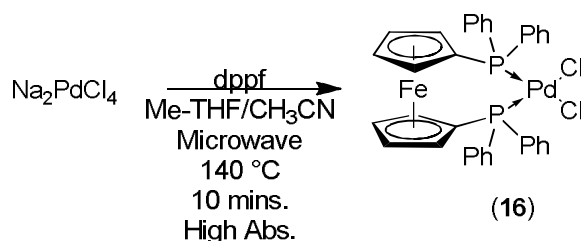
Using Method B, 1,1'-bis(ditertiarybutylphosphino) ferrocene (dtbpf) (1 eq., 0.161 g, 0.339 mmol.) was added to a solution of Na₂PdCl₄ (0.1 g, 0.339 mmol) in Me-THF/acetonitrile (3 mL / 0.1 mL) to give a yellow/brown solution, which was subjected to microwave conditions at 140 °C for 10 minutes at high absorption to give a red precipitate. The precipitate was

filtered, washed with water (2 mL to remove NaCl) and dried under vacuum. Distilled water (5 mL) was then added to the remaining reaction mixture, the aqueous phases were extracted, dried over MgSO₄ and concentrated *in vacuo* to give no further material) (0.221 g, 0.339 mmol, >99 % (>95% pure by ³¹P{¹H} NMR). ¹H NMR (300.06 MHz, CDCl₃) δ_H = 1.51-1.59 (m, 36H, CH₃), 4.45 (s, 4H, CpH), 4.54 (s, 4H, CpH), [Lit δ_H = 1.68 (3 x dd, 36H, J = 13.6 Hz, CH₃), 2.91-2.98 (m, 4H, CHP), 4.49 (bs, 4H, 2 x CH₂), 4.85 (bs, 4H, 2 x CH₂)]¹⁴⁶; ³¹P{¹H} NMR (121.466 MHz, CDCl₃) δ_P = 67.82 (s); LR-MS: [FAB] [M-Cl]⁺ = 615.10.

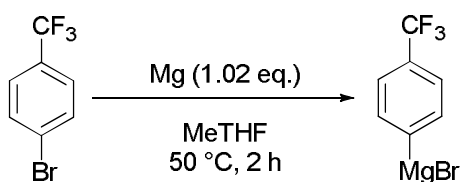
1-*bis*(ditertiarybutylphosphino)-1'-*bis*(diphenylphosphino)ferrocene palladium(II) dichloride [Pd(dtbdppf)Cl₂] (15)



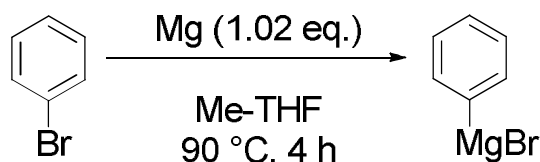
Using Method B, 1-*bis*(ditertiarybutyl)-1'-*bis*(diphenylphosphino)ferrocene (dtbdppf) (1 eq., 0.174 g, 0.339 mmol) was added to a solution of Na₂PdCl₄ (0.1 g, 0.339 mmol) in Me-THF/acetonitrile (3 mL / 0.1 mL) to give a red solution, which was subjected to microwave conditions at 140 °C for 10 minutes at high absorption to give a red precipitate. The precipitate was filtered, washed with water (2 mL to remove NaCl) and dried under vacuum. (Distilled water (5 mL) was then added to the remaining reaction mixture, the aqueous phases were extracted, dried over MgSO₄ and concentrated *in vacuo* to give no further material) (0.234 g, 0.339 mmol, >99 %, (99% pure by ³¹P{¹H} NMR). mp >230°C; ¹H NMR (300.06 MHz, CDCl₃) δ_H = 1.56 (d, 18H, J = 14.6 Hz, CH₃), 3.87 (s, 2H, CHP), 4.21 (s, 2H, CpH), 4.43 (s, 2H, CpH), 4.81 (s, 2H, CHP), 7.20-7.38 (m, 6H, ArH), 7.91-8.03 (m, 4H, ArH) [Lit δ_H = 1.63 (d, 18H, J = 16 Hz CH₃), 3.85-4.40 (bm, 4H, CHP), 7.32-7.52 (m, 6H, ArH), 7.88-8.23 (m, 4H, ArH)]¹⁴⁶; ³¹P{¹H} NMR (121.466 MHz, CDCl₃) δ_{P(tBu)} = 39.565 (d, 1P) (²J_{P-P} = 20.9 Hz), δ_{P(Ph)} = 81.275 (d, 1P) (²J_{P-P} = 20.9 Hz); ¹³C NMR (75.450 MHz, 298K, CDCl₃) δ_C = 31.8 (CH₃, ^tBu), 39.1 (C_{quat}), 53.3 (C_{quat}), 72.1(d) CpCH (J = 6.8 Hz), 72.2 (d) CpCH (J = 6.8 Hz), 75.4 (d) CpCH (J = 7.2 Hz), 128.0 (d) ArCH (J = 11.6 Hz), 130.7 (ArCH), 134.8 (C_{quat}), 135.0 (d) ArCH (J = 11.5 Hz); LR-MS: [FAB] [M-Cl]⁺ = 655.0.

1,1'-bis(diphenylphosphino)ferrocene palladium(II) dichloride [Pd(dppf)Cl₂] (16)

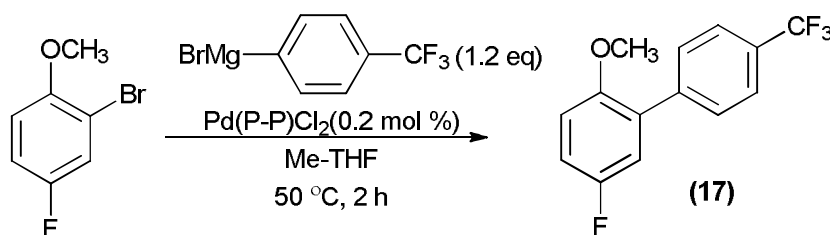
Using Method B, 1,1'-bis(diphenylphosphino) ferrocene (dppf) (1 eq., 0.188 g, 0.339 mmol) was added to a solution of Na₂PdCl₄ (0.1 g, 0.339 mmol) was dissolved in Me-THF/acetonitrile (3 mL / 0.1 mL to give a red orange solution, which was subjected to microwave conditions at 140 °C for 10 minutes at high absorption to give a red precipitate. The precipitate was filtered, washed with water (2 mL to remove NaCl) and dried under vacuum. (Distilled water (5 mL) was then added to the remaining reaction mixture, the aqueous phases were extracted, dried over MgSO₄ and concentrated *in vacuo* to give no further material) (0.248 g, 0.339 mmol, >99%, (>95% pure by ³¹P{¹H} NMR). ¹H NMR (300.06 MHz, CDCl₃) δ_H = 4.25 (s, 4H, CpH), 4.5 (s, 4H, CpH), 5.21 (s, 2H, CHP), 7.2-7.9 (m, 20H, ArH); ³¹P{¹H} NMR (121.466 MHz, CDCl₃) δ_P = 35.24 (s) [Lit δ_P = 34.5 (s)]¹³⁶; LR-MS: [FAB] [M-Cl]⁺ = 695.0.

“Synthesis of “Super concentrated” (5M) fluorinated Grignard (F₃C-*p*)ArMgBr)

4-Bromobenzotrifluoride (5 g, 3.07 mL, 22 mmol) in Me-THF (4.4 mL) was added DROPSWISE to the Mg (0.545 g, 1.02 eq., 22.4 mmol) NO INITIATOR NEEDED. CAUTION, EXOTHERM! (Heat generated sufficient to maintain gentle reflux). After addition, the reaction mixture was warmed to 50 °C for 2 h (until the Mg was consumed) to give a dark yellow solution. An aliquot was hydrolysed with ice-cold aqueous NH₄Cl and the organics dried over MgSO₄, ¹⁹F NMR spectroscopy of the organics showed a singlet at -61.028 p.p.m for benzotrifluoride. This confirms one species as the Grignard present before hydrolysis.

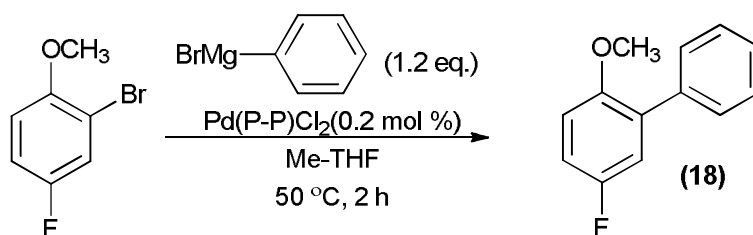
“Synthesis of “Super concentrated” (5M) Grignard (PhMgBr)

Bromobenzene (5 g, 3.36 mL, 32 mmol) in Me-THF (6.4 mL) was added DROPWISE to the Mg (0.789 g, 1.02 eq., 32.5 mmol) *via* an addition funnel. NO INITIATOR NEEDED. CAUTION, EXOTHERM! (Heat generated sufficient to maintain gentle reflux). After addition, the reaction mixture was warmed to 90 °C for 4 h (until the Mg was consumed) to give a bright orange solution. ^1H NMR showed a mixture of aryl peaks.

“Super concentrated” Grignard cross-coupling of 2-bromo-4-fluoroanisole ($\text{F}_3\text{CArMgBr}$) (17)

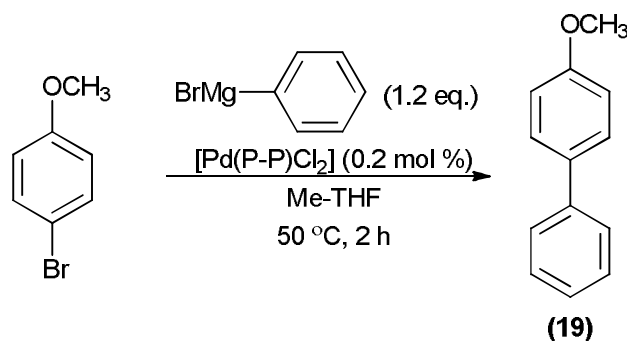
To a solution of the fluorinated Grignard in Me-THF (0.24 mL, 1.2 eq., 1.2 mmol), 2-bromo-4-fluoroanisole (0.205 g, 0.13 mL, 1 mmol) was added followed by the catalyst $[\text{Pd}(\text{dppf})\text{Cl}_2]$ (0.2 mol%, 1.46 mg) and the reaction mixture heated to 50 °C for 2 h. Excess Grignard was quenched with NH_4Cl , organics filtered through a plug of alumina. ^1H , ^{19}F NMR spectroscopy and GCMS showed the desired product. Excess Grignard was quenched with NH_4Cl , organics filtered through a plug of MgSO_4 and concentrated *in vacuo* to give a yellow oil. GCMS: Retention time, MS (EI) m/z (%): 18.345 mins (66%, $[\text{M}^+] = 270.1$ (100), 271.1 (15), 272.1 (1)) ($\text{C}_{14}\text{H}_{10}\text{F}_4\text{O}$ requires $[\text{M}^+] = 270.07$ (100), 271.07 (15.3), 272.07 (1.3)). Column chromatography (Petroleum ether 40-60) yielded a mixture of product and starting material (0.181 g, 67 % isolated yield of which 30% is product and 70% is SM due to coelution) as a colourless liquid. ^1H NMR (400 MHz, CDCl_3) $\delta_{\text{H}} = 3.79$ (3H, s, OCH_3), 6.88-7.01 (3H, m, ArCH), 7.19-7.24 (2H, m, ArCH), 7.52-7.62 (2H, m, ArCH); $^{19}\text{F}\{^1\text{H}\}$ NMR (376.5 MHz, CDCl_3) $\delta_{\text{F}} = -62.90$ (s), -122.65 (s) (Data in agreement with literature).¹⁴⁷

“Super concentrated” Grignard cross-coupling of 2-bromo-4-fluoroanisole (PhMgBr) (18)



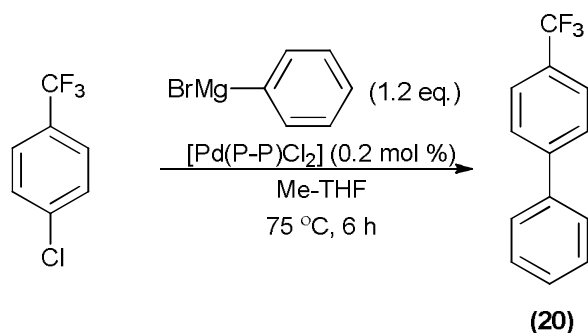
To a solution of the Grignard (PhMgBr) in Me-THF (0.24 mL, 1.2 eq., 1.2 mmol), 2-bromo-4-fluoroanisole (0.205 g, 0.13 mL, 1 mmol) was added followed by the catalyst [Pd(dppp)Cl₂] (0.2 mol%, 1.2 mg) and the reaction mixture heated to 50 °C for 2 h. Excess Grignard was quenched with NH₄Cl, organics filtered through a plug of MgSO₄ and concentrated *in vacuo* to give a yellow oil. GCMS: Retention time, MS (EI) *m/z* (%): 18.706 mins (96 %, [M⁺] = 202.1 (100), 203.1 (14)), (C₁₄H₁₀F₄O requires 202.08 (100), 203.08 (14.1)). Column chromatography (Petroleum ether 40-60) yielded the product as a colourless liquid (0.173 g, 0.86 mmol, 86 %) ¹H NMR (400 MHz, CDCl₃) δ_H = 3.82 (3H, s, OCH₃), 6.81 (1H, dd, *J* = 4.62, 8.8 Hz, ArCH), 6.87-6.94 (1H, m, ArCH), 6.96 (1H, dd, *J* = 3.2, 9.2 Hz, ArCH), 7.25 (1H, tt, *J* = 7.54, 1.4 Hz, ArCH), 7.34 (2H, t, *J* = 6.96 Hz, ArCH), 7.4-7.45 (2H, m, ArCH); ¹⁹F{¹H} NMR (376.5 MHz, CDCl₃) δ_F = -124.51; ¹³C NMR (100 MHz, CDCl₃) δ_C = 56.2, 112.4 (d, *J* = 8.5 Hz), 114.3 (d, *J* = 23.1 Hz), 117.4 (d, *J* = 23.1 Hz), 127.4, 128.2, 129.4, 132.0 (d, *J* = 10.1 Hz), 137.5, 152.7, 156.7 (d, *J* = 236.4 Hz); MS (EI) *m/z* (%): 202.1 (100.0) [M⁺], 203.1 (14.1). (Data in agreement with literature).⁵⁶

“Super concentrated” Grignard cross-coupling of 4-bromoanisole (PhMgBr) (19)



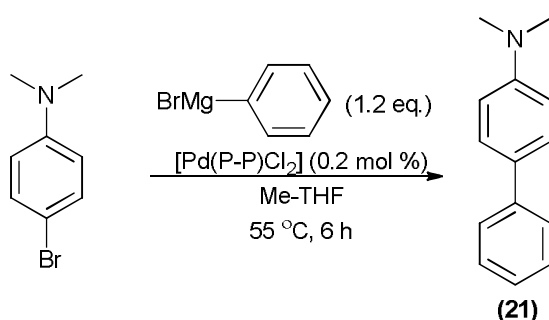
To a solution of the Grignard (PhMgBr) in Me-THF (0.24 mL, 1.2 eq., 1.2 mmol), 4-bromoanisole (0.187 g, 0.13 mL, 1mmol) was added followed by the catalyst [Pd(dppf)Cl₂] (0.2 mol%, 1.2 mg) and the reaction mixture heated to 50 °C for 2 h. Excess Grignard was quenched with NH₄Cl, organics filtered through a plug of MgSO₄ and concentrated *in vacuo* to give a yellow oil. GCMS: Retention time, MS (EI) m/z (%): 19.578 mins (66%, [M⁺] = 184.11 (100), 185.1 (15) (C₁₃H₁₂O requires [M⁺] = 184.09 (100), 185.09 (14.1))) (67 % product, 28 % SM, 5 % biaryl from Grignard) ¹H NMR (400 MHz, CDCl₃) δ_H = 3.82 (3H, s, OCH₃), 6.89 (2H, d, ArCH, *J* = 7.9 Hz), 7.02-7.6 (7H, m, ArCH) (Data in agreement with literature).³⁴

“Super concentrated” Grignard cross-coupling of 4-chlorobenzotrifluoride (PhMgBr)
(20)



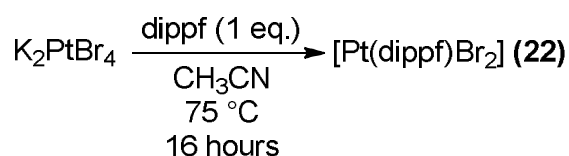
To a solution of the Grignard (PhMgBr) in Me-THF (0.24 mL, 1.2 eq., 1.2 mmol), 4-bromoanisole (0.181 g, 0.13 mL, 1mmol) was added followed by the catalyst [Pd(dppf)Cl₂] (0.2 mol%, 1.46 mg) and the reaction mixture heated to 75 °C for 6 h. Excess Grignard was quenched with NH₄Cl, organics filtered through a plug of MgSO₄ and concentrated *in vacuo* to give a yellow oil. GCMS: Retention time, MS (EI) m/z (%): 17.287 mins (97%, [M⁺] = 222.1 (100), 223.1 (15) (C₁₃H₉F₃ requires 222.07 (100), 223.07 (14.2)) (93% product, 7% SM) ¹H NMR (400 MHz, CDCl₃) δ_H = 7.01-7.60 (9H, m, ArCH); ¹⁹F{¹H} NMR (376.5 MHz, CDCl₃) δ_F = -62.886 (s) (Data in agreement with literature).⁶¹

“Super concentrated” Grignard cross-coupling of 4-bromo-*N,N'*-dimethylaniline (PhMgBr) (21)

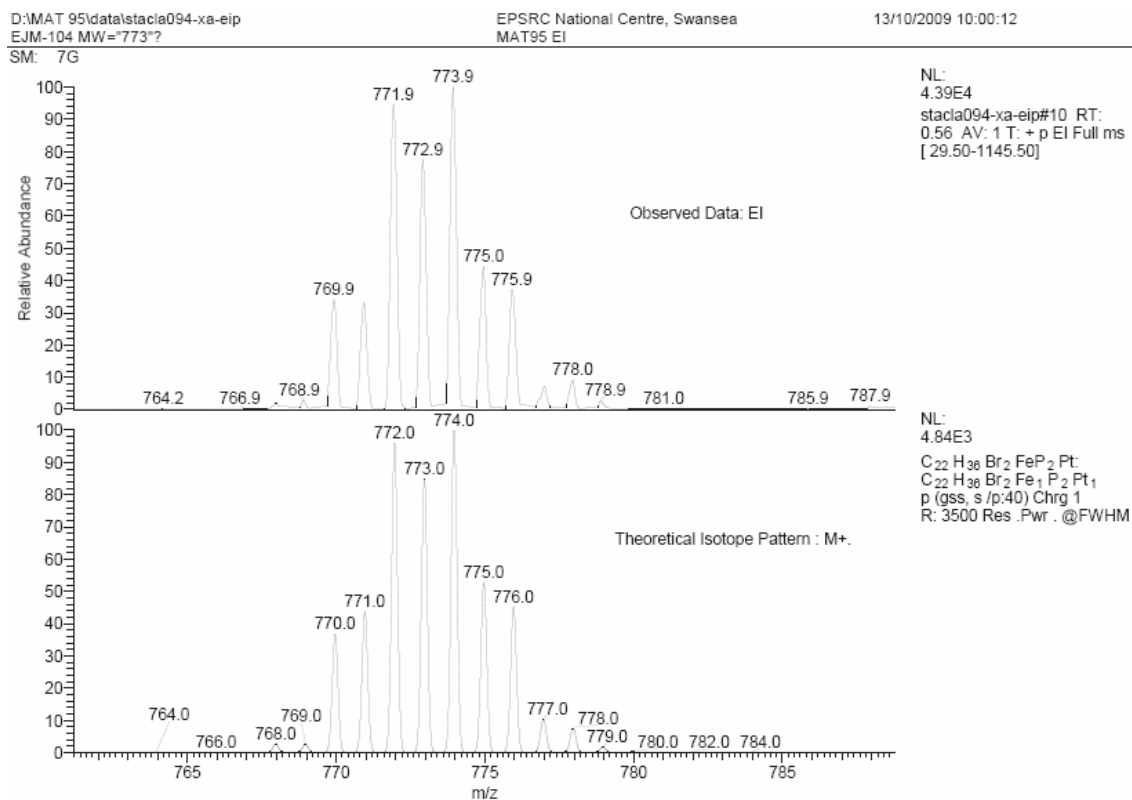


To a solution of the Grignard (PhMgBr) in Me-THF (0.24 mL, 1.2 eq., 1.2 mmol), 4-bromo-*N,N'*-dimethylaniline (0.2 g, 1mmol) was added followed by the catalyst [Pd(dppf)Cl₂] (0.2 mol%) and the reaction mixture heated to 55 °C for 6 h. Excess Grignard was quenched with NH₄Cl, organics filtered through a plug of MgSO₄ and concentrated *in vacuo* to give a yellow oil. GCMS: Retention time, MS (EI) *m/z* (%): 20.888 mins (66%, [M⁺] = 197.1 (100), 198.1 (16), 199.1 (1)) (C₁₄H₁₅N requires 197.12 (100), 198.12 (15.5), 199.13 (1.1)) (63% product, 37% SM). ¹H NMR (400 MHz, CDCl₃) δ_H = 3.21 (6H, s, N(CH₃)₂), 7.01-7.58 (9H, m, ArCH) (Data in agreement with literature).¹⁴⁸

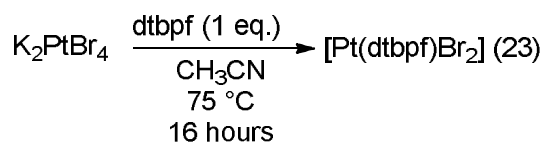
Synthesis of [Pt(dippf)Br₂] (22)



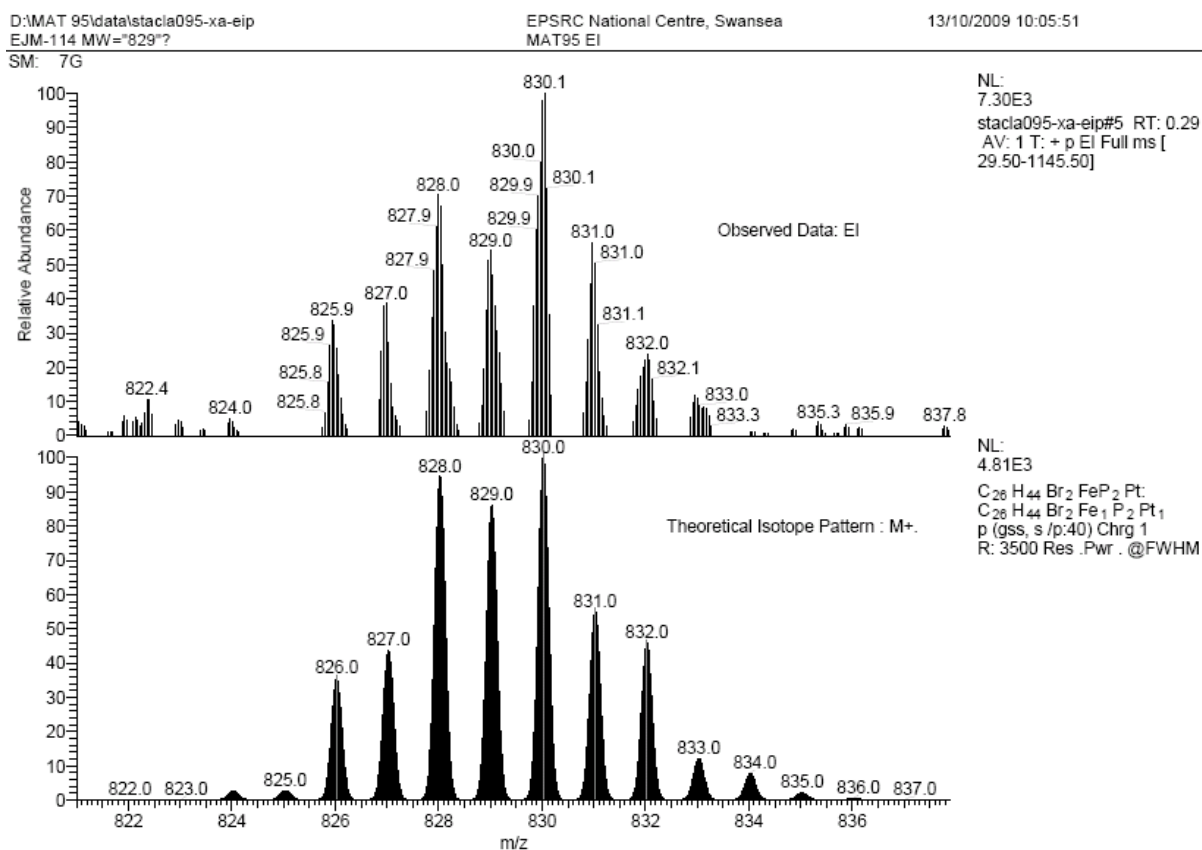
The diphosphine ligand (dippf) (0.064 g, 0.169 mmol) was added to K₂PtBr₄ (0.1 g, 0.169 mmol) followed by dry degassed acetonitrile (5 mL) and the reaction mixture heated to 75 °C for 16 hours. The yellow precipitate (0.146 g, 92%) was isolated by filtration, washed with water, dried under vacuum and required no further purification. ¹H NMR (400.130 MHz, CDCl₃) δ_H = 1.25 (m, 12H, CH₃), 1.75 (m, 12H, CH₃), 3.26 (m, 4H, CHP), 4.18 (s, 4H, CpH), 4.20 (s, 4H, CpH); ³¹P{¹H} NMR (161.976 MHz, CDCl₃) δ_P = 30.494 (s, 2P, ¹J_{P-Pt} = 3762.4 Hz); LR-MS: [FAB] [M⁺] = 773.0 (Isotope match – see below, Isotope matches of this quality were seen in all cases) (Data in accordance with the literature).¹³²



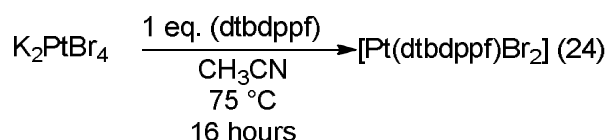
Synthesis of [Pt(dtbpf)Br₂] (23)



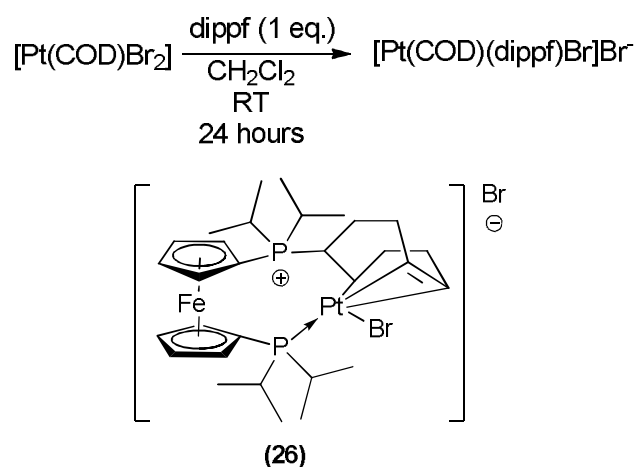
The diphosphine ligand (dtbpf) (0.051 g, 0.169 mmol) was added to K₂PtBr₄ (0.1 g, 0.169 mmol) followed by dry degassed acetonitrile (5 mL) and the reaction mixture heated to 75 °C for 16 hours. The orange precipitate (0.149 g, 89%) was isolated by filtration, washed with water and dried under vacuum and required no further purification. ¹H NMR (400.130 MHz, CDCl₃) δ_H = 1.25-2.21 (m, 36H, CH₃), 4.52 (s, 4H, CpH), 4.68 (s, 4H, CpH); ³¹P{¹H} NMR (161.976 MHz, CDCl₃) δ_P = 35.951 (s, 2P, ¹J_{P-Pt} = 3858.9 Hz) LR-MS: [FAB] [M⁺] = 830.1 (Isotope match – see below) (Data in accordance with the literature).¹⁴⁹



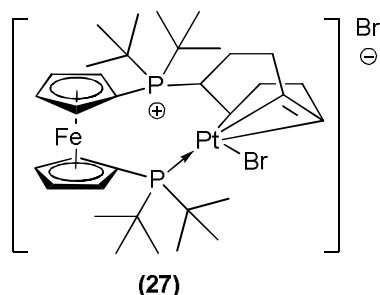
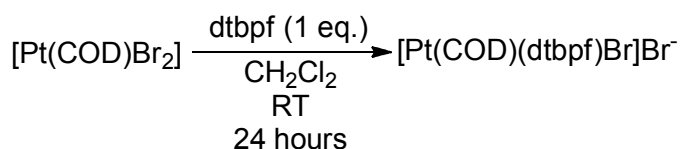
Synthesis of [Pt(dtbdppf)Br₂] (24)



The diphosphine ligand (dtbdppf) (0.087 g, 0.169 mmol) was added to K₂PtBr₄ (0.1 g, 0.169 mmol) followed by dry degassed acetonitrile (5 mL) and the reaction mixture heated to 75 °C for 16 hours. The yellow precipitate (0.138 g, 94%) was isolated by filtration, dried under vacuum and required no further purification. ¹H NMR (400.130 MHz, CDCl₃) δ_H = 1.52 (d, 18H, 6 x CH₃, J = 14.8 Hz), 3.84 (s, 1H, CHP), 4.17 (s, 1H, CHP), 4.40 (s, 4H, CpCH), 4.73 (s, 4H, CpCH), 7.36 (s, 6H, ArH), 7.98 (m, 4H, ArH); ³¹P{¹H} NMR (161.976 MHz, CDCl₃) δ_P = 13.88 (d, 2P, ¹J_{P-Pt} = 3371.8 Hz, ²J_{P-P} = 8.4 Hz), 46.54 (d, 2P, ¹J_{P-Pt} = 3753.8 Hz, ²J_{P-P} = 8.4 Hz); ¹³C NMR (75.450 MHz, 298K, CDCl₃) δ_C = 31.6 (CH₃, ¹Bu), 38.9 (C_{quat}), 52.4 (C_{quat}), 72.1(d) CpCH (J = 6.8 Hz), 72.3 (d) CpCH (J = 6.8 Hz), 74.2 (d) CpCH (J = 7.2 Hz), 127.9 (d) ArCH (J = 11.6 Hz), 130.7 (ArCH), 132.9 (C_{quat}), 134.9 (d) ArCH (J = 11.5 Hz); LR-MS: [FAB] [M-Br]^{+H} = 789.2 (Isotope match) (Data in accordance with the literature).¹³⁵

Synthesis of [Pt(COD)(dippf)Br][Br]⁻ (26)

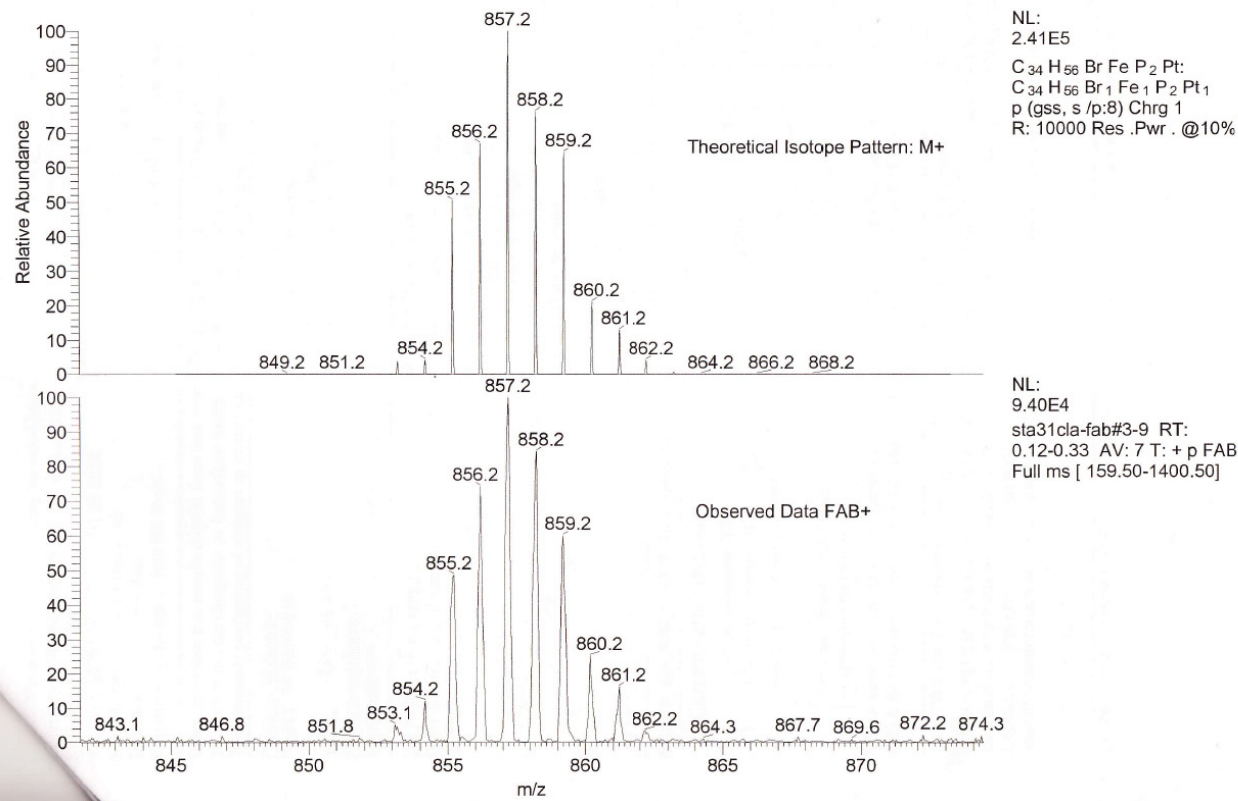
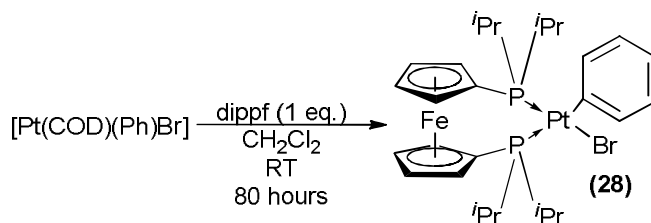
The diphosphine ligand (dippf) (1 eq. 0.091 g, 0.237 mmol) was added to a yellow solution of [Pt(COD)Br₂] (0.1 g, 0.237 mmol) in dry CH₂Cl₂ (10 mL) and stirred at RT for 24 hours. The reaction mixture was concentrated *in vacuo* to give an orange solid, which was isolated by filtration and washed with dry hexanes and recrystallized from DCM to give a yellow solid. (0.114 g, 0.142 mmol, 60 %); m.p. 160°C (decomp.); IR (KBr disc): 3407 (br), 2963 (br), 1717 (s), 1616 (s), 1458 (s), 1419 (s), 1387 (s), 1261 (s), 1161 (s), 1094 (s), 1031 (s), 800 (s), 690 (s), 639 (s) cm⁻¹; ¹H NMR (300.06 MHz, CDCl₃) δ_H = 0.57 (dd, 12H, 4 x CH₃, *J* = 6.9 Hz), 0.86 (d, 6H, 2 x CH₃, *J* = 6.8 Hz), 0.93 (d, 6H, 2 x CH₃, *J* = 6.7 Hz), 1.35 (d, 2H, CH₂, *J* = 6.8 Hz), 1.39 (d, 2H, CH₂, *J* = 6.8 Hz), 1.49 (d, 1H, CHP, *J* = 6.3 Hz), 1.53 (d, 1H, CHP, *J* = 6.3 Hz), 1.90 (d, 1H, CH, *J* = 12.7 Hz), 2.35 (m, 4H, 4 x CH(*i*Pr)), 4.20 (d, 4H, 2 x CH₂, *J* = 14 Hz), 4.70 (d, 4H, 2 x CH₂, *J* = 14 Hz), 5.40 (s, 1H, COD(Pt)*H*); ³¹P{¹H} NMR (121.466 MHz, CDCl₃) δ_P = 27.404 (s, 1P, ¹*J*_{P-Pt} = 4136 Hz), 36.33 (s, 1P, ¹*J*_{P-Pt} = 238 Hz); ¹³C NMR (75.450 MHz, 298K, CDCl₃) δ_C = 14.3, 15.3, 17.3, 17.7, 18.2, 18.4, 18.9, 20.8, 21.3, 23.9, 24.0, 24.5, 24.9, 25.3, 26.5, 27.0, 27.5, 30.8, 37.2, 42.3, 42.6, 52.5, 60.3, 61.5, 66.0, 66.7, 105.1, 108.2, 129.9, 131.0; LR-MS: [FAB] [M-Br]⁺ = 801.14 (matches predicted isotope profile); X-Ray quality crystals were grown by slow diffusion of DCM and hexanes. Anal. Calcd for C₃₀H₄₈BrFeP₂Pt(2.0 CH₂Cl₂): C, 36.55; H 4.95. Found: C 36.76; H 4.94; X-Ray: See Appendix A. Analysis was not a high quality structure due to a bis-DCM adduct and a solvate in the Elemental Analysis:

Synthesis of [Pt(COD)(dtbpf)Br][Br]⁻ (27)

The diphosphine ligand (dtbpf) (1 eq. 0.112 g, 0.237 mmol) was added to a yellow solution of [Pt(COD)Br₂] (0.1 g, 0.237 mmol) in dry CH₂Cl₂ (10 mL) and stirred at RT for 24 hours. The reaction mixture was concentrated *in vacuo* to give an orange solid, which was isolated by filtration and washed with dry hexanes and recrystallized from DCM. (0.081 g, 0.948 mmol, 40 %) m.p 134-136°C; IR (KBr disc): 3407 (br), 2970 (br), 2169 (s), 1723 (s), 1623 (s), 1479 (s), 1400 (s), 1374 (s), 1326 (s), 1261 (s), 1059 (s), 1041 (s), 923 (s), 834 (s), 805 (s), 727 (s), 636 (s), 604 (s), 577 (s), 549 (s) cm⁻¹; ¹H NMR (300.06 MHz, CDCl₃) δ_H = 1.12 (d, 18H, 6 x CH₃, *J* = 12 Hz), 1.39 (d, 18H, 6 x CH₃, *J* = 14 Hz), 1.51 (m, 2H, COD CH₂), 2.0-2.90 (m, 2H, COD CH₂), 2.99 (t, 2H, COD CH₂, *J* = 13.0 Hz), 4.33 (d, 1H, CHP, *J* = 6.3 Hz), 4.56 (s, 4H, CpCH), 4.79 (s, 4H, CpCH), 5.00 (m, 1H, COD CH), 5.13 (s, 1H, CHP), 5.72 (s, 1H, COD(Pt)H), 6.31 (s, 1H, COD(Pt)H); ³¹P{¹H} NMR (121.466 MHz, CDCl₃) δ_P = 38.254 (s, 1P, ¹*J*_{P-Pt} = 4128 Hz), 44.67 (s, 1P, ¹*J*_{P-Pt} = 296 Hz); ¹³C NMR (75.450 MHz, 298K, CDCl₃) δ_C = 10.3, 14.3, 25.3, 26.4, 26.7, 28.3, 30.0, 30.7, 31.7, 37.2, 38.4, 38.8, 40.3, 40.5, 40.8, 41.9, 43.0, 43.21, 74.5, 76.4, 100.3, 102.7, 112.2, 128.7; LR-MS: [FAB] [M]⁺ = 857.2 (matches predicted isotope profile, see below); Anal. Calcd for C₃₄H₅₅BrFeP₂Pt(2.0 CH₂Cl₂): C, 39.15; H 5.44. Found: C 38.85; H 5.28. After multiple attempts X-Ray crystals were found to be poor quality although an unrefined structure was suggestive of the complex as a *bis*-CH₂Cl₂ adduct.

EJM-093B MW=845?
E.MILTONEPSRC National Centre, Swansea
MAT95 LSIMS(NOBA)

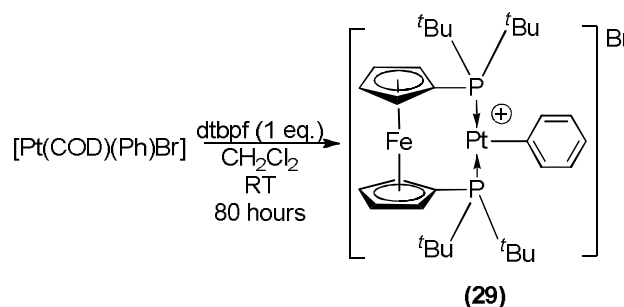
11/01/2007 12:56:16

**[Pt(dippf)(Ph)Br] (28)**

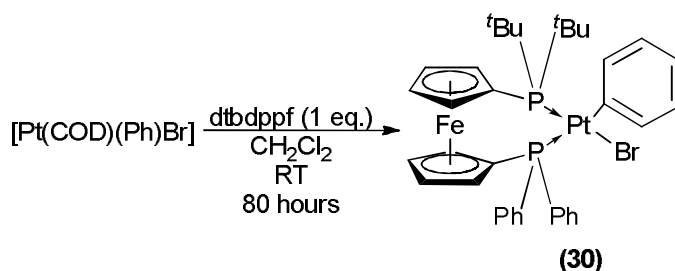
[Pt(COD)(Ph)Br] (40 mg, 0.08 mmol) was added to diisopropylphosphinoferrrocene (dippf) (34.1 mg, 0.08 mmol) followed by the addition of CH₂Cl₂ (10 mL) to give a yellow solution, which was stirred for 3 days at room temperature. The reaction mixture was concentrated *in vacuo* to a minimum volume of CH₂Cl₂. Warm petroleum ether (2 mL) was added and the reaction mixture was cooled to room temperature to give a yellow crystalline solid (25 mg, 3.13 μmol, 38.3%), which was isolated by filtration. ¹H NMR (300.06 MHz, CDCl₃) δ_H = 1.41-1.54 (m, 24H, CH₃), 2.32 (s, 1H, CHP), 2.98 (s, 1H, CHP), 4.38 (m, 8H, CpH), 7.01-7.56 (m, 5H, ArH); ³¹P{¹H} NMR (121.466 MHz, CDCl₃) δ_P = 22.16 (d, ¹J_{P-Pt} = 4411.9 Hz, ¹J_{P-P} = 12.8 Hz), 26.93 (d, ¹J_{P-Pt} = 1872.0 Hz, ¹J_{P-P} = 12.8 Hz); ¹³C NMR (75.450 MHz,

CDCl_3 δ_{C} = 17.6 (CH_3), 17.8 (CH_3), 18.5 (CH_3), 18.8 (CH_3), 19.8 (CH_3), 19.8 (CH_3), 24.4 (PC_{CpH}), 24.8 (PC_{CpH}), 24.9 (PC_{CpH}), 25.1 (PC_{CpH}), 70.0 (PC_{CpH}), 70.6 (PC_{CpH}), 71.8 (PC_{CpH}), 71.9 (PC_{CpH}), 121.7 (C_{ArH}), 126.2 (C_{ArH}), 136.7 ($\text{Pt-C}_{\text{ipso}}$); LR-MS: $[\text{MH}]^+$ = 770.100 (Isotope match); X-Ray: See Appendix A.

[Pt(dtbpf)(Ph)Br] (29)



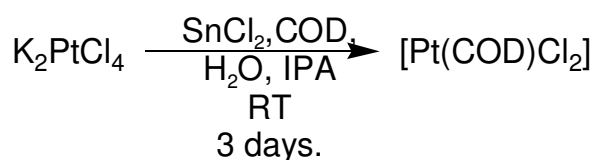
[Pt(COD)(Ph)Br] (40 mg, 0.08 mmol) was added to ditertiarybutylphosphinoferrocene (dtbpf) (38.7 mg, 0.08 mmol) followed by dry, degassed dichloromethane (10 mL) to give a yellow solution, which was stirred for 3 days. The reaction mixture was then concentrated *in vacuo* to a minimum volume of CH_2Cl_2 . Warm petroleum ether (2 mL) was added and the reaction mixture cooled to room temperature to give a dark yellow crystalline solid (25 mg, 3.07 μmol , 37.6 %), which was isolated by filtration. ^1H NMR (300.06 MHz, CDCl_3) δ_{H} = 1.41-1.54 (m, 36H, CH_3), 4.21 (s, 4H, CpH), 5.5-5.6 (m, 4H, CpH), 6.82-7.85 (m, 5H, ArCH); $^{31}\text{P}\{^1\text{H}\}$ NMR (121.466 MHz, CDCl_3) δ_{P} = 22.94 (s, $^1J_{\text{P-Pt}}$ = 2676.3 Hz); ^{13}C NMR (75.450 MHz, CDCl_3) δ_{C} = 30.0 (CH_3), 36.5 (C_{quat}) (t, J = 20.4 Hz), 52.1 (C_{quat}), 70.9 (PC_{CpH}), 79.1 (PC_{CpH}), 122.2 (C_{ArH}), 127.7 (C_{ArH}), 128.1 (C_{quat}), 135.0 (C_{ArH}); LR-MS: $[\text{MBr}]^-$ = 827.100 (Isotope match).

[Pt(dtbdppf)(Ph)Br] (30)

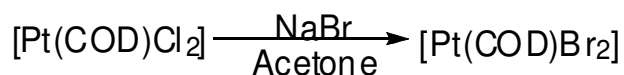
[Pt(COD)(Ph)Br] (33 mg, 0.072 mmol) was added to 1,1-*bis*-ditertiary butyl-1',1'-*bis*-diphenylphosphinoferrocene (dtbdppf) (37 mg, 0.72 mmol) followed by the addition of CH₂Cl₂ (10 mL) to give a yellow solution, which was stirred for 3 days at room temperature. The reaction mixture was concentrated *in vacuo* to a minimum volume of CH₂Cl₂. Warm petroleum ether (2 mL) was added and the reaction mixture was cooled to room temperature to give a yellow crystalline solid (33 mg, 3.8 μmol, 52.8%), which was isolated by filtration. ¹H NMR (300.06 MHz, CDCl₃) δ_H = 1.61 (d, 18H, CH₃, *J* = 12.6 Hz), 4.20 (m, 1H, CHP), 4.43 (s, 1H, CHP), 6.36 (s, 4H, CpH), 6.62 (m, 4H, CpH), 7.08-7.67 (m, 15H, ArH); ³¹P{¹H} NMR (121.466 MHz, CDCl₃) δ_P = 26.93 (d, ¹*J*_{P-Pt} 1787.1 Hz, ²*J*_{P-P} 11.5 Hz), 36.47 (d, ¹*J*_{P-Pt} = 4718.7 Hz, ²*J*_{P-P} 11.4 Hz); ¹³C NMR (75.450 MHz, CDCl₃) δ_C = 32.2 (d), (CH₃, *J* = 3.4 Hz), 38.6 (d), (*C*_{quat} ^tBu, *J* = 15.8 Hz), 71.7 (d), (CpCH, *J* = 4.6 Hz), 72.0 (d), (CpCH, *J* = 6.8 Hz), 73.06 (d), (CpCH, *J* = 6.3 Hz), 121.2 (PhCHP), 127.5 (d), (CpCH, *J* = 10.7 Hz), 129.8 (ArCH), 131.5 (*C*_{quat}), 132.4 (*C*_{quat}), 134.2 (d) (ArCH, *J* = 10.6 Hz), 136.4 (ArCH); LR-MS: [FAB] [M-Br]⁺ = 788.266 (Isotope match).

General procedure for transmetalation of [Pt(P-P)Br₂] with PhMgBr

The Pt complex (2.2×10^{-5} mol) was added to dry THF (5 mL), (the solution/slurry was cooled to 0 °C by a slush-ice bath if necessary). The Grignard solution (1 eq. 2.2×10^{-5} mol, 0.3 M, 73.3 μ L) was added and the reaction mixture (cooled if necessary) and stirred for 20 mins. Excess Grignard solution was quenched with NH₄Cl (5 mL) and the reaction mixture concentrated *in vacuo*. Organics were extracted into DCM (5 mL), washed with distilled water (5 mL), dried over MgSO₄ and concentrated *in vacuo* to give bright yellow solids. Pt species were identified by ³¹P{¹H}NMR spectroscopy.

[Pt(COD)Cl₂]

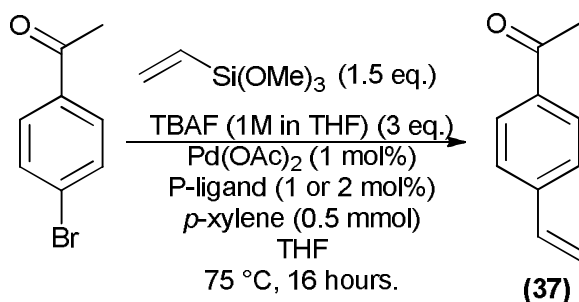
To a solution of K₂PtCl₄ (2 g, 4.818 mmol) in deionised water (32 mL), propan-2-ol (22 mL) followed by 1,5-cyclooctadiene (COD) (3.526 g, 3.260 mmol, 3.998 mL) and stannous(II) chloride (SnCl₂) (0.03 g, 0.132 mmol) to give a dark brown solution. The reaction mixture was stirred for 3 days after which the mixture had changed to an orange solution and an off white precipitate was observed. The mixture was filtered and the off white precipitate was washed with distilled water, (100 mL) ethanol (20 mL) and air dried to give an off-white solid (1.51 g, 4.528 mmol, 94%) ¹H NMR (300.06 MHz, CDCl₃) $\delta_{\text{H}} = 2.23$ (m, 4H, 2 CH₂), 2.65 (m, 4H, 2 CH₂), 5.72 (t, 4H, 2 x CH₂) (Data in agreement with literature).¹⁵⁹

[Pt(COD)Br₂]

To a suspension of [Pt(COD)Cl₂] (0.5 g, 1.5 mmol) in acetone (2 mL), sodium bromide (1.1 eq., 0.169 g, 1.65 mmol) in acetone (2 mL) was added. The white suspension immediately turned off-white on addition of the NaBr. The reaction mixture was stirred at RT for 1 hour and concentrated *in vacuo*. The brown-yellow residue was washed with distilled water (50 mL), filtered, recrystallized from DCM and allowed to air dry to give a yellow solid. (0.376 g, 0.890 mmol, 59.4%) ¹H NMR (300.06 MHz, CDCl₃) $\delta_{\text{H}} = 2.10$ (m, 4H, 2 x CH₂), 2.84 (m, 4H, 2 x CH₂), 5.62 (t, 4H, 2 x CH₂) (Data in agreement with literature).¹⁵⁹

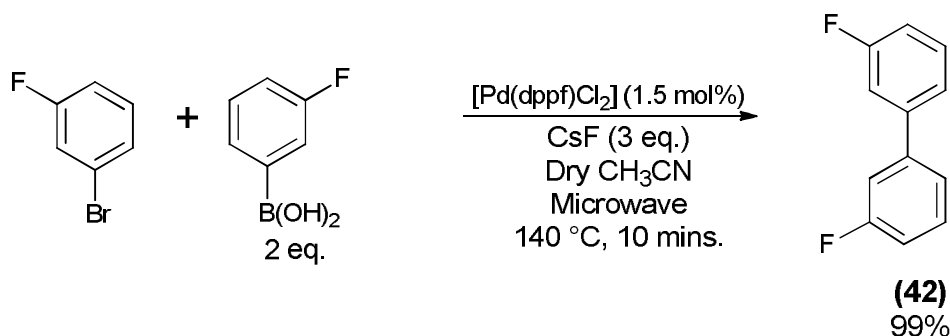
6.2 Hiyama & Suzuki cross-coupling reactions

Hiyama cross-coupling synthesis of 1-(4-vinylphenyl)ethanone (37)

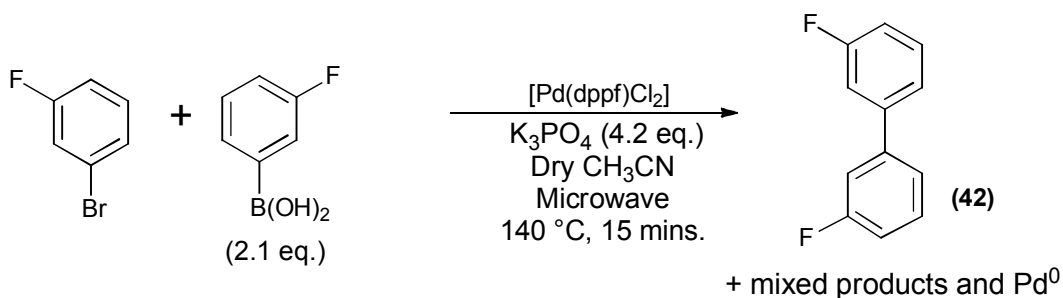


4-bromoacetophenone (0.2 g, 1.0 mmol), vinyltrimethoxysilane (0.223 g, 0.23 mL, 1.5 mmol) and *p*-Xylene (62 μL , 0.5 mmol) were dissolved in dry degassed THF (2 mL). A t=0 ^1H NMR spectra was taken to calibrate the internal standard. The Pd(OAc)_2 (0.0027 g, 1 mol%) and ligand (1 or 2 mol% respectively) were added and the tube heated to 75 °C for 16 h. Distilled water (5 mL) was then added to the reaction mixture, the aqueous phases were extracted with CH_2Cl_2 (5 mL), dried over MgSO_4 and concentrated *in vacuo* to give a red oil. Flash chromatography on silica (Et_2O /Hexanes 1:6) gave a colourless oil. ^1H NMR (300.06 MHz, CDCl_3) δ_{H} = 3.35 (s, 3H OCH_3), 5.40 (d, 1H vinylic CH , J = 10.8 Hz), 5.92 (d, 1H vinylic CH , J = 18 Hz), 6.78 (dd, 1H, vinylic CH , J = 10.5 Hz), 7.53 (d, 2H, ArH , J = 8.3 Hz, AB quartet), 7.95 (d, 2H, ArH , J = 8.3 Hz, AB quartet); ^{13}C NMR (75 MHz, CDCl_3) δ_{C} = 27.2, 114.4, 128.4, 128.9, 129.5, 130.0, 136.0 (quat), 136.2, 143.0, 197 (quat); MS (EI) m/z (%): 146 (100.0) [M^+], 147 (91) (Data in accordance with the literature).¹⁵⁰

Microwave assisted Suzuki cross-coupling synthesis of 3,3'-difluorobiphenyl (42)



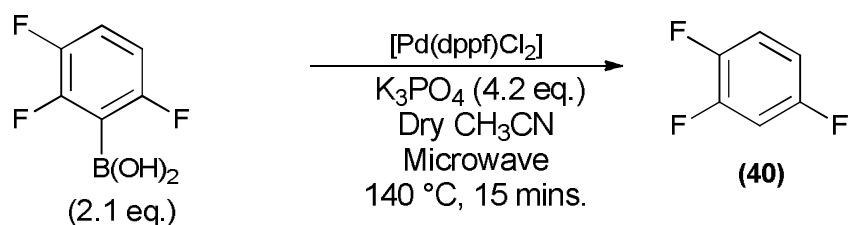
In a microwave vial, 1-bromo-3-fluorobenzene (0.100 g, 0.571 mmol., 0.063 mL) was dissolved in dry, degassed acetonitrile (2 mL), to this 3-fluoro-benzeneboronic acid (2 eq., 0.160 g, 1.142 mmol.) was added followed by CsF (3 eq., 0.178 g, 1.713 mmol.) and the Pd(dppf)Cl₂ (1.5 mol.%, 0.00418 g, 5.71 x 10⁻⁶ mol.), which was subjected to microwave conditions at 140 °C for 10 minutes at high absorption to give a red/orange solution. Distilled water (5 mL) was then added to the reaction mixture, the aqueous phases were extracted with CH₂Cl₂ (5 mL), dried over MgSO₄ and concentrated *in vacuo* to give a red solid, which was recrystallized from the slow evaporation of CH₂Cl₂ (2 mL) to give a red solid (0.108 g, 0.565 mmol, 99%). ¹H NMR (300.06 MHz, CDCl₃) δ_H = 6.90-7.18 (m, 1H), 7.12-7.51 (m, 5H), 7.72-7.82 (m, 1H), 7.84-7.98 (m, 1H, ArH); ¹³C NMR (75 MHz, CDCl₃) δ_C = 114.4, 115.1, 123.2, 130.8, 142.6, 162.0, 165.3; ¹⁹F {¹H} NMR (282.339 MHz, CDCl₃) δ_F = -113.32 (s, Ar-F) (Data in accordance with literature).¹⁵¹

Stoichiometric reactions between Pd(dppf)Cl₂ & 3-F(C₆H₄)B(OH)₂

In a microwave vial, 1-bromo-3-fluorobenzene (0.100 g, 0.571 mmol., 0.063 mL) was dissolved in dry, degassed acetonitrile (2 mL), to this 3-fluoro-benzeneboronic acid (2 eq., 0.160 g, 1.142 mmol.) was added followed by K₃PO₄ (4.2 eq., 0.509 g, 2.4 mmol.) and the [Pd(dppf)Cl₂] (0.418 g, 0.571 mmol.), which was subjected to microwave conditions at 140

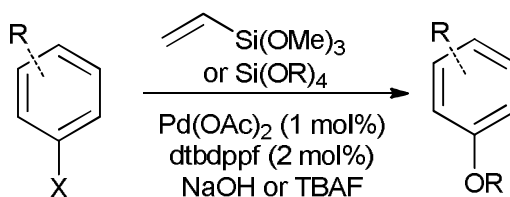
°C for 15 minutes at high absorption to give a red/orange solution. Distilled water (5 mL) was then added to the reaction mixture, the aqueous phases were extracted with CH₂Cl₂ (5 mL), dried over MgSO₄ and concentrated *in vacuo* to give a red solid (0.108 g, 0.565 mmol, 99%). ¹H NMR (300.06 MHz, CDCl₃) δ_H = 6.90-7.01 (m, 1H, ArH), 7.12-7.51 (m, 5H, ArH), 7.72-7.82 (m, 1H, ArH), 7.84-7.98 (m, 1H, ArH); ¹³C NMR (75 MHz, CDCl₃) δ_C = 114.4, 115.1, 123.2, 130.8, 142.6, 162.0, 165.3; ¹⁹F {¹H} NMR (282.339 MHz, CDCl₃) δ_F = -113.32 (s, Ar-F) (Data in accordance with literature).¹⁵¹

1,3,4-Trifluorobenzene (40)



In a microwave vial, 3-fluoro-benzeneboronic acid (2 eq., 0.160 g, 1.142 mmol.) and K₃PO₄ (4.2 eq., 0.509 g, 2.4 mmol.) and the [Pd(dppf)Cl₂] (0.418 g, 0.571 mmol.) were dissolved in dry, degassed acetonitrile (2 mL) and subjected to microwave conditions at 140 °C for 10 minutes at high absorption to give a red/orange solution. Distilled water (5 mL) was then added to the reaction mixture, the aqueous phases were extracted with CH₂Cl₂ (5 mL), dried over MgSO₄ and concentrated *in vacuo* to give a red solid, which was recrystallized from the slow evaporation of CH₂Cl₂ (2 mL) to give a red solid (0.108 g, 0.565 mmol, 99%) ¹H NMR (300.06 MHz, CDCl₃) δ_H = 6.90-6.96 (m, 1H, ArH), 7.01-7.19 (m, 1H, ArH), 7.20-7.30 (m, 1H, ArH); ¹⁹F {¹H} NMR (282.339 MHz, CDCl₃) δ_F = -117.10 (dd, *J* = 3 Hz, 15 Hz) Ar-F, -135.71 (dd, *J* = 3 Hz, 15 Hz), -145.33 (dd, *J* = 3 Hz, 15 Hz) (Data in accordance with literature).¹⁵²

6.3 Aryl Ether synthesis



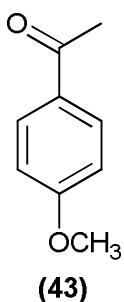
General procedure A for reactions using normal heating

The aryl halide (1 mmol) was added to a flame dried Schlenk tube containing a stirrer bead, followed by the silylether (1.5 mmol), *p*-Xylene (0.5 mmol, 62 μL) and dry, degassed toluene (5 mL). A ^1H NMR spectrum of this solution was taken to calibrate the internal standard. To this, Pd(OAc)_2 (0.0023 g, 0.1 mmol, 1 mol%), dtbdppf (0.0102 g, 0.2 mmol, 2 mol%) and powdered NaOH (0.05 g, 1.25 mmol) were added to the tube that was then sealed, flushed with nitrogen or argon and heated to reflux (or other temperatures) for the time specified.

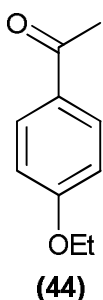
The reactions were analysed by ^1H NMR and GCMS. The products were isolated by removal of solvent followed by column chromatography (SiO_2) using hexane–diethyl ethers as eluent.

General procedure B Microwave heating conditions

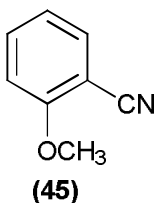
The aryl halide (1 mmol) was added to a flame dried Schlenk tube containing a stirrer bead, followed by the silyl-ether (1.5 mmol), *p*-Xylene (0.5 mmol, 62 μL) and dry, degassed toluene (5 mL). A ^1H NMR spectrum of this solution was taken to calibrate the internal standard. This was then added *via* syringe to Pd(OAc)_2 (0.0023 g, 0.1 mmol, 1 mol%), dtbdppf (0.0102 g, 0.2 mmol, 2 mol%) and powdered NaOH (0.05 g, 1.25 mmol) (or TBAF, 3 eq.), in a dry microwave tube flushed with nitrogen or argon. The reaction mixture was heated by microwave irradiation at 120 $^\circ\text{C}$ for 20 minutes, with analysis and isolation carried out as above.

1-(4-Methoxyphenyl)-ethanone (43)

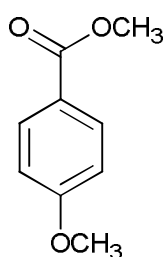
The title compound was prepared according to general procedure A, using 4-bromoacetophenone (0.2 g, 1 mmol) and vinyltrimethoxysilane (1.5 eq., 0.223 g, 0.23 mL, 1.5 mmol) and purified by column chromatography (Hexane:Et₂O= 9:1) to give a colourless oil (0.111 g, 74% yield) ¹H NMR (400 MHz, CDCl₃) δ_H = 2.48 (s, 3H, CH₃), 3.79 (s, 3H, OCH₃), 6.86 (d, 2H, *J* = 8.9 Hz, 2 x ArH), 7.86 (d, 2H, *J* = 9 Hz, 2 x ArH); ¹³C NMR (121 MHz, CDCl₃) δ_C = 25.3, 34.4, 112.6, 129.3, 129.6, 162, 197; MS (EI): *m/z* (%): 150.07 (100.0) [M⁺], 151.07 (9.9) (Data in accordance with literature).¹⁵³

1-(4-Ethoxyphenyl)-ethanone (44)

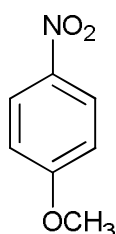
The title compound was prepared according to general procedure B, using 4-bromoacetophenone (0.2 g, 1 mmol) and vinyltriethoxysilane (1.5 eq., 0.246 g, 0.31 mL, 1.5 mmol) and purified by column chromatography (Hexane:Et₂O= 9:1) to give a colourless crystalline solid (0.126 g, 77% yield) ¹H NMR (300 MHz, CDCl₃) δ_H = 1.38 (t, 3H, *J* = 7 Hz, CH₃), 2.50 (s, 3H, CH₃), 4.03 (2H, q, *J* = 7 Hz, OCH₂), 6.86 (2H, d, *J* = 9 Hz, 2 x ArH), 7.86 (2H, d, *J* = 9 Hz, 2 x ArH); ¹³C NMR (121 MHz, CDCl₃) δ_C = 13.7, 25.6, 62.7, 113.1, 129.6, 161.9, 98; MS (EI) *m/z* (%): 164.08 (100.0) [M⁺], 165.09 (11) (Data in accordance with literature).¹⁵³

2-Methoxybenzonitrile (45)

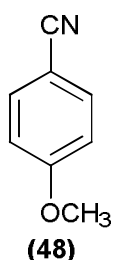
The title compound was prepared according to general procedure B, using 2-chlorobenzonitrile (0.181 g, 0.13 mL, 1 mmol) vinyltrimethoxysilane (0.223 g, 0.23 mL, 1.5 mmol) and purified by column chromatography (Hexane:Et₂O= 9:1) to give a colourless solid (0.096 g, 72% yield) ¹H NMR (300 MHz, CDCl₃) δ_H = 3.92 (s, 3H, OCH₃), 6.96-7.0 (2H, m, ArH), 7.51-7.59 (2H, m, ArH); ¹³C NMR (100 MHz, CDCl₃) δ = 54.9, 100.7, 110.3, 115.5, 119.7, 132.7, 133.4, 160.2; MS (EI) *m/z* (%): 133.05 (100.0) [M⁺], 134.06 (8.8) (Data in accordance with literature).¹⁵⁴

Methyl-4-methoxybenzoate (46)**(46)**

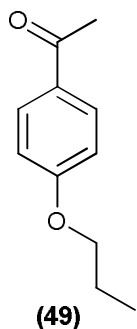
The title compound was prepared according to general procedure B, using methyl-4-bromobenzoate (0.215 g, 1 mmol) and vinyltrimethoxysilane (1.5 eq., 0.223 g, 0.23 mL, 1.5 mmol) and purified by column chromatography (Hexane:AcOEt= 6:1) to give a colourless solid (0.110 g, 66% yield) ^1H NMR (400 MHz, CDCl_3) δ_{H} = 3.85 (s, 3H, OCH_3), 3.88 (s, 3H, OCH_3), 6.91 (d, 2H, J = 9.0 Hz, 2 x ArH), 7.99 (d, 2H, J = 9.0 Hz, 2 x ArH); ^{13}C NMR (100 MHz, CDCl_3) δ_{C} = 51.8, 55.4, 113.5, 122.6, 131.5, 163.3, 166.8; MS (EI) m/z (%): 166.07 (100.0) [M^+], 167.07 (10.0), 168.07 (1.0) (Data in accordance with literature).¹⁰⁵

1-Methoxy-4-nitrobenzene (47)**(47)**

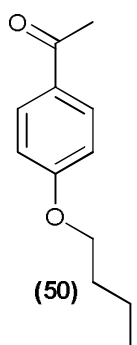
The title compound was prepared according to general procedure B, using 4-bromonitrobenzene (0.202 g, 1 mmol) and vinyltrimethoxysilane (1.5 eq., 0.223 g, 0.23 mL 1.5 mmol) and purified by column chromatography (Hexane:Et₂O= 9:1) to give a colourless solid (0.129 g, 84% yield) ^1H NMR (400 MHz, CDCl_3) δ_{H} = 3.91 (s, 3H, OCH_3), 6.96 (d, 2H, J = 9 Hz, 2 x ArH), 8.20 (d, 2H, J = 9 Hz, 2 x ArH); ^{13}C NMR (100 MHz, CDCl_3) δ_{C} = 59.9, 114.0, 125.9, 141.5, 164.5; MS (EI) m/z (%) = 153.04 (100.0) [M^+], 154.05 (7.8) (Data in accordance with literature).¹⁵⁵

4-Methoxybenzonitrile (48)**(48)**

The title compound was prepared according to general procedure B, using 4-bromobenzonitrile (0.182 g, 1 mmol) and vinyltrimethoxysilane (1.5 eq., 0.223 g, 0.23 mL, 1.5 mmol) and purified by column chromatography (Hexane:Et₂O= 9:1) to give a pale yellow solid (0.097 g, 73% yield) ^1H NMR (300 MHz, CDCl_3) δ_{H} = 3.80 (s, 3H, OCH_3), 6.88 (d, 2H, J = 9 Hz, 2 x ArH), 7.52 (d, 2H, J = 9 Hz, 2 x ArH); ^{13}C NMR (100 MHz, CDCl_3) δ_{C} = 54.5, 102.9, 113.7, 118.7, 132.9, 161.8; MS (EI) m/z (%): 133.05 (100.0) [M^+], 134.06 (8.8) (Data in accordance with literature).¹⁵⁶

1-(4-*n*-Propoxyphenyl)-ethanone (49)

The title compound was prepared according to general procedure B, using 4-bromoacetophenone (0.2 g, 1 mmol) and tetra-*n*-propoxysilane (1.5 eq., 0.267 g, 0.43 mL, 1.5 mmol.) and purified by column chromatography (Hexane:Et₂O= 9:1) to give a colourless oil (0.116 g, 65% yield) ¹H NMR (300 MHz, CDCl₃) δ_H = 0.98 (t, 3H, *J* = 7 Hz, CH₃), 1.77 (septet, 2H, *J* = 7 Hz, CH₂), 2.48 (s, 3H, CH₃), 3.92 (t, 2H, *J* = 6.7 Hz, CH₂), 6.86 (d, 2H, *J* = 9 Hz, 2 x ArH), 7.86 (d, 2H, *J* = 9 Hz, ArH); ¹³C NMR (121 MHz, CDCl₃) δ_C = 9.4, 21.4, 25.3, 68.7, 113.1, 129.1, 129.6, 162.1, 195.8; MS (EI) *m/z* (%): 178.1 (100.0) [M⁺], 179.1 (12) (Data in accordance with literature).¹⁵⁷

1-(4-*n*-Butoxyphenyl)-ethanone (50)

The title compound was prepared according to general procedure B, using 4-bromoacetophenone (0.2 g, 1 mmol), tetra-*n*-butoxysilane (1.5 eq., 0.288 g, 0.53 mL, 1.5 mmol) and TBAF (1M solution in THF) (3 eq., 3 mL, 3 mmol) as an activator and purified by column chromatography (Hexane:Et₂O= 9:1) to give a colourless oil (0.140 g, 73% yield) ¹H NMR (300 MHz, CDCl₃) δ_H = 0.85 (t, 3H, *J* = 7.5 Hz, CH₃), 1.30 (sextet, 2H, *J* = 7.5 Hz, CH₂), 1.49 (quintet, 2H, *J* = 6.6 Hz, CH₂), 2.50 (s, 3H, CH₃), 3.70 (t, 2H, *J* = 6.8 Hz, CH₂), 7.39 (d, 2H, *J* = 8.3 Hz, 2 x ArH), 7.90 (d, 2H, *J* = 8.3 Hz, 2 x ArH); ¹³C NMR (121 MHz, CDCl₃) δ_C = 14.2, 19.6, 26.8, 31.54, 68.4, 114.5, 131, 163.5, 197.3; MS (EI) *m/z* (%): 192.12 (100.0) [M⁺], 193.12 (13.0) (Data in accordance with literature).¹²⁵

Chapter 7. References

1. P. W. N. M. van Leeuwen, *Homogeneous Catalysis - Understanding the Art*, Kluwer Academic Publishers, Dordrecht, 2004.
2. K. C. Nicolaou, P. G. Bulger and D. Sarlah, *Angew. Chem., Int. Ed.*, 2005, **44**, 4442-4489.
3. N. Miyaura, K. Yamada and A. Suzuki, *Tetrahedron Lett.*, 1979, **20**, 3437-3440.
4. F. Bellina, A. Carpita and R. Rossi, *Synthesis*, 2004, **2004**, 2419-2440.
5. C. A. Tolman, *Chem. Rev.*, 1977, **77**, 313-348.
6. C. P. Casey and G. T. Whiteker, *Isr. J. Chem.*, 1990, **30**, 299-304.
7. M. Kranenburg, Y. E. M. van der Burgt, P. C. J. Kamer, P. W. N. M. van Leeuwen, K. Goubitz and J. Fraanje, *Organomet.*, 1995, **14**, 3081-3089.
8. P. W. N. M. Van Leeuwen, P. C. J. Kamer and J. N. H. Reek, *Pure Appl. Chem.*, 1999, **71**, 1443-1452.
9. M. N. B. Gensow, Z. Freixa and P. W. N. M. van Leeuwen, *Chem. Soc. Rev.*, 2009, **38**, 1099-1118.
10. P. C. J. Kamer, P. W. N. M. van Leeuwen and J. N. H. Reek, *Acc. Chem. Res.*, 2001, **34**, 895-904.
11. C. P. Casey, G. T. Whiteker, M. G. Melville, L. M. Petrovich, J. A. Gavney and D. R. Powell, *J. Am. Chem. Soc.*, 1992, **114**, 5535-5543.
12. A. Zapf, *Angew. Chem., Int. Ed.*, 2003, **42**, 5394-5399.
13. P. Espinet and A. M. Echavarren, *Angew. Chem., Int. Ed.*, 2004, **43**, 4704-4734.
14. J. M. Brown and N. A. Cooley, *Chem. Rev.*, 2002, **88**, 1031-1046.
15. C. Amatore, E. Carre, A. Jutand, M. A. M'Barki and G. Meyer, *Organomet.*, 1995, **14**, 5605-5614.
16. C. Amatore, A. Jutand and A. Suarez, *J. Am. Chem. Soc.*, 1993, **115**, 9531-9541.
17. C. Amatore, A. Jutand and A. Thuilliez, *Organomet.*, 2001, **20**, 3241-3249.
18. I. D. Hills, M. R. Netherton and G. C. Fu, *Angew. Chem., Int. Ed.*, 2003, **42**, 5749-5752.
19. M. Portnoy and D. Milstein, *Organomet.*, 1993, **12**, 1665-1673.
20. J. M. Brown and P. J. Guiry, *Inorg. Chim. Acta*, 1994, **220**, 249-259.
21. D. A. Culkin and J. F. Hartwig, *Organomet.*, 2004, **23**, 3398-3416.

22. R. K. Merwin, R. C. Schnabel, J. D. Koola and D. M. Roddick, *Organomet.*, 1992, **11**, 2972-2978.
23. M. Tschoerner, P. S. Pregosin and A. Albinati, *Organomet.*, 1999, **18**, 670-678.
24. I. J. S. Fairlamb, A. R. Kapdi and A. F. Lee, *Org. Lett.*, 2004, **6**, 4435-4438.
25. Y. Mace, A. R. Kapdi, I. J. S. Fairlamb and A. Jutand, *Organomet.*, 2006, **25**, 1795-1800.
26. E. Galardon, S. Ramdeehul, J. M. Brown, A. Cowley, K. K. Hii and A. Jutand, *Angew. Chem., Int. Ed.*, 2002, **41**, 1760-1763.
27. J. Zou, Q. Yu and Z. Shang, *J. Chem. Soc., Perkin Trans. 2*, 2001, 1439-1443.
28. F. Barrios-Landeros and J. F. Hartwig, *J. Am. Chem. Soc.*, 2005, **127**, 6944-6945.
29. P. DeShong and S. Hodges, *Abstracts of Papers, 224th ACS National Meeting, Boston, MA, United States, August 18-22, 2002*, 2002, ORGN-677.
30. K. Gouda, E. Hagiwara, Y. Hatanaka and T. Hiyama, *J. Org. Chem.*, 1996, **61**, 7232-7233.
31. Y. Hatanaka and T. Hiyama, *J. Org. Chem.*, 1988, **53**, 918-920.
32. T. Hiyama and Y. Hatanaka, *Pure and Applied Chemistry*, 1994, **66**, 1471-1478.
33. M. E. Mowery and P. DeShong, *Org. Lett.*, 1999, **1**, 2137-2140.
34. S. Riggleman and P. DeShong, *J. Org. Chem.*, 2003, **68**, 8106-8109.
35. M. L. Clarke and M. Heydt, *Organomet.*, 2005, **24**, 6475-6478.
36. P. Nilsson, G. Puxty and O. F. Wendt, *Organomet.*, 2006, **25**, 1285-1292.
37. S. E. Denmark and R. F. Sweis, *J. Am. Chem. Soc.*, 2004, **126**, 4876-4882.
38. S. E. Denmark, R. F. Sweis and D. Wehrli, *J. Am. Chem. Soc.*, 2004, **126**, 4865-4875.
39. S. Shekhar and J. F. Hartwig, *J. Am. Chem. Soc.*, 2004, **126**, 13016-13027.
40. J. J. Low and W. A. Goddard, III, *J. Am. Chem. Soc.*, 1986, **108**, 6115-6128.
41. K. Tatsumi, R. Hoffmann, A. Yamamoto and J. K. Stille, *Bulletin of the Chemical Society of Japan*, 1981, **54**, 1857-1867.
42. T. Hayashi, M. Konishi, Y. Kobori, M. Kumada, T. Higuchi and K. Hirotsu, *J. Am. Chem. Soc.*, 1984, **106**, 158-163.
43. M. Kranenburg, P. C. J. Kamer and P. W. N. M. van. Leeuwen, *Eur. J. Inorg. Chem.*, 1998, 155-157.
44. G. Mann and J. F. Hartwig, *Tetrahedron Lett.*, 1997, **38**, 8005-8008.
45. G. Mann, Q. Shelby, A. H. Roy and J. F. Hartwig, *Organomet.*, 2003, **22**, 2775-2789.
46. L. M. Alcazar-Roman and J. F. Hartwig, *J. Am. Chem. Soc.*, 2001, **123**, 12905-12906.

47. E. Negishi, A. O. King and N. Okukado, *J. Org. Chem.*, 1977, **42**, 1821-1823.
48. J. F. Fauvarque and A. Jutand, *J. Organomet. Chem.*, 1977, **132**, C17-C19.
49. J. E. Milne and S. L. Buchwald, *J. Am. Chem. Soc.*, 2004, **126**, 13028-13032.
50. E. J. G. Anctil and V. Snieckus, *J. Organomet. Chem.*, 2002, **653**, 150-160.
51. Z. Huang, M. Qian, D. J. Babinski and E. Negishi, *Organomet.*, 2005, **24**, 475-478.
52. Q. Liu, Y. Lan, J. Liu, G. Li, Y.-D. Wu and A. Lei, *J. Am. Chem. Soc.*, 2009, **131**, 10201-10210.
53. C. Wang, T. Tobrman, Z. Xu and E. Negishi, *Org. Lett.*, 2009, **11**, 4092-4095.
54. E. Negishi, Z. Huang, G. Wang, S. Mohan, C. Wang and H. Hattori, *Acc. Chem. Res.*, 2008, **41**, 1474-1485.
55. G. Wang, Z. Huang and E. Negishi, *Tetrahedron Lett.*, 2009, **50**, 3220-3223.
56. T. J. Colacot and H. A. Shea, *Org. Lett.*, 2004, **6**, 3731-3734.
57. U. Christmann and R. Vilar, *Angew. Chem., Int. Ed.*, 2005, **44**, 366-374.
58. J. H. Kirchhoff, C. Dai and G. C. Fu, *Angew. Chem., Int. Ed.*, 2002, **41**, 1945-1947.
59. W. A. Herrmann, C. Brossmer, C.-P. Reisinger, T. H. Riermeier, K. Oefele and M. Beller, *Chem. Eur. J.*, 1997, **3**, 1357-1364.
60. T. E. Barder, S. D. Walker, J. R. Martinelli and S. L. Buchwald, *J. Am. Chem. Soc.*, 2005, **127**, 4685-4696.
61. X. Bei, H. W. Turner, W. H. Weinberg, A. S. Guram and J. L. Petersen, *J. Org. Chem.*, 1999, **64**, 6797-6803.
62. M. L. Clarke, D. J. Cole-Hamilton and J. D. Woollins, *J. Chem. Soc., Dalton Trans.*, 2001, 2721-2723.
63. J. P. Wolfe and S. L. Buchwald, *Angew. Chem., Int. Ed.*, 1999, **38**, 2413-2416.
64. A. F. Littke, C. Dai and G. C. Fu, *J. Am. Chem. Soc.*, 2000, **122**, 4020-4028.
65. J. P. Wolfe, R. A. Singer, B. H. Yang and S. L. Buchwald, *J. Am. Chem. Soc.*, 1999, **121**, 9550-9561.
66. R. B. Bedford, C. S. J. Cazin, M. B. Hursthouse, M. E. Light and V. J. M. Scordia, *Dalton Transactions*, 2004, 3864-3868.
67. S. W. Wright, D. L. Hageman and L. D. McClure, *J. Org. Chem.*, 2002, **59**, 6095-6097.
68. P. S. Braterman, R. J. Cross and G. B. Young, *J. Chem. Soc., Dalton Trans* 1977, **1**, 1892-1897.
69. G. Y. Li, *J. Org. Chem.*, 2002, **67**, 3643-3650.

70. S. M. Reid, R. C. Boyle, J. T. Mague and M. J. Fink, *J. Am. Chem. Soc.*, 2003, **125**, 7816-7817.
71. M. S. Wong and X. L. Zhang, *Tetrahedron Lett.*, 2001, **42**, 4087-4089.
72. H. G. Kuivila, J. F. Reuwer and J. A. Mangravite, *J. Am. Chem. Soc.*, 1964, **86**, 2666-2670.
73. M. Feuerstein, F. Berthiol, H. Doucet and M. Santelli, *Synlett*, 2002, **11**, 1807-1810.
74. T. Thiemann, K. Umeno, J. Wang, Y. Tabuchi, K. Arima, M. Watanabe, Y. Tanaka, H. Gorohmaru and S. Mataka, *J. Chem. Soc. Perkin Trans. 1*, 2002, 2090-2110.
75. H. Chaumeil, S. Signorella and C. Le Drian, *Tetrahedron*, 2000, **56**, 9655-9662.
76. S. T. Handy, Y. Zhang and H. Bregman, *J. Org. Chem.*, 2004, **69**, 2362-2366.
77. T. Watanabe, N. Miyaura and A. Suzuki, *Synlett*, 1992, **3**, 207-210.
78. J. Yin, M. P. Rainka, X.-X. Zhang and S. L. Buchwald, *J. Am. Chem. Soc.*, 2002, **124**, 1162-1163.
79. M. L. Clarke, M. B. France, J. A. Fuentes, E. J. Milton and G. J. Roff, *Beilstein J. Org. Chem.*, 2007, **3**, 18.
80. D. Milstein and J. K. Stille, *J. Am. Chem. Soc.*, 1979, **101**, 4992-4998.
81. A. L. Casado and P. Espinet, *J. Am. Chem. Soc.*, 1998, **120**, 8978-8985.
82. J. A. Casares, P. Espinet and G. Salas, *Chem. Eur. J.*, 2002, **8**, 4843-4853.
83. C. Amatore, A. A. Bahsoun, A. Jutand, G. Meyer, N. Ndedi and L. Ricard, *J. Am. Chem. Soc.*, 2003, **125**, 4212-4222.
84. C. Wolf and R. Lerebours, *J. Org. Chem.*, 2003, **68**, 7551-7554.
85. G. Y. Li, *Angew. Chem., Int. Ed.*, 2001, **40**, 1513-1516.
86. K. Menzel and G. C. Fu, *J. Am. Chem. Soc.*, 2003, **125**, 3718-3719.
87. H. Tang, K. Menzel and G. C. Fu, *Angew. Chem., Int. Ed.*, 2003, **42**, 5079-5082.
88. J. R. Naber and S. L. Buchwald, *Adv. Synth. Catal.*, 2008, **350**, 957-961.
89. V. Farina, S. Kapadia, B. Krishnan, C. Wang and L. S. Liebeskind, *J. Org. Chem.*, 2002, **59**, 5905-5911.
90. D. Gelman and S. L. Buchwald, *Angew. Chem., Int. Ed.*, 2003, **42**, 5993-5996.
91. A. L. Casado and P. Espinet, *Organomet.*, 2003, **22**, 1305-1309.
92. K. Tamao, K. Sumitani and M. Kumada, *J. Am. Chem. Soc.*, 1972, **94**, 4374-4376.
93. K. Tamao, K. Sumitani, Y. Kiso, M. Zembayashi, A. Fujioka, S. Kodama, I. Nakajima, A. Minato and M. Kumada, *Bull. Chem. Soc. Jpn.*, 1976, **49**, 1958.
94. R. J. P. Corriu and J. P. Masse, *J. Chem. Soc. Chem. Commun.*, 1972, 144.

95. A. C. Frisch, N. Shaikh, A. Zapf and M. Beller, *Angew. Chem., Int. Ed.*, 2002, **41**, 4056-4059.
96. C. Wolf and H. Xu, *J. Org. Chem.*, 2007, **73**, 162-167.
97. A. Alimardanov, L. Schmieder-van de Vondervoort, A. H. M. de Vries and J. G. de Vries, *Adv. Synth. Catal.*, 2004, **346**, 1812-1817.
98. G. Y. Li, *J. Organomet. Chem.*, 2002, **653**, 63-68.
99. J. A. Miller and R. P. Farrell, *Tetrahedron Lett.*, 1998, **39**, 7275-7278.
100. K. Tamao, K. Kobayashi and Y. Ito, *Tetrahedron Lett.*, 1989, **30**, 6051-6054.
101. E. Alacid and C. Najera, *Adv. Synth. Catal.*, 2006, **348**, 2085-2091.
102. M. L. Clarke, *Adv. Synth. Catal.*, 2005, **347**, 303-307.
103. S. E. Denmark and J. M. Kallemeyn, *J. Am. Chem. Soc.*, 2006, **128**, 15958-15959.
104. T. Hiyama and Y. Hatanaka, *Pure Appl. Chem.*, 1994, **66**, 1471-1478.
105. R. Lerebours and C. Wolf, *J. Am. Chem. Soc.*, 2006, **128**, 13052-13053.
106. E. J. Milton, M. L. Clarke and J. A. Fuentes, *unpublished results*.
107. S. E. Denmark, D. Wehrli and J. Y. Choi, *Org. Lett.*, 2000, **2**, 2491-2494.
108. S. E. Denmark and C. S. Regens, *Acc. Chem. Res.*, 2008, **41**, 1486-1499.
109. M. L. Clarke, E. J. Milton and K. S. Damian, *unpublished results*.
110. E. J. Corey and G. A. Reichard, *Tetrahedron Lett.*, 1989, **30**, 5207-5210.
111. A. W. Czarnik, *Acc. Chem. Res.*, 1996, **29**, 112-113.
112. J. Deeter, J. Frazier, G. Staten, M. Staszak and L. Weigel, *Tetrahedron Lett.*, 1990, **31**, 7101-7104.
113. T. X. Metro, D. G. Pardo and J. Cossy, *J. Org. Chem.*, 2008, **73**, 707-710.
114. J. F. Hartwig, *Inorg. Chem.*, 2007, **46**, 1936-1947.
115. M. Yamashita and J. F. Hartwig, *J. Am. Chem. Soc.*, 2004, **126**, 5344-5345.
116. R. A. Altman, A. Shafir, A. Choi, P. A. Lichtor and S. L. Buchwald, *J. Org. Chem.*, 2008, **73**, 284-286.
117. M. A. Keegstra, T. H. A. Peters and L. Brandsma, *Tetrahedron*, 1992, **48**, 3633-3652.
118. J. Lindley, *Tetrahedron*, 1984, **40**, 1433-1456.
119. M. T. Ning Xia, *Chem. Eur. J.*, 2008, **14**, 6037-6039.
120. C. A. Parrish and S. L. Buchwald, *J. Org. Chem.*, 2001, **66**, 2498-2500.
121. J. Bonnamour and C. Bolm, *Org. Lett.*, 2008, **10**, 2665-2667.
122. A. C. Olivia-Bistri, C. Bolm, *Angew. Chem., Int. Ed.*, 2008, **47**, 586-588.

123. K. W. Anderson, T. Ikawa, R. E. Tundel and S. L. Buchwald, *J. Am. Chem. Soc.*, 2006, **128**, 10694-10695.
124. A. Aranyos, D. W. Old, A. Kiyomori, J. P. Wolfe, J. P. Sadighi and S. L. Buchwald, *J. Am. Chem. Soc.*, 1999, **121**, 4369-4378.
125. K. E. Torraca, X. Huang, C. A. Parrish and S. L. Buchwald, *J. Am. Chem. Soc.*, 2001, **123**, 10770-10771.
126. K. E. Torraca, S. I. Kuwabe and S. L. Buchwald, *J. Am. Chem. Soc.*, 2000, **122**, 12907-12908.
127. A. V. Vorogushin, X. Huang and S. L. Buchwald, *J. Am. Chem. Soc.*, 2005, **127**, 8146-8149.
128. R. A. Widenhoefer, H. A. Zhong and S. L. Buchwald, *J. Am. Chem. Soc.*, 1997, **119**, 6787-6795.
129. R. Han and G. L. Hillhouse, *J. Am. Chem. Soc.*, 1997, **119**, 8135-8136.
130. T. J. Colacot, R. A. Teichman, R. Cea-Olivares, J. G. Alvarado-Rodríguez, R. A. Toscano and W. J. Boyko, *J. Organomet. Chem.*, 1998, **557**, 169-179.
131. A. R. Elsagir, F. Gassner, H. Górls and E. Dinjus, *J. Organomet. Chem.*, 2000, **597**, 139-145.
132. J. H. L. Ong, C. Nataro, J. A. Golen and A. L. Rheingold, *Organomet.*, 2003, **22**, 5027-5032.
133. M. Sato, H. Shigeta, M. Sekino and S. Akabori, *J. Organomet. Chem.*, 1993, **458**, 199-204.
134. M. A. Zuideveld, B. H. G. Swennenhuis, P. C. J. Kamer and P. W. N. M. van Leeuwen, *J. Organomet. Chem.*, 2001, **637-639**, 805-808.
135. S. L. Kahn, M. K. Breheney, S. L. Martinak, S. M. Fosbenner, A. R. Seibert, W. S. Kassel, W. G. Dougherty and C. Nataro, *Organomet.*, 2009, **28**, 2119-2126.
136. T. J. Colacot, H. Qian, R. Cea-Olivares and S. Hernandez-Ortega, *J. Organomet. Chem.*, 2001, **637-639**, 691-697.
137. M. L. Clarke and E. J. Milton, *Green Chem.*, 2009, Accepted December 2009.
138. G. Mann and J. F. Hartwig, *J. Am. Chem. Soc.*, 1996, **118**, 13109-13110.
139. A. V. Vorogushin, X. Huang and S. L. Buchwald, *J. Am. Chem. Soc.*, 2005, **127**, 8146-8149.
140. M. C. Willis, D. Taylor and A. T. Gillmore, *Chem. Comm.*, 2003, 2222-2223.
141. M. C. Willis, D. Taylor and A. T. Gillmore, *Tetrahedron*, 2006, **62**, 11513-11520.

142. M. C. Willis, *Angew. Chem., Int. Ed.*, 2007, **46**, 3402-3404.
143. J. A. Davies and R. J. Staples, *Polyhedron*, 1991, **10**, 909-917.
144. H. A. Brune, E. Hupfer, G. Schmidtberg and A. Baur, *J. Organomet. Chem.*, 1992, **424**, 225-241.
145. R. Klotzbücher and H. A. Brune, *J. Organomet. Chem.*, 1986, **299**, 399-407.
146. I. R. Butler, W. R. Cullen, T. J. Kim, S. J. Rettig and J. Trotter, *Organomet.*, 1985, **4**, 972-980.
147. R. K. Atwal and R. Bolton, *Aust. J. Chem.*, 1987, **40**, 241-247.
148. G. A. Molander and B. Biolatto, *J. Org. Chem.*, 2003, **68**, 4302-4314.
149. F. N. Blanco, L. E. Hagopian, W. R. McNamara, J. A. Golen, A. L. Rheingold and C. Nataro, *Organomet.*, 2006, **25**, 4292-4300.
150. A. M. Echavarren and J. K. Stille, *J. Am. Chem. Soc.*, 2002, **109**, 5478-5486.
151. M. A. Cooper, H.E. Weber and S.L. Manatt, *J. Am. Chem. Soc.*, 1971, **93**, 2369.
152. P. L. Coe, A.L Stuart and D. J. Moody, *J. Chem. Soc., Perkin Trans. 1*, 1998, 1807.
153. K. Smith, Z. Zhenua and P. K. G. Hodgson, *J. Mol. Cat. A.*, 1998, **134**, 121.
154. R. K. Arvela and N. E. Leadbeater, *J. Org. Chem.*, 2003, **68**, 9122.
155. G. G. Wubbels and K. M. Johnson, *Org. Lett.*, 2006, **8**, 1451.
156. C. O. Kangani, B. W. Day and D. E. Kelley, *Tetrahedron Lett.*, 2008, **49**, 914-918.
157. K. Sugamoto, Y. Matsushitu, T. Yamamoto and T. Matsui, *Synth. Comm.*, 2005, **35**, 1865.
158. D. H. Farrar and G. Ferguson, *J. Chem. Crystallogr.*, 1982, **12**, 465-471.
159. H. C. Clark and L. E. Manzer, *J. Organomet. Chem.*, 1973, **59**, 411-428.

Appendix A - X-Ray Crystallography Data

(For X-Ray Data tables see attached CD-R)



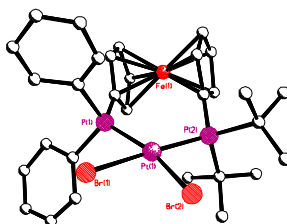
[Pt(dtbdppf)Br₂] – (24)

Table 1. Crystal data and structure refinement for emmc4.

Identification code	emmc4	
Empirical formula	C ₃₁ H ₃₇ Br ₂ Cl ₃ Fe P ₂ Pt	
Formula weight	988.66	
Temperature	93(2) K	
Wavelength	0.71073 Å	
Crystal system	Triclinic	
Space group	P-1	
Unit cell dimensions	a = 10.514(2) Å	α = 88.63(3)°.
	b = 10.929(3) Å	β = 79.66(3)°.
	c = 18.156(7) Å	γ = 61.71(2)°.
Volume	1802.7(9) Å ³	
Z	2	
Density (calculated)	1.821 Mg/m ³	
Absorption coefficient	6.826 mm ⁻¹	
F(000)	956	
Crystal size	0.1000 x 0.0800 x 0.0100 mm ³	
Theta range for data collection	2.12 to 25.34°.	
Index ranges	-12 ≤ h ≤ 11, -13 ≤ k ≤ 8, -21 ≤ l ≤ 21	
Reflections collected	11123	
Independent reflections	6086 [R(int) = 0.1060]	
Completeness to theta = 25.00°	93.1 %	
Absorption correction	Multiscan	
Max. and min. transmission	1.0000 and 0.5292	
Refinement method	Full-matrix least-squares on F ²	
Data / restraints / parameters	6086 / 54 / 358	
Goodness-of-fit on F ²	1.279	
Final R indices [I > 2σ(I)]	R1 = 0.1334, wR2 = 0.3458	
R indices (all data)	R1 = 0.1670, wR2 = 0.3824	
Extinction coefficient	0.0052(12)	
Largest diff. peak and hole	11.347 and -2.994 e.Å ⁻³	

Table 3. Bond lengths [\AA] and angles [$^\circ$] for emmc4.

Pt(1)-P(1)	2.280(5)
Pt(1)-P(2)	2.328(6)
Pt(1)-Br(2)	2.478(3)
Pt(1)-Br(1)	2.494(3)
Fe(1)-C(6)	1.99(2)
Fe(1)-C(1)	2.02(2)
Fe(1)-C(2)	2.02(2)
Fe(1)-C(10)	2.05(2)
Fe(1)-C(4)	2.02(2)
Fe(1)-C(7)	2.06(2)
Fe(1)-C(5)	2.07(2)
Fe(1)-C(9)	2.04(3)
Fe(1)-C(8)	2.07(2)
Fe(1)-C(3)	2.10(3)
P(1)-Pt(1)-P(2)	101.9(2)
P(1)-Pt(1)-Br(2)	164.65(17)
P(2)-Pt(1)-Br(2)	93.46(16)
P(1)-Pt(1)-Br(1)	81.07(16)
P(2)-Pt(1)-Br(1)	177.04(15)
Br(2)-Pt(1)-Br(1)	83.58(10)

Table 6. Torsion angles [$^\circ$] for emmc4.

C(2)-C(3)-C(4)-C(5)	4(3)
---------------------	------

Symmetry transformations used to generate equivalent atoms:

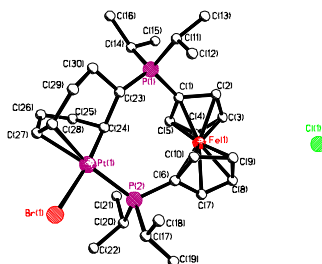
[Pt(COD)(dippf)Br]Br⁻ – (26)

Table 1. Crystal data and structure refinement for emmc6.

Identification code	emmc6	
Empirical formula	C ₃₀ H ₄₆ Br Cl Fe P ₂ Pt	
Formula weight	834.91	
Temperature	93(2) K	
Wavelength	0.71073 Å	
Crystal system	Monoclinic	
Space group	P2(1)/c	
Unit cell dimensions	a = 10.360(6) Å	α = 90°.
	b = 15.804(8) Å	β = 102.80(2)°.
	c = 20.875(14) Å	γ = 90°.
Volume	3333(3) Å ³	
Z	4	
Density (calculated)	1.664 Mg/m ³	
Absorption coefficient	6.020 mm ⁻¹	
F(000)	1648	
Crystal size	0.2000 x 0.0300 x 0.0100 mm ³	
Theta range for data collection	1.63 to 25.30°.	
Index ranges	-12 ≤ h ≤ 12, -14 ≤ k ≤ 18, -19 ≤ l ≤ 25	
Reflections collected	19922	
Independent reflections	5956 [R(int) = 0.1498]	
Completeness to theta = 25.00°	98.5 %	
Absorption correction	Multiscan	
Max. and min. transmission	1.0000 and 0.3022	
Refinement method	Full-matrix least-squares on F ²	
Data / restraints / parameters	5956 / 18 / 326	
Goodness-of-fit on F ²	1.322	
Final R indices [I > 2σ(I)]	R1 = 0.1587, wR2 = 0.3842	
R indices (all data)	R1 = 0.2173, wR2 = 0.4276	
Largest diff. peak and hole	8.721 and -2.587 e.Å ⁻³	

Table 3. Bond lengths [\AA] and angles [$^\circ$] for emmc6.

Br(1)-Pt(1)	2.547(3)
Fe(1)-C(3)	1.97(3)
Fe(1)-C(5)	1.99(2)
Fe(1)-C(9)	2.02(2)
Fe(1)-C(10)	2.03(2)
Fe(1)-C(1)	2.04(4)
Fe(1)-C(8)	2.05(3)
Fe(1)-C(4)	2.06(3)
Fe(1)-C(7)	2.08(4)
Fe(1)-C(6)	2.07(2)
Fe(1)-C(2)	2.11(3)
Pt(1)-C(24)	1.98(2)
Pt(1)-C(27)	2.23(3)
Pt(1)-C(28)	2.22(3)
Pt(1)-P(2)	2.284(8)
C(24)-Pt(1)-C(27)	80.6(12)
C(24)-Pt(1)-C(28)	90.1(11)
C(27)-Pt(1)-C(28)	37.4(12)
C(24)-Pt(1)-P(2)	93.0(9)
C(27)-Pt(1)-P(2)	162.3(8)
C(28)-Pt(1)-P(2)	160.0(11)
C(24)-Pt(1)-Br(1)	172.0(9)
C(27)-Pt(1)-Br(1)	92.1(8)
C(28)-Pt(1)-Br(1)	85.9(8)
P(2)-Pt(1)-Br(1)	93.10(18)

Symmetry transformations used to generate equivalent atoms:

Table 6. Torsion angles [°] for emmc6.

C(24)-Pt(1)-P(2)-C(6)	36.3(13)
C(27)-Pt(1)-P(2)-C(6)	104(3)
C(28)-Pt(1)-P(2)-C(6)	-62(3)
Br(1)-Pt(1)-P(2)-C(6)	-148.8(10)
C(24)-Pt(1)-P(2)-C(20)	-86.5(12)
C(27)-Pt(1)-P(2)-C(20)	-18(3)
C(28)-Pt(1)-P(2)-C(20)	175(2)
Br(1)-Pt(1)-P(2)-C(20)	88.4(9)
C(24)-Pt(1)-P(2)-C(17)	155.9(12)
C(27)-Pt(1)-P(2)-C(17)	-136(3)
C(28)-Pt(1)-P(2)-C(17)	57(3)
Br(1)-Pt(1)-P(2)-C(17)	-29.3(10)
C(20)-P(2)-C(6)-C(10)	178(2)
C(17)-P(2)-C(6)-C(10)	-71(3)
Pt(1)-P(2)-C(6)-C(10)	53(3)
C(20)-P(2)-C(6)-C(7)	-30(3)
C(17)-P(2)-C(6)-C(7)	82(3)
Pt(1)-P(2)-C(6)-C(7)	-155(2)
C(20)-P(2)-C(6)-Fe(1)	79(3)
C(17)-P(2)-C(6)-Fe(1)	-170(3)
Pt(1)-P(2)-C(6)-Fe(1)	-47(3)
Pt(1)-P(2)-C(20)-C(21)	61(2)
C(1)-P(1)-C(23)-C(30)	179(2)
C(14)-P(1)-C(23)-C(30)	-63(3)
C(11)-P(1)-C(23)-C(30)	60(3)
C(1)-P(1)-C(23)-C(24)	-42(2)
C(14)-P(1)-C(23)-C(24)	76(2)
C(11)-P(1)-C(23)-C(24)	-161(2)
C(30)-C(23)-C(24)-C(25)	53(3)
P(1)-C(23)-C(24)-C(25)	-86(3)
C(30)-C(23)-C(24)-Pt(1)	-69(3)
P(1)-C(23)-C(24)-Pt(1)	152.7(16)
C(27)-Pt(1)-C(24)-C(25)	-35.8(16)
C(28)-Pt(1)-C(24)-C(25)	-72.2(19)
P(2)-Pt(1)-C(24)-C(25)	127.5(15)
Br(1)-Pt(1)-C(24)-C(25)	-12(7)

Appendix A.) X-Ray Crystallography Data

C(27)-Pt(1)-C(24)-C(23)	88(2)
C(28)-Pt(1)-C(24)-C(23)	52(2)
P(2)-Pt(1)-C(24)-C(23)	-109(2)
Br(1)-Pt(1)-C(24)-C(23)	111(5)
C(23)-C(24)-C(25)-C(26)	-80(2)
Pt(1)-C(24)-C(25)-C(26)	46(2)
C(24)-C(25)-C(26)-C(27)	-26(3)
C(25)-C(26)-C(27)-C(28)	76(4)
C(25)-C(26)-C(27)-Pt(1)	-3(3)
C(24)-Pt(1)-C(27)-C(28)	-102.7(19)
P(2)-Pt(1)-C(27)-C(28)	-173(2)
Br(1)-Pt(1)-C(27)-C(28)	80.4(17)
C(24)-Pt(1)-C(27)-C(26)	23.7(19)
C(28)-Pt(1)-C(27)-C(26)	126(3)
P(2)-Pt(1)-C(27)-C(26)	-46(4)
Br(1)-Pt(1)-C(27)-C(26)	-153.1(18)
C(26)-C(27)-C(28)-C(29)	8(5)
Pt(1)-C(27)-C(28)-C(29)	105(3)
C(26)-C(27)-C(28)-Pt(1)	-97(3)
C(24)-Pt(1)-C(28)-C(29)	-47(2)
C(27)-Pt(1)-C(28)-C(29)	-121(3)
P(2)-Pt(1)-C(28)-C(29)	52(4)
Br(1)-Pt(1)-C(28)-C(29)	140(2)
C(24)-Pt(1)-C(28)-C(27)	74.2(19)
P(2)-Pt(1)-C(28)-C(27)	173.4(18)
Br(1)-Pt(1)-C(28)-C(27)	-98.9(17)
C(27)-C(28)-C(29)-C(30)	-26(5)
Pt(1)-C(28)-C(29)-C(30)	57(4)
C(24)-C(23)-C(30)-C(29)	60(3)
P(1)-C(23)-C(30)-C(29)	-161(2)
C(28)-C(29)-C(30)-C(23)	-59(4)

Symmetry transformations used to generate equivalent atoms:

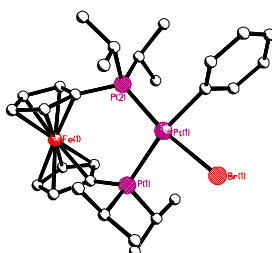
[Pt(dippf)(Ph)Br] – (28)

Table 9. Crystal data and structure refinement for EMMC1.

Identification code	emmc1	
Empirical formula	C ₂₉ H ₄₃ Br Cl ₂ Fe P ₂ Pt	
Formula weight	855.32	
Temperature	93(2) K	
Wavelength	0.71073 Å	
Crystal system	Monoclinic	
Space group	P2(1)/c	
Unit cell dimensions	a = 16.325(2) Å	α = 90°.
b = 11.8520(13) Å	β = 99.627(4)°.	
c = 16.365(2) Å	γ = 90°.	
Volume	3121.7(7) Å ³	
Z	4	
Density (calculated)	1.820 Mg/m ³	
Absorption coefficient	6.513 mm ⁻¹	
F(000)	1680	
Crystal size	0.0300 x 0.0300 x 0.0300 mm ³	
Theta range for data collection	2.13 to 25.37°.	
Index ranges	-14 ≤ h ≤ 19, -13 ≤ k ≤ 14, -18 ≤ l ≤ 19	
Reflections collected	19985	
Independent reflections	5652 [R(int) = 0.0296]	
Completeness to theta = 25.37°	98.6 %	
Absorption correction	Multiscan	
Max. and min. transmission	1.0000 and 0.8607	
Refinement method	Full-matrix least-squares on F ²	
Data / restraints / parameters	5652 / 0 / 326	
Goodness-of-fit on F ²	1.040	
Final R indices [I > 2σ(I)]	R1 = 0.0242, wR2 = 0.0487	
R indices (all data)	R1 = 0.0285, wR2 = 0.0500	
Largest diff. peak and hole	1.671 and -0.941 e.Å ⁻³	

Table 11. Bond lengths [\AA] and angles [$^\circ$] for EMMC1.

Pt(1)-C(23)	2.070(3)
Pt(1)-P(2)	2.2545(9)
Pt(1)-P(1)	2.3622(9)
Pt(1)-Br(1)	2.5036(4)
Fe(1)-C(5)	2.016(3)
Fe(1)-C(6)	2.023(3)
Fe(1)-C(1)	2.026(3)
Fe(1)-C(7)	2.029(3)
Fe(1)-C(10)	2.035(4)
Fe(1)-C(2)	2.049(4)
Fe(1)-C(9)	2.051(4)
Fe(1)-C(4)	2.056(4)
Fe(1)-C(8)	2.057(4)
Fe(1)-C(3)	2.071(4)
C(23)-Pt(1)-P(2)	87.69(10)
C(23)-Pt(1)-P(1)	168.18(10)
P(2)-Pt(1)-P(1)	102.56(3)
C(23)-Pt(1)-Br(1)	82.55(10)
P(2)-Pt(1)-Br(1)	169.53(2)
P(1)-Pt(1)-Br(1)	87.56(3)
C(5)-Fe(1)-C(6)	110.17(14)
P(1)-C(1)-Fe(1)	126.98(19)
C(6)-C(7)-Fe(1)	68.97(19)

Symmetry transformations used to generate equivalent atoms:

Table 14. Torsion angles [$^\circ$] for EMMC1.

Fe(1)-C(1)-P(1)-C(11)	93.7(2)
C(5)-C(1)-P(1)-Pt(1)	51.4(3)
C(2)-C(1)-P(1)-Pt(1)	-130.6(3)
Fe(1)-C(1)-P(1)-Pt(1)	-37.8(3)
C(23)-Pt(1)-P(1)-C(1)	-127.2(5)
P(2)-Pt(1)-P(1)-C(1)	22.31(14)
Br(1)-Pt(1)-P(1)-C(1)	-160.42(14)
C(23)-Pt(1)-P(1)-C(14)	-11.7(5)
P(2)-Pt(1)-P(1)-C(14)	137.84(13)
Br(1)-Pt(1)-P(1)-C(14)	-44.90(13)
C(23)-Pt(1)-P(1)-C(11)	107.7(5)

Appendix A.) X-Ray Crystallography Data

P(2)-Pt(1)-P(1)-C(11)	-102.76(13)
Br(1)-Pt(1)-P(1)-C(11)	74.50(13)
C(1)-P(1)-C(11)-C(12)	-81.6(3)
C(14)-P(1)-C(11)-C(12)	174.7(2)
Pt(1)-P(1)-C(11)-C(12)	51.8(3)
C(1)-P(1)-C(11)-C(13)	154.0(3)
Pt(1)-P(1)-C(11)-C(13)	-72.6(3)
Br(1)-Pt(1)-P(2)-C(6)	-158.51(16)
Br(1)-Pt(1)-P(2)-C(20)	78.12(19)

Symmetry transformations used to generate equivalent atoms:

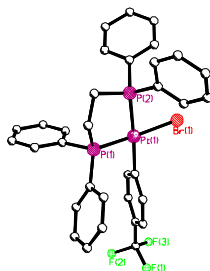
[Pt(dppe)(*p*-CF₃(C₆H₄))Br] – (54)

Table 15. Crystal data and structure refinement for emmc2.

Identification code	emmc2	
Empirical formula	C ₃₃ H ₂₈ Br F ₃ P ₂ Pt	
Formula weight	818.49	
Temperature	93(2) K	
Wavelength	0.71073 Å	
Crystal system	Monoclinic	
Space group	P2(1)/c	
Unit cell dimensions	a = 12.613(3) Å	α = 90°.
	b = 15.854(3) Å	β = 111.868(7)°.
	c = 16.062(4) Å	γ = 90°.
Volume	2980.7(11) Å ³	
Z	4	
Density (calculated)	1.824 Mg/m ³	
Absorption coefficient	6.196 mm ⁻¹	
F(000)	1584	
Crystal size	0.1000 x 0.1000 x 0.1000 mm ³	
Theta range for data collection	1.88 to 25.35°.	
Index ranges	-15 ≤ h ≤ 14, -18 ≤ k ≤ 13, -14 ≤ l ≤ 19	
Reflections collected	17882	
Independent reflections	5236 [R(int) = 0.0297]	
Completeness to theta = 25.00°	97.0 %	
Absorption correction	Multiscan	
Max. and min. transmission	1.0000 and 0.4936	
Refinement method	Full-matrix least-squares on F ²	
Data / restraints / parameters	5236 / 0 / 362	
Goodness-of-fit on F ²	1.049	
Final R indices [I > 2σ(I)]	R1 = 0.0231, wR2 = 0.0540	
R indices (all data)	R1 = 0.0260, wR2 = 0.0556	
Largest diff. peak and hole	1.448 and -1.179 e.Å ⁻³	

Table 17. Bond lengths [\AA] and angles [$^\circ$] for emmc2.

Pt(1)-C(27)	2.066(3)
Pt(1)-P(1)	2.2107(9)
Pt(1)-P(2)	2.3086(8)
Pt(1)-Br(1)	2.5161(6)
P(1)-C(9)	1.805(3)
P(1)-C(3)	1.822(3)
P(1)-C(1)	1.835(3)
P(1)-Pt(1)-P(2)	85.61(3)
C(27)-Pt(1)-Br(1)	91.89(8)
P(1)-Pt(1)-Br(1)	177.48(2)
P(2)-Pt(1)-Br(1)	91.90(3)

Symmetry transformations used to generate equivalent atoms:

Table 20. Torsion angles [$^\circ$] for emmc2.

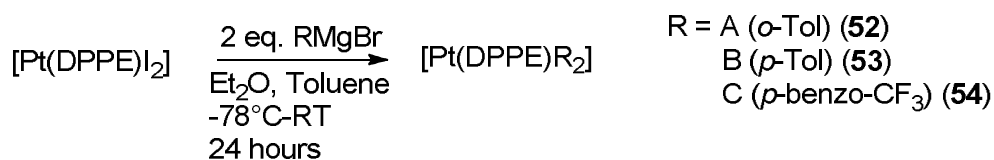
C(27)-Pt(1)-P(1)-C(9)	40.31(16)
P(2)-Pt(1)-P(1)-C(9)	-139.19(13)
Br(1)-Pt(1)-P(1)-C(9)	-130.8(5)
C(27)-Pt(1)-P(1)-C(3)	-85.24(14)
P(2)-Pt(1)-P(1)-C(3)	95.25(11)
Br(1)-Pt(1)-P(1)-C(3)	103.7(5)
C(27)-Pt(1)-P(1)-C(1)	160.65(14)
P(2)-Pt(1)-P(1)-C(1)	-18.85(12)
Br(1)-Pt(1)-P(1)-C(1)	-10.5(6)
Pt(1)-P(1)-C(1)-C(2)	46.1(2)
P(1)-C(1)-C(2)-P(2)	-51.6(3)
P(1)-Pt(1)-P(2)-C(21)	-125.24(12)
Br(1)-Pt(1)-P(2)-C(21)	55.13(12)
C(27)-Pt(1)-P(2)-C(15)	101.9(13)
P(1)-Pt(1)-P(2)-C(15)	109.33(11)
Br(1)-Pt(1)-P(2)-C(15)	-70.30(11)
C(27)-Pt(1)-P(2)-C(2)	-13.3(13)
P(1)-Pt(1)-P(2)-C(2)	-5.89(11)
Br(1)-Pt(1)-P(2)-C(2)	174.48(11)

Symmetry transformations used to generate equivalent atoms:

Appendix B - Synthesis of [Pt(dppe)(p-CF₃(C₆H₄))Br] (54)

Studies on the reactivity of various metal complexes with nucleophiles with respect to the phosphine ligands are of fundamental interest and can enable more efficient catalysis, thus providing an impetus for this study. Our aim was to vary the substituents on the aryl ring of the Pt complex and probe the effect this has on the transmetalation. A range of complexes of the form [Pt(dppe)(Ar)Br] were chosen, where Ar = C₆H₄(*o*-Tol) (**52**), C₆H₄(*p*-Tol) (**53**), C₆H₄(*p*-CF₃) (**54**). Synthesis of the *bis*-aryl complexes was achieved *via* [Pt(dppe)Cl₂] or [Pt(dppe)I₂] and an excess of the Grignard reagents containing the desired aryl groups respectively. Monitoring the reaction by ³¹P NMR showed the formation of the *bis*-aryl, unsymmetrical or dibromide complex respectively.

A mixture of products was observed with the *o*-Tol analogue when the Grignard reagent was added at -78°C and the reaction warmed to room temperature. The C₆H₄(*p*-Tol) and C₆H₄(*p*-CF₃) analogues were successfully synthesised under identical conditions in moderate yields (~60 %), (Scheme 65).

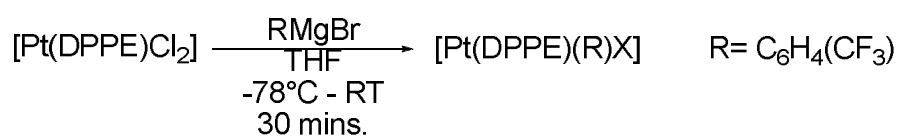


Scheme 65. Synthesis of bis-aryl complexes

Problems also arose on trying to create the unsymmetrical complex by generating 0.8 molar equivalents of HBr *in situ* (Acetyl bromide in CH₂Cl₂/MeOH in a 1:1 ratio) to displace one of the aryl groups. On each attempt, either the dibromide species was generated within minutes, or the *bis*-aryl complex remained. This reaction seemed to be more successful with the acetyl bromide being added as a solution in methanol to the reaction mixture.

Given the problematic nature of the generation of HBr *in situ*, a direct reaction between $[Pt(dppe)Cl_2]$ and one equivalent of Grignard reagent (ArMgBr) for a short reaction time (30 minutes) was attempted (Scheme 22).

For Ar = *o*-Tol (**52**), *p*-To (**53**), this approach was not successful. However for the Ar = $C_6H_4(p-CF_3)$ (**54**), a good yield (~80 %) of a mixture of $[Pt(dppe)(Ar)Cl]$ and $[Pt(dppe)(Ar)Br]$ was observed. Treatment with NaBr in acetone, gave full conversion to the pure $[Pt(dppe)C_6H_4(p-CF_3)Br]$ complex **54** observed by 1H , ^{31}P and ^{13}C NMR spectroscopy.



Scheme 66. Synthesis of $[Pt(dppe)(R)X]$

X-Ray quality crystals of $[Pt(dppe)(C_6H_4-pCF_3)Br]$ were grown by slow evaporation of NMR solvent $CDCl_3$ or by slow diffusion of DCM and hexanes. Figure 23 shows a representation of $[Pt(dppe)(C_6H_4CF_3)Br]$ (**54**) and square plane geometry about the Pt as expected (Figure 23, Table 24).

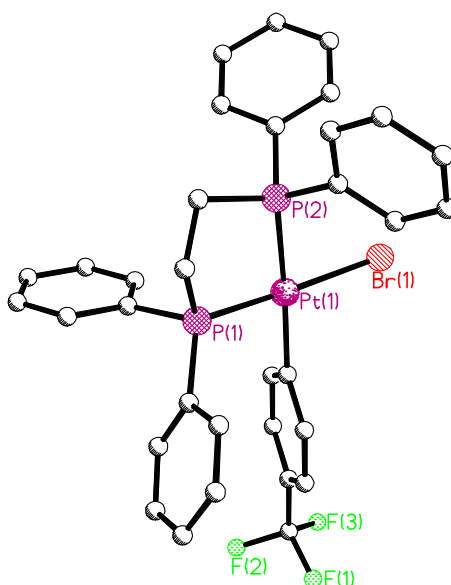


Figure 23. X-Ray structure of (**54**)

	Bond Angle (°)		Bond Length (Å)
P(2)-Pt(1)-P(1)	85.61(3)	Pt(1)-C(27)	2.066(3)
C(27)-Pt(1)-Br(1)	91.89(8)	Pt(1)-Br(1)	2.516(6)
P(2)-Pt(1)-Br(1)	91.90(3)	P(1)-Pt(1)	2.211(9)
P(1)-Pt(1)-Br(1)	177.48(2)	P(2)-Pt(1)	2.309(8)
C(27)-Pt(1)-P(1)	90.60(8)		
C(27)-Pt(1)-P(2)	176.17(8)		

Table 24. Selected Bond Angles (°) and Lengths (Å) for $[Pt(dppe)C_6H_4(p-CF_3)](54)$

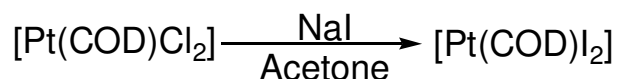
The work of Farrar *et al.*¹⁵⁸ showed that the $[Pt(dppe)Cl_2]$ structure has a distorted square planar geometry with a Cl-Pt-Cl bond angle of 90.2° and the DPPE backbone having a P-Pt-P bite angle of 86.3°. The average Pt-P bond length is 2.208 Å and the Pt-Cl is 2.348 Å. Complex **55** (Table 8) also adopts a slightly distorted square planar geometry about the Pt, where the C(27)-Pt(1)-Br(1) bond angle is 91.90° and the DPPE has a relatively small P-Pt-P “bite” angle of 85.61°.

The differing *trans* influence of the aryl and bromide ligands is reflected in the bond lengths of the phosphorus atoms *trans* to the aryl group attached (2.309 Å) compared to those *trans* to the Pt-Br bond (2.211 Å).

Complex **54** would have formed part of a comparison study varying the substituents on the aryl ring system however, due to the syntheses of these complexes proving to be problematic after multiple attempts only complex **54** was obtained.

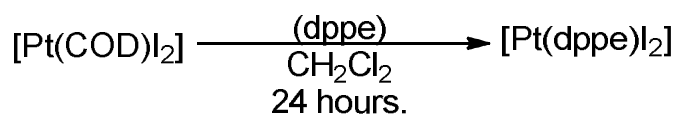
Experimental

$[Pt(COD)I_2]$

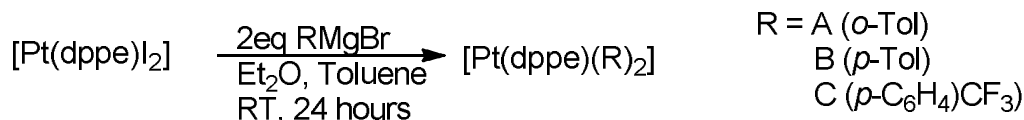


To a suspension of $[Pt(COD)Cl_2]$ (2 g, 5.99 mmol) in acetone (2 mL), sodium iodide (1eq, 0.899 g, 5.99 mmol) in acetone (2 mL) was added. The white suspension immediately turned bright yellow on addition of the NaI. The reaction mixture was concentrated *in vacuo*, washed with distilled water (50 mL), filtered, and allowed to air dry to give a yellow solid (3.09 g, 5.99 mmol, >99%) (1H NMR (300.06 MHz, $CDCl_3$) δ_H = 1.98 (m, 4H, 2 x CH_2), 2.48 (m, 4H, 2 x CH_2), 5.82 (t, 4H, 2 x CH_2) (Data in agreement with literature).¹⁵⁹

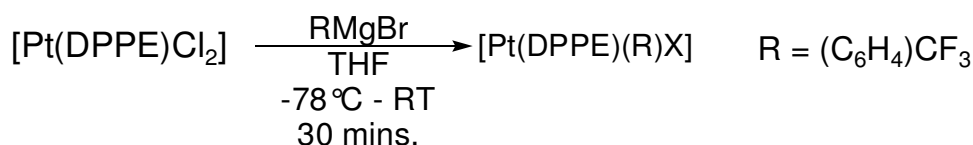
$[Pt(dppe)I_2]$



Dppe (1.1 eq., 0.594 g, 1.491 mmol) (colourless solid) was added to a solution of $[Pt(COD)I_2]$ (0.7 g, 1.356 mmol) in CH_2Cl_2 (5 mL) to give a yellow solution, this was stirred for 24 hours at room temperature. An off-white precipitate was formed, which was washed with hexanes and concentrated *in vacuo* to give a yellow solid (1.41g, 1.347 mmol, 99.31%). 1H NMR (300.06 MHz, $CDCl_3$) δ_H = 2.21 (m, 4H, 2 x CH_2), 7.21-7.82 (m, 20H, ArH); $^{31}P\{^1H\}$ NMR (121.466 MHz, $CDCl_3$) δ_P = 47.27 (s, $^1J_{P-Pt}$ = 3369.8 Hz) [Lit δ_P = 46.0 (s, $^1J_{P-Pt}$ = 3337 Hz)].¹⁴³

[Pt(dppe)(R)₂]

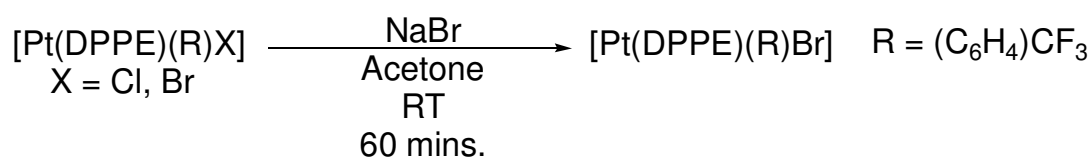
The Grignard reagent (12.37 eq., 2.919 mmol, 2 mL as 1.46 M in Et₂O) was added at -78°C to a yellow solution of [Pt(dppe)I₂] (0.2 g, 0.236 mmol) in toluene (1 mL). The reaction was stirred overnight at room temperature. The reaction mixture was hydrolysed with ice cold saturated NH₄Cl solution (CARE!). Organics were extracted into Et₂O (10 mL), dried over MgSO₄ and concentrated *in vacuo* to give orange/yellow solids respectively (0.142 mmol, 60 %). ¹H NMR (300.06 MHz, CDCl₃) (A) δ_H = 1.6-2.1 (m, 6H, CH₃), 6.46 (m, 2H, CH₂), 6.91-7.9 (m, 28H, ArH), [Lit δ_H = 2.0 (s, 6H, CH₃), 6.4 (m, 2H, CH₂), 6.4-8.0 (m, 28H, ArH),]¹⁴⁴ ¹H NMR (300 MHz, CDCl₃) (B) δ_H = 2.08-2.48 (m, 6H, CH₃), 6.49 (m, 2H, CH₂), 6.91-7.89 (m, 28H, ArH), [Lit δ_H = 2.08 (s, 6H, CH₃), 6.6 (d, 2H, CH₂), 6.9-7.9 (m, 28H, ArH)]¹⁴⁵; ³¹P{¹H} NMR (121.466 MHz, CDCl₃) δ_P = 42.12 (s, ¹J_{P-Pt} = 1688.4 Hz). ¹H NMR (300.06 MHz, CDCl₃) (C) δ_H = 2.3 (m, 6H, CH₃), 6.9 (m, 2H, CH₂), 6.8-7.6 (m, 28H, ArH), [Lit δ_H = 6.8-7.8 (m, 28H, ArH)]¹⁴⁵; ³¹P{¹H} NMR (121.466 MHz, CDCl₃) δ_P = 43.30 (s, ¹J_{P-Pt} = 1741.5 Hz)

[Pt(dppe)(R)X] X= Cl, Br

RMgBr (0.244 mmol, 0.167 mL, 1.46 M solution in Et₂O) was added dropwise at -78°C to a slurry of [Pt(dppe)Cl₂] (0.075 g, 0.113 mmol) in dry degassed THF (10 mL). The reaction mixture was allowed to warm to room temperature and stir for 30 minutes. Excess Grignard reagent was quenched with cold saturated NH₄Cl solution. Organics were extracted into Et₂O (10 mL), dried over MgSO₄ and concentrated *in vacuo* (ca. 2 mL). The solution was cooled to -78°C to obtain a crystalline yellow solid, which was isolated by filtration and dried under high vacuum (0.100 g, 0.1 mmol, 88.5%). ³¹P NMR showed 2 complexes; Cl and Br

analogues in a 1:1 ratio. ³¹P{¹H} NMR (121.466 MHz, CDCl₃) [(dppe)Pt(C₆H₄CF₃)Br] δ_P = 40.36 (s, 1P, ¹J_{P-Pt} = 1683.9 Hz, ²J_{P-P} = 36.8 Hz), 40.66 (d, 1P, ¹J_{P-Pt} = 4076.4 Hz, ²J_{P-P} = 36.8 Hz); [(dppe)Pt(C₆H₄CF₃)Cl] δ_P = 39.27 (s, 1P, ¹J_{P-Pt} = 1685.6 Hz, ²J_{P-P} = 3.2 Hz), 39.29 (s, 1P, ¹J_{P-Pt} = 4100.7 Hz, ²J_{P-P} = 3.2 Hz), This complex was directly treated with excess NaBr to form the pure bromide complex as discussed below.

[Pt(dppe) p-CF₃(C₆H₄)Br] (54)



NaBr (4 eq. 0.0466 g, 0.452 mmol) was dissolved in acetone (5 mL) and added to a slurry of [Pt(dppe)(C₆H₄CF₃)X] (0.1 g, 0.113 mmol) in acetone (3 mL). The reaction mixture was stirred at room temperature for 90 minutes and concentrated *in vacuo*. Organics were extracted into Et₂O (10 mL), dried over MgSO₄ and concentrated *in vacuo* to give a yellow solid, which was recrystallized from CH₂Cl₂/pentane, filtered and dried under high vacuum to give a crystalline yellow solid (0.100g, 0.11 mmol, 97 %) (**54**). ¹H NMR (300.06 MHz, CDCl₃) δ_H = 2.42 (m, 4H, 2 CH₂), 6.80-7.92 (m, 24H, ArH); ³¹P{¹H} NMR (121.466 MHz, CDCl₃) δ_P = 40.63 (d, 1P, ¹J_{P-Pt} = 1684.1 Hz, ²J_{P-P} = 4.5 Hz), 40.66 (d, 1P, ¹J_{P-Pt} = 4073.1 Hz, ²J_{P-P} = 4.5 Hz); ¹³C NMR (75.450 MHz, 298K, CDCl₃) δ_C = 66.3 (s, CH₂), 123.8, (t, ArCF₃), 131.5, (s, *p*-C_{Ar}H), 132.0 (s, *p*-C_{Ar}H), 133.6 (d, *o*-C_{Ar}H), 134.2 (d, *o*-C_{Ar}H), 137.2, (s, C_{Ar}H); ¹⁹F{¹H} NMR (282.339 MHz, CDCl₃) δ_F = -62.33 (s, Ar-CF₃); LR-MS: [FAB] [MBr]⁻ = 738.10; Also characterised by X-Ray Diffraction (See Appendix A).